PNNL-10947
UC-721

Sulfur Polymer Cement as a Low-Level Waste Glass Matrix Encapsulant

P. Sliva
Y. B. Peng
D. K. Peeler
L. R. Bunnell
P. J. Turner
P. F. Martin
X. Feng

January 1996

Prepared for
the U.S. Department of Energy
Contract DE-AC06-76RLO 1830

Pacific Northwest National Laboratory
Operated for the U.S. Department of Energy
by Battelle

Battelle

PNNL-10947

DISCLAIMER

PACIFIC NORTHWEST LABORATORY
operated by
BATTELLE MEMORIAL INSTITUTE
for the
UNITED STATES DEPARTMENT OF ENERGY
under Contract DE-AC06-76RLO 1830

Printed in the United States of America

Available to DOE and DOE contractors from the Office of Scientific and Technical Information, P.O. Box 62, Oak Ridge, TN 37831; prices available from (615) 576-8401. FTS 626-8401.

Available to the public from the National Technical Information Service, U.S. Department of Commerce, 5285 Port Royal Rd., Springfield, VA 22161.

PNNL-10947
UC-721

Sulfur Polymer Cement as a Low-Level Waste Glass Matrix Encapsulant

P. Sliva
Y. B. Peng
D. K. Peeler
L. R. Bunnell
P. J. Turner
P. F. Martin
X. Feng

January 1996

Prepared for
the U.S. Department of Energy
under Contract DE-AC06-76RLO 1830

Pacific Northwest National Laboratory
Richland, Washington 99352

Summary

Sulfur polymer cement (SPC) is being considered as a matrix encapsulant for the Hanford low-level (activity) waste glass. SPC is an elemental sulfur polymer-stabilized thermoplastic that is fluid at 120° to 140°C. The candidate process would encapsulate the waste glass by mixing the glass cullet with the SPC and casting it into the container. As the primary barrier to groundwater and a key factor in controlling the local environment of the disposal system after it has been compromised, SPC plays a key role in the waste form's long-term performance assessment.

Work in fiscal year 1995 targeted several technical areas of matrix encapsulation involving SPC. A literature review was performed to evaluate potential matrix-encapsulant materials. The dissolution and corrosion behavior of SPC under static conditions was determined as a function of temperature, pH, and sample surface area/solution volume. Preliminary dynamic flow-through testing was performed. SPC formulation and properties were investigated, including controlled crystallization, phase formation, modifying polymer effects on crystallization, and SPC processibility. The interface between SPC and simulated LLW glass was examined. Interfacial chemistry and stability, the effect of water on the glass/SPC interface, and the effect of molten sulfur on the glass surface chemistry were established. Preliminary scoping experiments involving SPC's Tc gettering capabilities were performed. Compressive strengths of SPC and SPC/glass composites, both before and after lifetime radiation dose exposure, were determined.

Results from the static MCC-1-type tests on SPC indicated that the reaction rate was highly dependent on both temperature and initial aqueous conditions. Higher temperature tests (i.e., 90°C) indicated that the SPC did not perform well under the conditions evaluated. This could have been a result of the test temperature approaching or exceeding the "transition" temperature of the SPC. At room temperature, SPC was stable and insoluble in water throughout the test duration in this project, where no pH change and/or weight loss were observed.

Based on static tests, solution pH has the greatest effect on SPC corrosion. The corrosion rate in 0.0107m LiOH was higher than in deionized water (DIW) by a factor of 2 at the 1-day test and a factor of 23 at 56 days in room temperature tests; a factor of 6 at 1-day and a factor of 55 at 56-day tests at 40°C; a factor of 100 to 300 from 1-day to 56-day in 70°C tests; and a factor of 100 for 1-, 7-, and 14-day tests at 90°C. The difference between the reaction rate in DIW and in alkaline water increases with time and increases with temperature.

Based on statistical results, temperature affects SPC corrosion rate, but the effect is less than that of solution pH. The temperature effects were different in DIW and in alkaline solutions:

- At room temperature: The corrosion rate in 0.0107m LiOH decreased from 40° to 20°C by about 2 times in the 1-day test to about 6 times in 56 days. The temperature effects were constant from 7 to 56 days. The corrosion rate difference between 40° and 20°C tests in DIW was insignificant during the early test periods and gradually increased to a factor of two at 56 days; i.e., the temperature effects were very small and slowly increased with time.

- At 40°C: The corrosion rate in 0.0107m LiOH decreased from 70° to 40°C by about 40 times at the 1-day test and by 10 times at 56 days. The temperature effects decreased with time. The

corrosion rate difference in DIW was maintained at about 2 times throughout 1 to 56 days; i.e., the temperature effects did not change with time.

- At 70°C: The SPC corrosion rate between 70° and 90°C differed by 7 to 1.3 times for tests in 0.0107m LiOH, and by 4 to 10 times for tests in DIW from day one to day 56. The temperature difference for tests in 0.0107m LiOH decreased with time while the difference increased with time for the tests in DIW.

Activation energy could not be calculated from the static tests because too many variables were not under control (pH, oxygen fugacity, etc).

Sulfuric acids released from SPC drove down the pH to an equilibrium value of approximately 3.5. The starting pH of 11.82 decreased to approximately 9.0 in just one day and reached a constant value of approximately 3.5 after only 28 days at 90°C. However, the static tests at lower temperature or in DIW approached this pH much slower and no pH change was observed for tests at room temperature.

The final phases in SPC depend not only on the polymer modification but also on the thermal history of the SPC. Polymer modification is necessary to retain the beta-crystalline sulfur at lower temperatures. When the cooling rates are slower than 1.5°C/min, the final crystalline phase is alpha sulfur regardless of the polymer modification.

The role of the polymer modification is not as important to stabilizing the beta sulfur form as it is in controlling the microstructure. Pure sulfur crystallizes and forms large alpha crystals (millimeters to centimeters). With the addition of polymer, the crystal growth is limited and controlled by the polymer in such a way that all crystals are plate-like of micron thickness.

A better understanding of SPC has been obtained in terms of its chemistry and thermal processing. New SPC formulations are possible. In particular, if control of the microstructure is most critical to achieve mechanical integrity of a sulfur cement, inorganic modifiers can be considered to impinge on the crystal growth. The same microstructure can be obtained without the use of organic species like polymer in SPC formulation.

Processing conditions have been defined in terms of temperature, processibility, reproducibility, and safety. Removal of entrapped air will reduce void volume. Curing at a higher temperature will complete the sulfur-polymer reaction.

Simulated LLW glass surface chemistry changes very little after exposure to molten SPC (during simulated processing of simulated LLW glass/SPC waste forms), compared to changes caused by water exposure even for a relatively short time at a lower temperature. There is no anticipated change in the glass corrosion mechanism.

The simulated LLW glass/SPC interface exhibited good wetting and bonding. The chemical affinity between calcium and sulfur that this investigation revealed should be explored further. A calcium sulfate thin layer can be created on the glass surface and can act as a barrier to preserve the interface.

The worst-case simulation indicated that SPC may accelerate the glass leaching at an early stage

(within 13 days at 50°C) when compared with inert encapsulants like quartz. However, SPC encapsulation greatly minimized the glass leaching when compared with no encapsulation. Well bonded glass/SPC interfaces exposed to 50°C water for 1330 hours (55 days) had no detectable interfacial opening or deterioration.

Sulfur polymer cement, both neat and in composite form with simulated LLW glass, is a fairly strong material capable of mechanical damage without catastrophic failure. Gamma irradiation to projected lifetime dose stiffens and strengthens the SPC by an unknown mechanism.

This report was originally being written as a year-end status report. However, after the report was completed, the work was terminated. Consequently, a portion of the work was left incomplete, especially the single-pass flow-through tests and the technetium gettering studies. It was decided to include most of the preliminary results from these studies as a basis for future work. Caution should be exercised not to generalize beyond the results and conclusions presented.

Acknowledgments

Douglas Mackey performed most of the work relating to controlled cooling and crystallization of sulfur polymer cement (SPC). He also assisted in glass/SPC interfacial characterization experiments, in data acquisition and documentation and presentation, and many other supporting function of this investigation. Our thanks go to Martin Resources, Inc. for supplying the SPC. We also acknowledge and thank the following investigation team members:

- David McCready for the X-ray diffraction work in SPC phase identification and quantitative analysis;
- Mark Engelhard, Don Baer, and Ashley Shultz for their XPS and SIMS analysis of SPC and glass;
- Karl Pool, for his insight into sulfur chemistry, sulfur speciation, and detection. In addition, he directed most of the solution inductively coupled plasma analysis and other analyses, like IC;
- Peter McGrail for assisting in the SPC dissolution kinetics study and data interpretation;
- Jim Coleman, Jim Young, and Susan McKinley for their scanning electron microscopy work;
- Ross Gordon and Kevin Simmons for their differential scanning calorimetry and thermal expansion work;
- Bruce Lerner for the FTIR and Raman Analysis;
- Mike Schweiger for providing the low-level waste glass and other support for this project;
- Meiling Gong for directing some of the solution inductively coupled plasma analysis and polymer extraction work;
- Tom Chen and Eve Tracy for the SPC viscosity measurements;
- John Vienna for the SPC gas chromatography/mass analysis;
- Bobbi Romine, Jan Miles, and Kyla Noyola for much of the office support for this investigation;
- Wendy K. Hahn for helping to perform some of the single-pass flow-through tests;
- Cheryl Eiholzer and Fred Mann, for their guidance and being so great to work with; and
- Joe Westsik for his support and guidance on this investigation.

Acronyms, Abbreviations, and Initialisms

BNL	Brookhaven National Laboratory
DIW	Deionized water
DSC	Differential scanning calorimetry
EDX	Energy-dispersive X-ray
Eh	Oxygen potential
FTIR	Fourier transform infrared (spectroscopy)
FY	Fiscal year
GC	Gas chromatography
IC	Ion chromatography
ICP	Inductively coupled plasma
IR	Infrared
LATA	Los Alamos Technical Associates
LLW	Low-level waste
LS	Liquid scintillation
LVDT	Linear variable differential transformer
Kd	Distribution coefficient
MCC	Materials Characterization Center
PA	Performance assessment
PFA	Perfluoroalkoxy (Dupont Teflon™ fluoropolymer resin)
PCT	Product consistency test
PNNL	Pacific Northwest National Laboratory
PTFE	Polytetrafluoroethylene
SC	Sulfur concrete
SEM	Scanning electron microscopy/microscope
SIMS	Secondary ion mass spectometry
SPC	Sulfur polymer cement
SSA	Specific surface area
WHC	Westinghouse Hanford Company
XPS	X-ray photoelectron spectroscopy
XRD	X-ray diffraction

Contents

Figures

Tables

1.0 Introduction and Background

Hanford Site low-level waste (LLW) will be vitrified and stored at the Hanford Reservation, which could also serve as the final disposal site. The waste glass will be transported from the vitrification plant and emplaced at the storage/disposal site. Storage/disposal will be in near-surface engineered facility. Westinghouse Hanford Company (WHC) has responsibility for implementing this strategy for the U.S. Department of Energy. The Pacific Northwest National Laboratory is providing technical support to this effort. Specific storage/disposal criteria have yet to be developed for the vitrified LLW at the Hanford Site.

The scope of product packaging is to identify and develop the best packaging for the glass from the time it exits the melter until it is emplaced at the storage/disposal site. The underlying basis for developing the best packaging is to meet all safety, permit, and regulatory requirements. Consequently, product packaging is intimately interfaced with long-term performance assessment (PA) and processing requirements.

Undetermined at this time are the specifics involving the waste glass once it exits the melter; for example, the glass could be poured directly into large monolith container forms, molded into large monoliths, or it could be molded into marble-like spheres. A leading candidate is quenching the glass in water to form cullet. The marbles or cullet could be encapsulated in a matrix within the storage/disposal container.

Containers of embedded waste-glass marbles or large monolithic glass blocks could be stacked in a storage/disposal facility; the entire facility could then be backfilled with a barrier material. Each of these options will motivate choices for transportation, retrievable storage, and final disposal.

A key choice for both retrievable storage and final disposal of vitrified LLW is whether or not to use an embedding matrix material. A matrix material offers possible advantages over a waste glass alone. The matrix material can provide an additional barrier to isolate the glass from degradation mechanisms, such as dissolution by water. Embedding matrix materials can contain "getters" that complex specific ions which could be released from the glass over time. It is possible for matrix materials to regulate the local environment around the waste glass. Embedding the glass in a matrix material could enhance the waste form's overall performance. However, the need for matrix materials to meet performance assessment requirements has yet to be determined.

Numerous investigations have evaluated waste-matrix materials (Wiemers et al. 1992; Darnell et al. 1992; Kalb et al. 1991; Ringwood 1980; Boomer et al. 1990); however, all of these studies have focused on incorporating the waste directly into the proposed material (i.e., instead of glass). These investigations offer little insight into embedding waste-containing glass into the matrix material and using the matrix material as a second barrier, especially when the matrix material has the potential to alter the waste-glass surface during the embedding process.

In fiscal year (FY) 1994, Los Alamos Technical Associates (LATA) was contracted by Westinghouse Hanford Company to assess potential matrix materials for the Hanford Site LLW glass (LATA 1994). Los Alamos Technical Associates reviewed several potential matrix materials,

including polyethylene, soils/clays, sulfur polymer cement, bitumen, cement-based grout, and various metals. Based on a set of weighted criteria, the leading candidate was sulfur polymer cement.

Westinghouse Hanford Company and Pacific Northwest National Laboratory staff members determined the key issues concerning the use of a matrix material and its influence on performance assessment, glass processing, and glass composition formulation. These issues are presented in an outline in Appendix A, which represents an incomplete working list of packaging concerns that warrant investigation during the life of the program and was used as a basis for determining the FY 1995 work scope.

The objective of the FY 1995 product-packaging work was to begin evaluating the most promising matrix materials that could embed LLW glass produced from the Hanford Site tank wastes. Sulfur polymer cement, the leading candidate from the LATA report, was to be evaluated.

2.0 Product Packaging Testing Approach

Tests were conducted to increase understanding and provide data to several key technical areas, including performance assessment, glass processing, and glass composition formulation. An investigation of sulfur polymer cement was to begin in FY 1995, as outlined in Appendix A. Testing priority responded first to needed data input for performance-assessment calculations, followed by any processing and glass formulation requirements. Although other crucial information may be needed for a specific process or glass formulation function, performance assessment needs were the primary motivation for matrix material evaluation. The following subtask descriptions identify proposed sample test matrices for product packaging in FY 1995. Not all of the work under each matrix was completed; however, describing the full test matrix was considered expedient at this time. Also, some of the test areas listed below were combined during testing and are consequently reported and discussed as such.

2.1 Subtask Descriptions

2.1.1 Evaluate Alternate Matrix Materials

Alternate matrix materials will be evaluated by reviewing reports on matrix materials for LLW, including the FY 1994 LATA report; compiling a list of most promising matrix materials for LLW glass along with their deficiencies; ascertaining if the deficiency(ies) can be overcome and effort expected to do so; and completing a "short list." In addition to sulfur polymer cement, one or two most-promising matrix material candidates will be selected.

2.1.2 Sample Preparation/Testing/Characterization

Prepare Samples

Samples will be prepared using the current baseline simulant vendor glass (20% sodium); then one or two glasses at higher waste loadings (up to 40% sodium) will be chosen. Glass/matrix and matrix (alone) samples will be prepared for testing. Consider whether or not the test samples are representative of prospective storage/disposal scenarios.

Dissolution

Preliminary scoping tests

The reaction kinetics of sulfur polymer cement without glass will be determined as a function of time at four temperatures from 40-90°C; four pHs from neutral to very basic; fixed oxygen partial pressure, based on the known O_2 diffusion rate through a Teflon™ container wall (relatively oxidizing), using duplicate specimens. The results of these preliminary tests may change or preclude some of the short- and long-term aqueous durability testing listed below, or may lead to similar testing of samples containing glass.

Short- and long-term durability

Short-term aqueous durability of the following will be evaluated: monoliths (few cm^3) (MCC-1, flow-through if needed); SPC, glass, glass/SPC-cored, glass/SPC as-molded (glass cullet encased in SPC), blanks, duplicate specimens, different waste loadings. The primary measurable is Na concentration in solution as a function of time and other variables.

Long-term aqueous durability of the following will be determined: ground (PCT, flow-through if high[er] surface area needed); SPC, glass, glass/SPC, blanks, duplicate specimens, different waste loadings. The primary measurable is the concentration of Na, B, and S in solution as a function of time and other variables such as temperature, solution Eh and pH.

Relevant data on long-term durability can also be derived from vapor-phase hydration (corrosion) testing. A sample matrix, similar to that listed above, can be tested under elevated temperatures in a saturated vapor. Corrosion tests will be performed as needed to corroborate the other long-term data collected.

Glass/Matrix Interface Chemistry

Interface chemistry before and after embedding glass in the SPC, and before and after dissolution testing will be evaluated. Glass coupons may be dipped in molten SPC, exposed to molten SPC for long periods to simulate a slow-cooled waste canister, and dissolution-tested. Changes in the surface chemistry of the glass or the matrix material that could alter the materials' chemistry will be characterized. Samples will be cross-sectioned after testing and analyzed for ion migration, typically accomplished with X-ray mapping (e.g., Na or B migration from the glass into the sulfur).

Glass/Matrix Interface Mechanical Properties

Interface mechanical properties before and after embedding glass into the SPC, before and after dissolution testing, and before and after radiation (gamma) exposure will be characterized. To do so, sample preparation will be similar to interface chemistry, except that the presence of mechanical bonding will be evaluated. Testing will involve determining tensile and/or shear modes; load-to-failure will be measured. Changes in the surface chemistry of the glass or the matrix material may alter the bonding between the glass and the matrix material.

Sulfur Oxidation

Much of the information concerning sulfur oxidation will result from the preliminary scoping tests (listed above, under Dissolution) and data collected from biodegradation testing. The quantity of sulfur oxidized as a function of time will be measured. This test is specific to sulfur polymer cement.

Compressive Strength

Compressive strength before and after dissolution testing, before and after radiation exposure (gamma); SPC, glass, glass/SPC, glass loading, spheres and shards, multiple samples for statistics will be measured. Samples will be cylinders, loaded axially. Load-at-failure will be measured. Fracture surfaces will be evaluated for failure origin and mode. Testing will be done at a temperature relevant to storage, and diametral expansion prior to failure will be used as a measure of plasticity.

Compressive strength will identify processing flaws, help determine efficient glass loading, and radiation- or dissolution-induced defects.

Pore Volume and Pore Distribution

Pore volume and pore distribution properties before and after dissolution testing, before and after radiation exposure (gamma); SPC, and glass/SPC will be evaluated. The pore volume and pore distribution measured will identify any interconnected porosity in the matrix material and its pore size distribution, which is crucial to the matrix material's capability to act as an environmental barrier for the waste glass.

Radiation Effects

Radiation effects on sulfur polymer cement and glass/SPC monoliths (few cm^3), two to three different doses, will be assessed. Radiation testing will be performed in conjunction with mechanical property, chemistry, oxidation, and dissolution testing. Additional testing may include determining if off-gassing is occurring. The tests will be performed in the 3730 Building.

Technetium Gettering

Sulfur polymer cement and glass/SPC samples, using sodium pertechnetate as the technetium source, will be evaluated for technetium gettering. Distribution coefficient (Kd) experiments using sample morphology, oxygen partial pressure, pH, temperature, and the presence of other potential disposal-system materials as the variables will be run.

2.1.3 Sulfur Cement Formulation Variability

By testing alternate sulfur cements, the viability and applicability of other sulfur-based compounds will be determined.

3.0 Sample Preparation, Testing, and Characterization

Samples prepared for all of the testing performed consisted either of sulfur polymer cement (SPC) alone (designated neat) or of a composite prepared from LLW glass particles embedded into the SPC. This section covers characterization of the starting materials and a general sample preparation description. Details of procedures or processes performed on samples for a specific test are discussed with that test.

3.1 Sulfur Polymer Cement

ASTM C1159-90 defines sulfur polymer cement (SPC) as "a polymer product consisting of small amounts of chemical modifying additives dispersed in sulfur." In practice, SPC is made by the reaction of a blend of dicyclopentadiene and oligomers of cyclopentadienes with elemental sulfur. Typical SPC formulation contains 2 wt% dicyclopentadiene and 2.5 wt% oligomers of cyclopentadienes. SPC is intended and used as an acid-resistant construction material in the form of sulfur concrete (SC). This material has been investigated extensively as a potential primary encapsulant for various low-level wastes that cannot be appropriately encapsulated with ordinary Portland cement (Mayberry et al 1993; Kalb et al 1991; Kalb et al 1990).

Sulfur polymer cement is water-impermeable. It has a low melting temperature (120° to 140°C) and a low viscosity (below 100 centipoise) when melted. It is suitable for pouring and pumping. All of these characteristics of SPC make it ideal, potentially, as a retrievable encapsulant for vitrified low-level waste glass or as a water barrier (wall or backfill) in an engineered disposal system.

The sulfur polymer cement used in this study was commercially produced (Chement 2000, Martin Resources, Inc., Odessa, TX). Two main lots were used in this investigation. SPC lot 122794 was produced before 1990, and was used so that results from this investigation could be compared with previous results from Pacific Northwest Laboratory (PNL) and elsewhere. A lot from recent improved processing was also obtained from Martin Resources and was denoted (SPC lot 030695). The manufacturer's certification of analysis, listed in Table 3.1, agrees with the ASTM C1159-90 requirements for SPC chemical and physical properties.

3.1.1 Initial Characterization of As-Received Sulfur Polymer Cement

There were significant visual differences between the two main SPC lots used in this investigation. SPC lot 122794 was composed of granules 6 mm or smaller. The color was yellowish on the outer surface of the granules and dark gray inside. A small portion (about 5 to 10%) of the granules was yellowish in color throughout the entire grain. SPC lot 030695 was received in chips about 5-mm thick. The color was yellowish throughout the granule.

X-ray diffraction patterns were collected for both SPC lots (see Figure 3.1). Also collected was the XRD spectrum of the yellowish surface layer of SPC lot 122794. This yellowish surface material was identified as alpha-crystalline sulfur, while the dark gray interior of the same lot was identified as mostly beta-crystalline sulfur. SPC lot 030695 was predominantly alpha-crystalline sulfur. The amorphous content of SPC lot 030695 was also relatively lower since the XRD spectrum (Figure 3.1, op) has a lower background compared to that of SPC lot 122794 (Figure 3.1, bottom).

Table 3.1. Properties of SPC (Chement 2000)

Property	Manufacturer's Value	Analyzed/Measured Lot 122794	Analyzed/Measured Lot 030695
Carbon Content (wt% as C)	4.5 to 5.5	4.05 to 4.06	3.7 to 3.8
Hydrogen Content (wt% as H)	0.45 to 0.55	< 0.5	< 0.5
Sulfur Content (wt% as S)	94.0 to 96.0	92.6 to 92.9	93.2 to 94.0
Viscosity at 135° C (centipoise)	25 to 100	83	88
Specific Gravity(g/ml)	1.88 to 1.92		

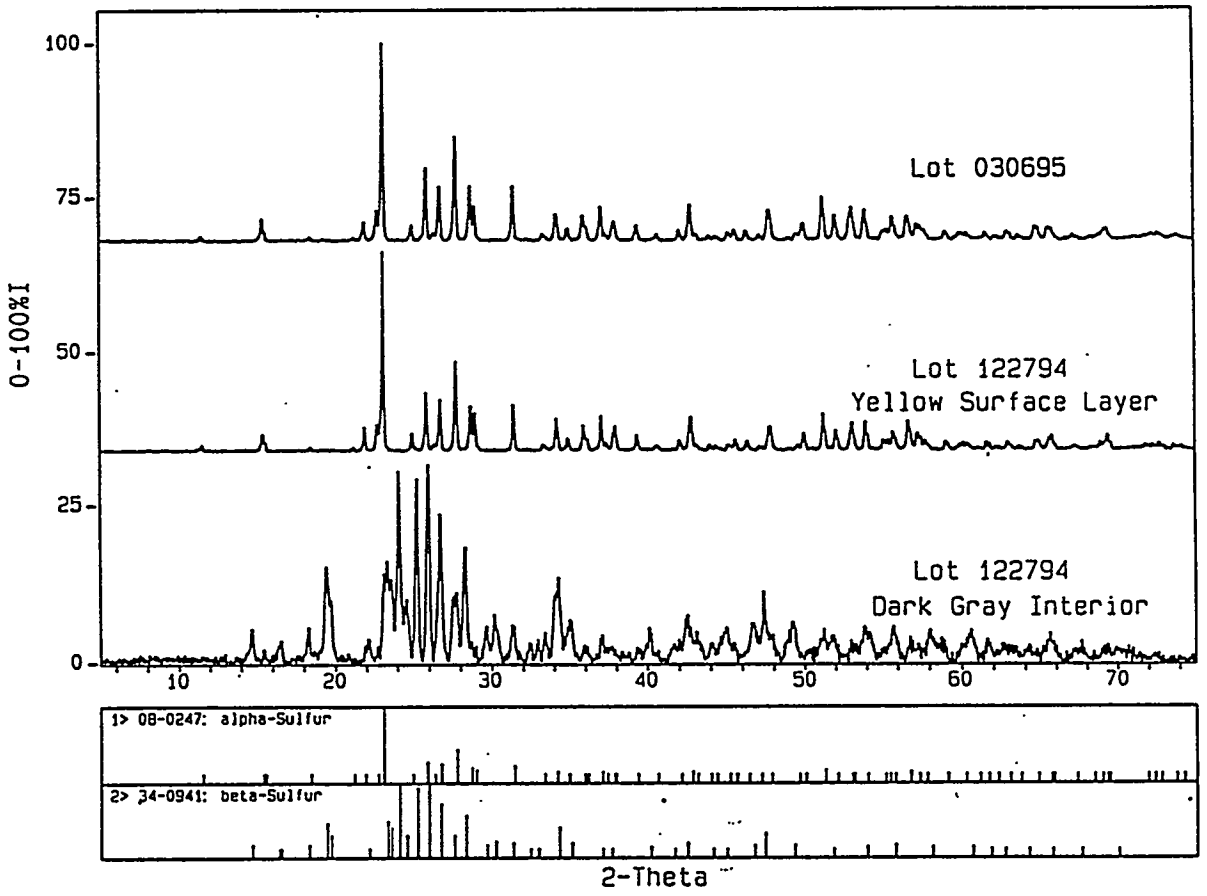

Figure 3.1. X-Ray Diffraction Patterns of As-Received Sulfur Polymer Cement. Top: Lot 030695, alpha sulfur. Middle: Lot 122794, only material from yellow surface layer, alpha sulfur. Bottom: Lot 122794, only dark gray material from granule core, major amount of beta sulfur and major amount of amorphous sulfur, some alpha sulfur.

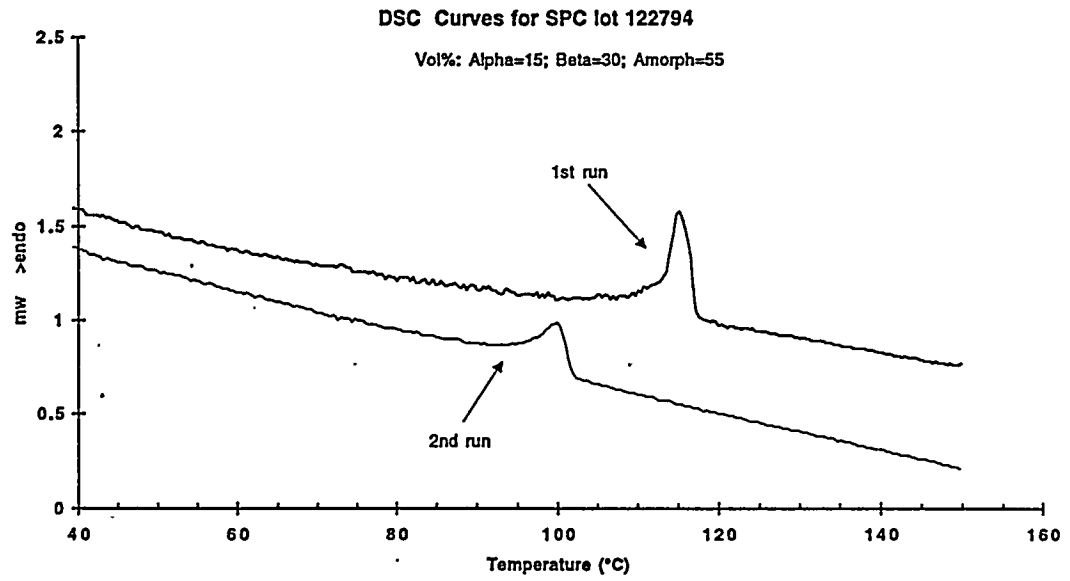

Figure 3.2. DSC Curves for SPC Lot 122794. The heating rate was 5°C/min. The sample was cooled naturally after the first run and allowed to sit a minimum of 10 hours before reheating in the second run.

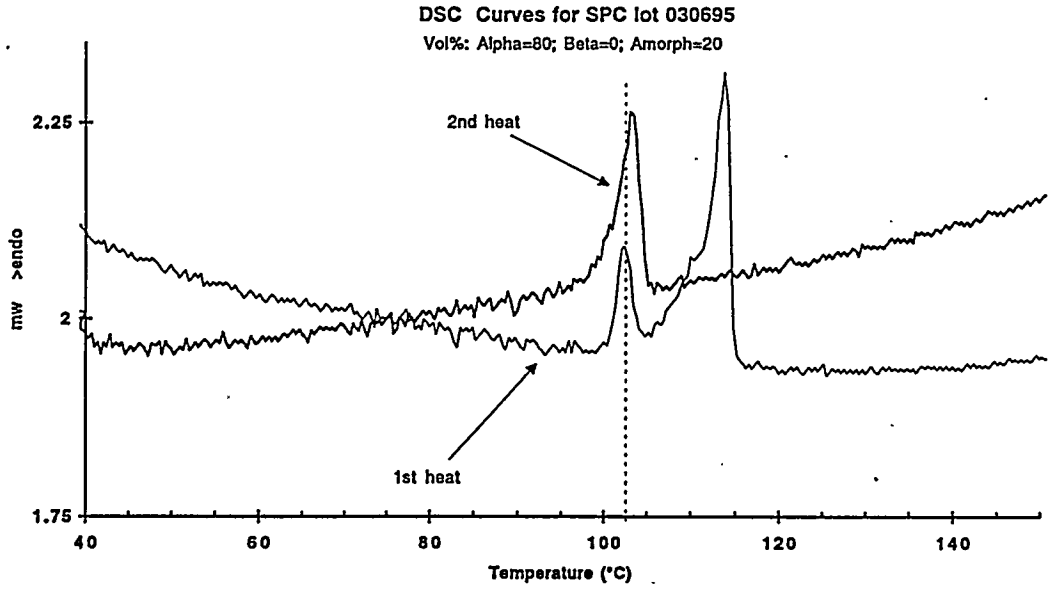

Figure 3.3. DSC Curves for SPC Lot 030695. The heating rate was 5°C/min. The sample was cooled naturally after the first run and allowed to sit a minimum of 10 hours before reheating in the second run.

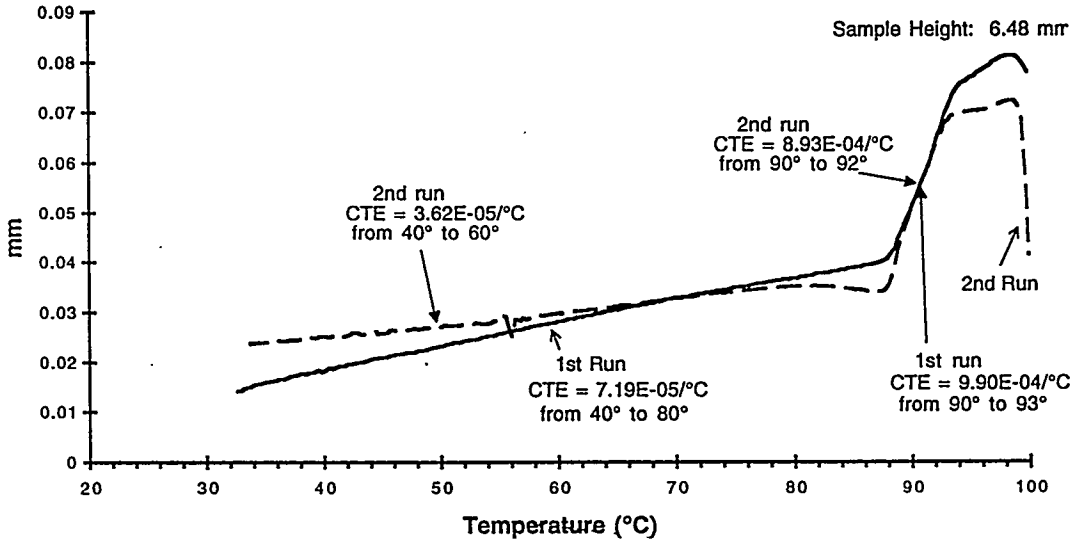

Figure 3.4. Thermal Expansion and Glass Transition Temperature of SPC Lot 122794. The heating rate was 5°C/min and the sample length was 6.48 mm.

Differential scanning calorimetric (DSC) spectra of both SPC lot 122794 and lot 030695 are shown in Figures 3.2 and 3.3, respectively. Sample size was about 10 mg and the heating rate was 5°C/min. When 150°C was reached, the sample was allowed to cool naturally. Reheating was done after the samples cooled to room temperature for 10 hours or longer. For SPC lot 122794, melting of the beta-crystalline phase was detected in the first run, while only alpha melting was detected in the second run. Melting of the beta-crystalline phase was not detected either in the second run for SPC lot 030695. However, both alpha- and beta-crystalline phase melting was detected in the first run for SPC lot 030695.

The thermal expansion curves shown in Figure 3.4 provided information relating to the glass transition temperature and the thermal expansion coefficient for SPC lot 122794. The expansion coefficient varied between the first and second runs. Both runs showed the glass transition temperature in the range of 88° to 90°C.

Viscosities for SPC lot 122795 and 030695 were 83 and 88 centipoise, respectively, at 135°C.

Table 3.2. Nominal and Analyzed LD6-5412 Glass Composition

Component	Nominal (wt%)	Analyzed (wt %)
SiO_2	55.91	55.44
Na_2O	20.00	20.41
Al_2O_3	12.00	12.17
B_2O_3	5.00	5.05
CaO	4.00	4.12
K_2O	1.46	1.66
Cl	0.35	
F	0.29	
SO_3	0.21	0.18
P_2O_5	0.19	0.22
Cs_2O	0.15	
SrO	0.11	
Cr_2O_3	0.04	0.05
Fe_2O_3	0.00	0.11
Others	0.29	0.58

3.1.2 Low-Level Waste Glass

One representative glass was chosen from PNL's LLW vendor glass series.[a] This glass was identified as LD6-5412; its chemical composition is listed in Table 3.2. This glass contained 20 wt% Na_2O, which is the main constituent of Hanford low-level wastes. The 7-day product consistency test (PCT) at 90°C showed the glass dissolution rate as 0.38 g/m^2, based on sodium release. This glass showed good processibility and had good solubility for minor components and metal components that are normally present in a waste stream.

Chemical batching and glass melting were done according to PNL Procedure PSL-417-GBM. Glass frits were obtained by casting the glass melt directly into water in a stainless-steel container. Glass fibers were obtained by pulling from the melt in the crucible. Glass bars were obtained by casting in steel molds, followed by annealing. Square glass bars (5 mm x 5 mm) were cut from annealed casts. Various surface finishes used in glass/SPC interface characterization included fractured, and diamond-polished. Mineral oil and acetone were used in most of the sample preparation steps where contact with water would alter the glass surface chemistry.

(a) X. Feng, et al. 1995. "Evaluation of Phase II Glass Formulations for Vitrification of Hanford Site Low-Level Waste." PVTD-T3B-95-206. Pacific Northwest Laboratory, Richland, Washington.

4.0 Dissolution and Corrosion of Sulfur Polymer Cement

The waste form is proposed to be low-level waste glass cullet embedded in sulfur polymer cement (SPC) (Mitchell 1995). In a disposal environment, after the containers corrode, groundwater may come in contact with the SPC first because the glass is encapsulated in the SPC. After time, glass will become a component of the system. Because the disposal system has not yet been defined, characterization of the groundwater expected to reach the SPC/glass waste form is unknown. Therefore, ranges of pH conditions and SPC/glass configurations (SPC alone and SPC/LLW) glass were included in the test matrix.

To attain a fundamental understanding of the reaction kinetics (dissolution behavior) of SPC in various aqueous environments, a suite of "short-term" laboratory tests was performed, including both static (MCC-type) and dynamic (single-pass flow-through) tests. The results of these tests will provide insight into the reaction kinetics of SPC, and provide necessary data to link performance assessment criteria for the low-level waste product packaging system to near-surface disposal site conditions. Information regarding the corrosion rate (including temperature and pH dependence), activation energy, and properties inherent to the SPC material are needed for performance assessment.

4.1 Experimental Considerations

4.1.1 Static Tests

The MCC-1 leaching test was performed in accordance with PNNL Technical Procedure PSL-417-LCH, Rev. 0 ("Leaching Test Using MCC-1P and MCC-3S Methods"). Monolithic samples were immersed in a solution within Teflon[1] vessels in a controlled experimental environment. Tests conditions that are controlled include the pH of the aqueous environment, temperature, and the surface area-to-volume ratio. Table 4.1 shows the test conditions of the static (MCC-type) tests. Table 4.2 shows the experimental conditions for the static-testing program.

Two different aqueous systems were used for the static tests, deionized water (DIW) and a 0.0107m LiOH buffer solution. These two aqueous systems were used to provide an environment consistent with the current LLW testing program at PNNL.

The monolithic samples were placed on a Teflon-coated, mesh support screen to expose the entire surface area (~400 mm^2) to the aqueous environment. The test was run at a surface area-to-volume ratio of $10m^{-1}$ (adjusted by the addition of the aqueous solution to a known/measured surface area). The pre-labeled Teflon vessels containing the SPC monolith were placed into a calibrated isothermal oven held at a predetermined temperature (40°, 70°, or 90°C). Tests run at 20°C were nominal laboratory room temperatures in which the temperature was electronically recorded to ensure no unusual spikes occurred in the normal temperature. After the predetermined test duration, the Teflon vessel was removed from the oven, opened, and the solid SPC sample carefully removed. The

[1] Registered Trademark, Du Pont de Nemours, Wilmington, Delaware.

Table 4.1. Test Conditions for the Static MCC-1 Type Tests

Test Temperature(s)	90°, 70°, 40°, and 20°C
Aqueous Systems	Deionized water 0.0107m LiOH buffer
Sample Type	Monoliths
Sample Size	~ 1 gram
Sample Dimensions	~ 6.4 x 6.4 x 12.6 mm
Sample Surface Area	~ 400 mm^2
Surface Area-to-Volume Ratio	10 m^{-1}
Sample Density	~ 1.93 g/cm^3
Sampling Times	1, 7, 14, 21, 28, 56, TBD* days

* TBD: To be determined.

sample was then placed in a 40°C oven to dry and then archived for further solids analysis (if necessary). A measurement of the solution pH (cooled to room temperature) was also taken and recorded. An aliquot (~10 ml) from the aqueous solution was removed from the vessel for ICP/AES analysis for total sulfur content, reported in parts per million. The remaining aqueous solution was archived under room temperature conditions. Sampling times were typically 1, 7, 14, 21, 28, and 56 days. To-be-determined (TBD) tests were run for a later sampling time, as warranted by the initial test results. Each test condition was run in duplicate to ensure reproducibility. The labelling system used in the program was as follows:

SPC-X-YZ-#

where X is the temperature,
Y is an estimate of the initial aqueous solution pH,
Z is the sampling day, and
is the number of the duplicate tests (either 1 or 2).

Table 4.2. Test Matrix of Static Tests

Temperature	Aqueous System	pH 20°C	Identification
90°C	0.1265m LiOH*	12.61	SPC-90-12Z-#
	0.0107m LiOH	11.82	SPC-90-10Z-X
	DIW	6.11	SPC-90-7Z-#
70°C	0.0107m LiOH	11.65	SPC-70-10Z-#
	DIW	6.18	SPC-70-DZ-#
40°C	0.0107m LiOH	11.65	SPC-40-10Z-#
	DIW	5.81	SPC-40-DZ-#
20°C	0.0107m LiOH	11.65	SPC-20-10Z-#
	DIW	5.81	SPC-20-DZ-#

* The 0.1265m LiOH buffer was used in a scoping tests only.

4.1.2 Flow-Through Tests

A schematic of the single-pass flow-through (SPFT) test equipment is shown in Figure 4.1. The test equipment uses 13 holding reservoirs to evaluate the dissolution kinetics of various waste-form compositions under different aqueous environments. Twelve of the 13 holding reservoirs are 2000-ml vessels in which a range of pH buffer solutions can be placed to evaluate the effect of pH on a single waste form composition. A single large holding reservoir (25-liter carboy) processes a constant pH solution to twelve independent cells/lines, from which the dissolution kinetics of 12 varying waste-form compositions can be evaluated at a constant pH. During testing, nitrogen was used continually as a cover gas for the buffer solution-holding reservoirs to eliminate the potential effect of CO_2 on pH.

Once the test conditions (buffers, flow rates, temperature, etc.) were defined and verified through pre-test procedures, a predetermined quantity of SPC monolith was added to the solution in each preheated, two-port sample vessel. The vessels were sealed and buffer solution flow began by activation of the pump(s) and the nitrogen source. The buffer composition was chosen to minimize overlapping elements associated with the buffer solution and the SPC and/or LLW glass. Nitrogen flowed into the three-port vessels and aided in the transfer of buffer solution to and through the two-port sample vessels into the sample-collection vessels. The test conditions were meant to keep the leachant undersaturated with respect to precipitation of secondary phases, but above elemental detection limits of the analytical equipment to be used. Flow rates were monitored and samples were collected as specified on the pre-test data sheets. Testing was done in accordance with "GDL-FTP: Single-Pass Flow-Through Test Procedure, Rev. 0."

The dynamic SPFT test used controlled chemical conditions, including pH and temperature, to obtain a measure of the forward rate of dissolution. The results of these tests (elemental concentrations from leachant samples taken as a function of time) provided supplementary information necessary to model the SPC dissolution kinetics. SPC monoliths were tested under various aqueous environments and four temperatures (20°, 40°, 70°, and 90°C).

Two suites of flow-through tests were performed, pH dependence on dissolution rate and temperature dependence on dissolution rate.

In the pH tests, the pH dependence on dissolution rate was evaluated. A series of tests was run at 40°C using seven different buffer solutions ranging in pH from 6 to 12. Table 4.3 shows the seven buffer solution compositions.

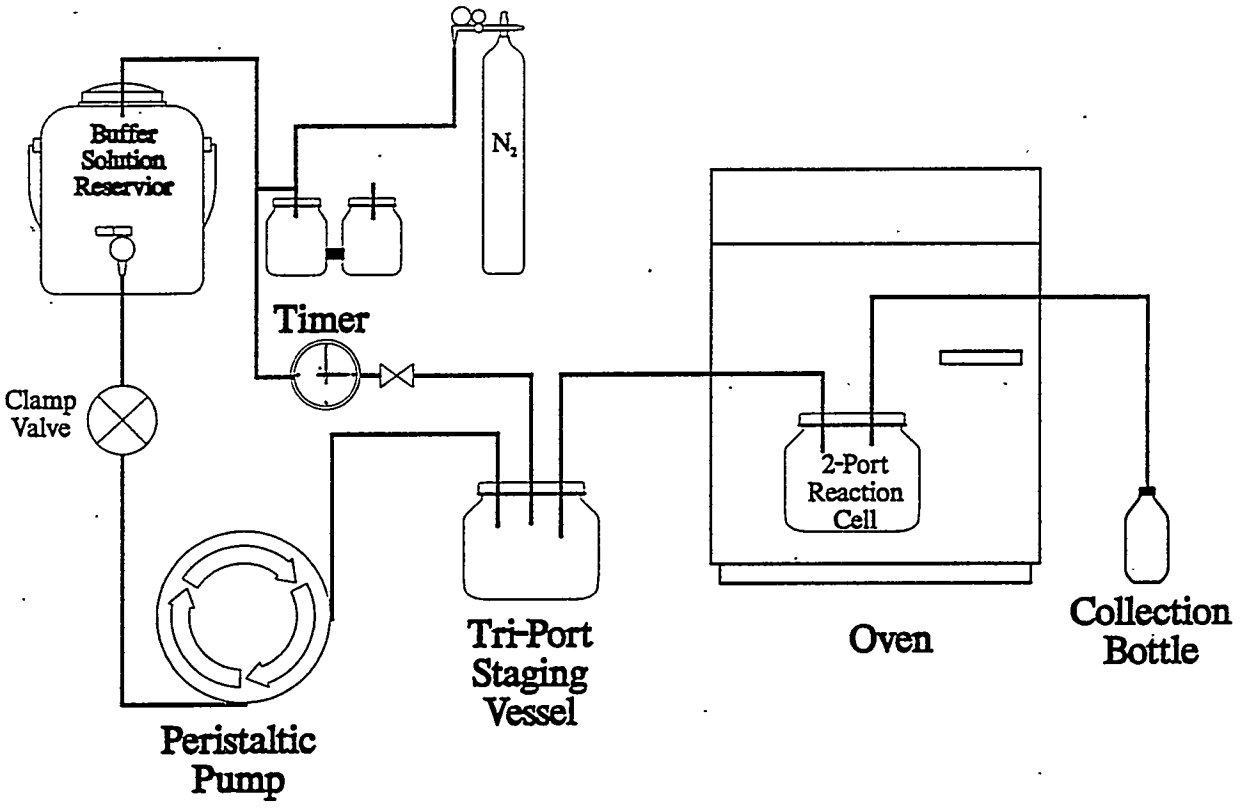

Figure 4.1. Schematic of Single-Pass Flow-Through Apparatus

Table 4.3. Compositions of Seven Buffer Solutions Used in the pH Dependence Tests

Buffer	Composition	I	pH (20°C)	pH (90°C)
1	0.005m KHphth + 0.0041m LiOH	0.0131	5.92	6.41
2	0.005m H_3BO_3 + 0.0003m LiOH	0.0003	8.09	7.74
3	0.005m H_3BO_3 + 0.0020m LiOH	0.0019	9.07	8.68
4	0.005m H_3BO_3 + 0.0044m LiOH	0.0044	10.02	9.30
5	0.005m LiCL + 0.0050m LiOH	0.0104	11.05	9.98
6	0.04M CAPS + 0.03 M NaOH			
7	0.005m LiCl + 0.0107m LiOH	0.0153	11.95	10.39

Table 4.4 identifies the test conditions which were verified through pre-test procedures. A SPC monolith (approximately 1 gram) was used in each sample vessel. At 40°C, a nominal flow rate of 30 ml/day was used. These rates were based on previous testing experiences (e.g., test temperature, relative sample durability, and buffer pH). The test conditions were designed to keep the leachant undersaturated with respect to precipitation of secondary phases, but above elemental detection limits of the analytical equipment (ICP-AES) used. Flow rates were monitored daily to ensure that proper flow rates were maintained (±10%) for the duration of the test. If needed, flow rates were adjusted by adjusting the pump speed setting.

Samples were collected on days 1, 3, 5, and 7 (at a minimum). To ensure steady-state release concentrations were reached at the lower temperatures, sampling times were extended to 21 days for the 40°C tests. Fifteen milliliters of effluent were removed from each collection vessel and placed into separate, pre-labelled, Teflon scintillation vials. The samples were then analyzed for pH and ICP-AES measurements for total sulfur content (ppm). Before ICP/AES analysis, the samples were treated with NH_3 and H_2O_2, followed by an acidification process using 2% HNO_3.

To determine temperature dependence on dissolution rate, SPC monoliths were tested using the SPFT at temperatures of 40°, 70°, and 90°C. A 0.0107m LiOH buffer solution was used to provide continuity with the existing LLW testing program. The sample type, size, dimension, surface area,

Table 4.4. Test Conditions Established During Pre-Test Set-Up

Test Temperature(s)	90°C, 70°C, and 40°C
Buffers Used	7
Nominal Flow Rate	100, 65, and 30 ml/day (dependent on temperature)
Sample Size	1 gram
Sample Type	Monolith
Sample Surface Area	~ 400 mm^2
Cover Gas	Nitrogen
Gas Flow Timer Interval	4 times/day
Sampling Times	Minimum of 1, 3, 5, and 7 days

Table 4.5. Composition of Buffer Solutions Used for Temperature-Dependence Testing

Buffer	Composition	I (Ionic Strength)	pH (20°C)*	pH (40°C)	pH (70°C)	pH (90°C)
#1	0.005m LiCl + 0.0107m LiOH	0.0153	11.95	11.50	10.78	10.39

* Measured at room temperature (nominally 20°C). Higher temperature pH values were calculated using EQ3NR codes.

and density are consistent with those listed in Table 4.4 (static tests). The LiOH buffer solution composition used is given in Table 4.5, along with the calculated solution pH and ionic strength value (using EQ3NR codes). Solution pHs at 20°C were experimentally measured values, whereas the pH values at higher temperatures were calculated.

4.2 Results

4.2.1 Preliminary/Scoping Static Tests

A scoping test was performed to establish a baseline from which a final test matrix could be established. This preliminary/scoping static test was performed at 90°C using a 0.1265m LiOH

Table 4.6. Results of SPC Scoping Test at 90°C

Sample	Sulfur (ppm)	pH (out)	% Weight Change
SPC-90-121-1	-	11.83	10.97
SPC-90-121-2	6300	11.81	11.21
SPC-90-127-1	4750	9.01	26.49
SPC-90-127-2	4970	8.85	28.00
SPC-90-1214-1	4000	3.87	22.68
SPC-90-1214-2	4770	8.85	24.95
SPC-122	20,200 (3490)	3.68	23.00
SPC-1228	21,000 (4230)	8.57	28.96
SPC-1256	2870	3.41	23.01
SPC-1256	3280	3.63	24.46

buffer solution. The buffer solution had a pH of 12.61 (measured at room temperature) and a calculated pH of 11.33 at 90°C. Aliquots were sampled and submitted for ICP analysis for total sulfur content (ppm). Table 4.6 shows the results of this scoping test.

The SPC-90-1228 duplicate samples had an extremely high release of sulfur (20,200 and 21,000 ppm, respectively). In fact, using a mass balance calculation, the values reported suggest that almost 50 to 60% of the sample should have been corroded. By visual inspection of the solid sample retrieved from the test, this was not the case. The weight loss calculation from the solid samples (23% and 28.96%), although high, did not account for the excessively high sulfur values from ICP. Archived samples were resubmitted for ICP analysis; the results are reported in parentheses (3490 and 4230 ppm, respectively).

It should be noted that the SPC dissolution into the LiOH buffer solution occurred almost instantaneously. After one day under these harsh conditions, the SPC lost on average approximately 10% of its initial weight. The release of sulfur into the system resulted in continual decrease in pH. From an initial pH of 12.61 (buffer solution alone), the solution pH dropped continually to a value of approximately 3.5 after 56 days. It should also be noted that due to the use of a LiOH buffer, the buffer capacity of the system had to be overcome before the pH would decrease.

The results of this test indicate that the testing conditions were excessive in the sense that the reactions occurred at an extremely rapid rate. These conditions may never occur in the disposal facility and were used only as preliminary scoping tests. From the results of this test, a test matrix was established.

To slow the dissolution process relative to the scoping test, the matrix (see Table 4.2) included tests at lower temperatures (90°, 70°, 40°, and 20°C) and lower aqueous pH conditions of 11.65 (0.0107m LiOH buffer) and approximately 6.10 (DIW, dependent upon CO_2). The results of these tests are discussed below.

4.2.2 Static Tests Results

The static tests were performed at 90°, 70°, 40°, and 20°C under two aqueous solutions (0.0107m LiOH buffer and DIW). These tests conditions were used for several purposes, as follows: (1) to slow the reaction or dissolution of the SPC monoliths to obtain reliable data based on the scoping tests results; (2) to simulate disposal facility temperatures; (3) to obtain temperature dependence on the reaction kinetics; and (4) to provide an environment consistent with the current LLW glass testing program. The results of the static test matrices are discussed in order of decreasing temperatures.

The results of the 90°C DIW tests are shown in Table 4.7. There are two columns of ICP results, acid and base/acid. The acid samples were acidified with 2% HNO_3 before performing the ICP analysis whereas the base/acid samples were treated with NH_3 and H_2O_2 and then acidified with 2% HNO_3 before ICP analysis. The difference between the two pretreatments was that the base/acid converted all of the sulfide, sulfite, and thiosulfate into sulfate, whereas the acid-only treatment converted ionic sulfur species to a mixture of metastable and potentially volatile compounds. Although the results were fairly consistent from this test matrix, the acid pretreatment process has been
observed to provide nonreproducible data. Therefore, all SPC samples were treated with the base/acid before ICP analysis; the base/acid values reported will be discussed here.

The lower total sulfur values (ppm) as compared to the scoping tests suggested that the reaction rate slowed. However, there was a continual increase in total sulfur released to the aqueous system with the associated continual decrease in pH (generating sulfuric acid). Figure 4.2 shows the data.

The dissolution of the SPC monoliths was strongly dependent on the pH of the aqueous solution and was seen by the 90°C, 0.0107m LiOH buffer solution results (see Table 4.8 and Figure 4.3). The dissolution rates in DIW were a factor of 100 lower than in 0.0107m LiOH for 1-, 7-, and 14-day tests, as shown in Figure 4.4. The increase in pH increased the rate of SPC dissolution due to the associated reactions between sulfur-related acids ($H_2S_2O_3$, H_2SO_4, etc.) and LiOH. The sulfur-acids released from SPC drove the pH down to an equilibrium value of approximately 3.5. The starting pH of 11.82 decreased to approximately 9.0 in just one day and reached a constant value of approximately 3.5 after only 28 days at 90°C.

In addition to the weight changes observed in these samples, the color and surface morphology were also observed to change, as shown in Figure 4.5. The color changed from the dark red of the 1-day sample (SPC-101-1) to the light brown color of the 56-day sample (SPC-1056-1). The 56-day sample was also analyzed by XRD and it showed a single alpha-sulfur phase.

Table 4.7. Results of the SPC Static Test at 90°C and Deionized Water

Sample Identification	S (ppm) acid	S (ppm) base/acid	pH (out)	% Weight Change
SPC-90-71-1	3.3	1.6	4.52	6.01
SPC-90-71-2	3.0	1.8	4.53	6.97
SPC-90-77-1	2.6	3.4	3.89	1.18
SPC-90-77-2	3.0	3.4	3.93	1.04
SPC-90-714-1	5.2	5.4	3.61	0.03
SPC-90-714-2	4.5	4.8	3.64	-0.02
SPC-90-728-1	8.0	8.0	3.43	-0.13
SPC-90-728-2	7.9	8.0	3.41	-0.02
SPC-90-756-1	12.7	13.2	3.21	0.25
SPC-90-756-2	13.2	13.8	3.21	0.20

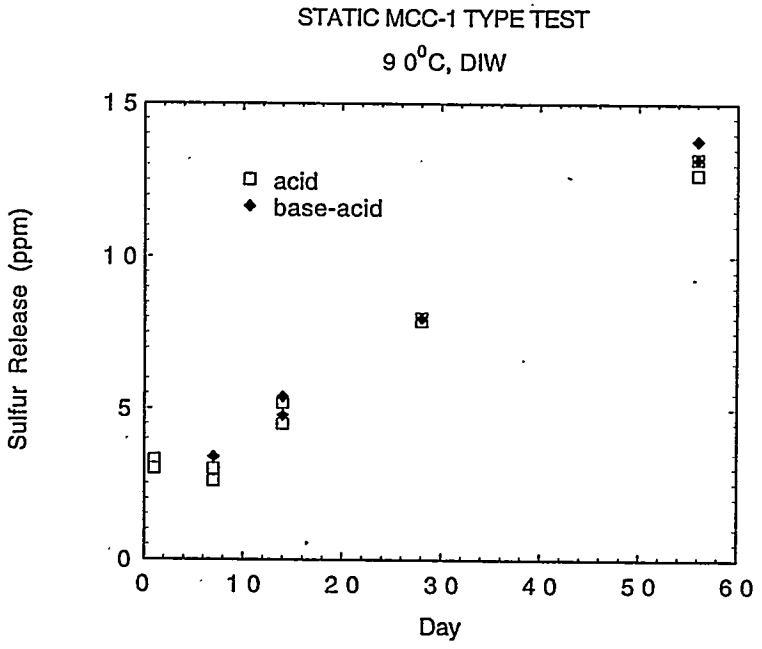

Figure 4.2. Results of the 90°C, Deionized Water Static Tests. Both acid and base/acid results are plotted.

Table 4.8. Results of the SPC Static Test at 90°C and 0.0107m LiOH

Sample Identification	S (ppm) acid	S (ppm) base/acid	pH (out)	% Weight Change
SPC-101-1	335	340	8.65	1.65
SPC-101-2	325	340	9.55	1.70
SPC-107-1	340	350	3.86	1.50
SPC-107-2	340	360	3.87	1.68
SPC-1014-1	350	350	3.63	1.56
SPC-1014-2	350	350	3.70	1.43
SPC-1028-1	556	-	3.46	1.53
SPC-1028-2	547	-	3.38	1.52
SPC-1056-1	667	-	3.30	1.52
SPC-1056-2	624	-	3.28	1.59

Both ICP pretreatment (acid and base/acid) values are reported in Figure 4.3. It can be seen that there is very little difference (within analytical error) through day 14 on the two types of analytical methods. Samples from days 28 and 56 were not rerun using the base/acid technique due to insufficient archived sample being available.

As expected, the reaction rate is dependent on the temperature (i.e., as temperature decreases the dissolution rate as measured by the release of sulfur into solution also decreases). Table 4.7 shows the measured release rates of sulfur in solution as a function of time for the 70°C static tests in DIW.

As in all other static tests, as the test duration increases, the total sulfur content in solution increases and the pH of the solution decreases. The total sulfur concentration in solution appears to dramatically lower (almost an order of magnitude) as compared to the 90°C test results. This may indicate that the SPC samples run at 90°C were close to, if not exceeding, the transition temperature of the polymer particularly for the 0.1265m LiOH buffer solution (scoping test) (see Figures 3.2-3.4). This may suggest that the stability of SPC in an aqueous environment depends on both test temperature and pH of the solution.

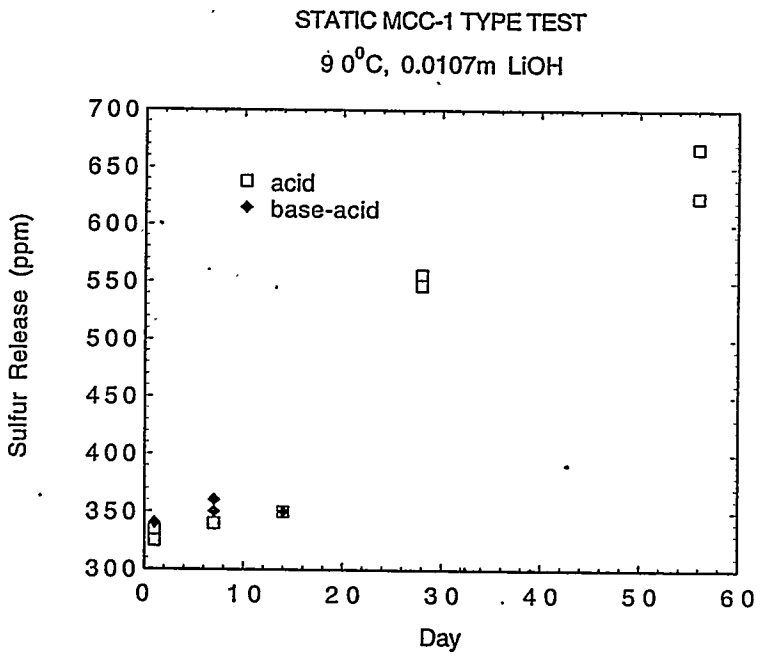

Figure 4.3. SPC MCC-1 Tests at 90°C and in 0.0107m LiOH Buffer Solution. Acid versus base/acid results show no difference.

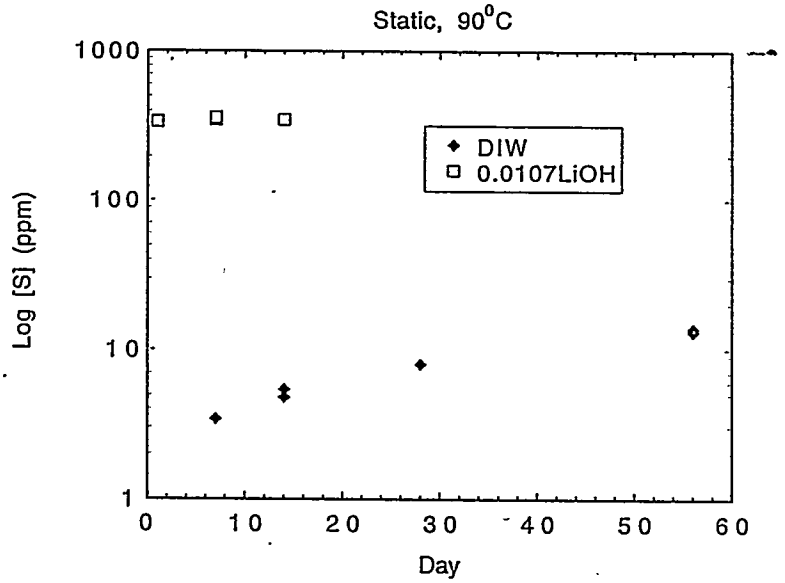

Figure 4.4. SPC Static 90°C Tests: 0.0107m LiOH Versus the DIW Buffer Solutions

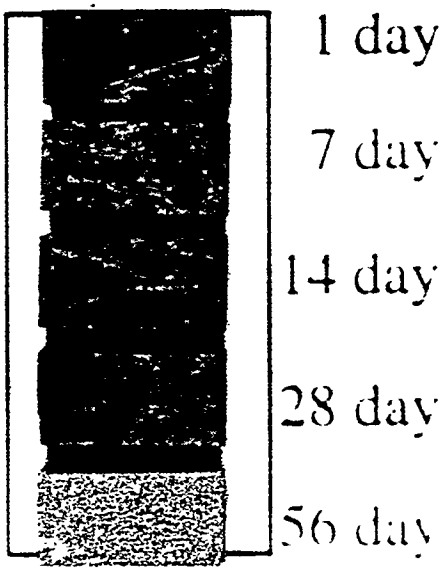

Figure 4.5. Optical Micrograph Showing the Color and Morphology Change After MCC-1 Tests of SPC in 0.0107m LiOH at 90°C. These are samples of SPC-101-1 to SPC-1056-1.

Table 4.9. Results of the SPC Static Test at 70°C and Deionized Water

Sample	S (ppm) Run #1	Run #2	pH (out)	% Weight Change
SPC-70-D1-1	(X)	(0.27)	5.77	0.0005
SPC-70-D1-2	0.45	(0.27)	5.92	0.0005
SPC-70-D7-1	0.81	(0.65)	4.99	0.0000
SPC-70-D7-2	0.55	(0.70)	4.65	0.0003
SPC-70-D14-1	0.92	(0.85)	4.47	-0.0002
SPC-70-D14-2	0.65	(0.55)	4.59	0.0001
SPC-70-D21-1	1.2	(1.1)	4.56	0.0001
SPC-70-D21-2	1.1	(1.1)	4.27	0.0000
SPC-70-D28-1	1.0	(0.93)	4.31	0.0002
SPC-70-D28-2	1.1	(1.0)	4.22	0.0003
SPC-70-D56-1	1.3		4.13	0.0005
SPC-70-D56-2	1.4		4.14	0.0004
SPC-70-DTBD-1	In Progress		-	-
SPC-70-DTBD-2	In Progress		-	-

Although deionized water has no buffering capacity, the system pH did not appear to drop as quickly during the initial 28 days, compared to the 90°C test in DIW (which dropped to the equilibrium value of 3.5 within the initial 28 days). This suggests that the reaction rate at 70°C was much lower, which was consistent with the observation that there was very little weight change from the solid samples.

All ICP values reported used the base/acid pretreatment technique. The two values in Table 4.9, under the base/acid column, are values from different ICP analyses (Run 1 and Run 2) of the sample which had been archived. All the four data points for each sample (duplicates of Run 1 and duplicates of Run 2) are shown in Figure 4.6, which shows the same trend of SPC corrosion.

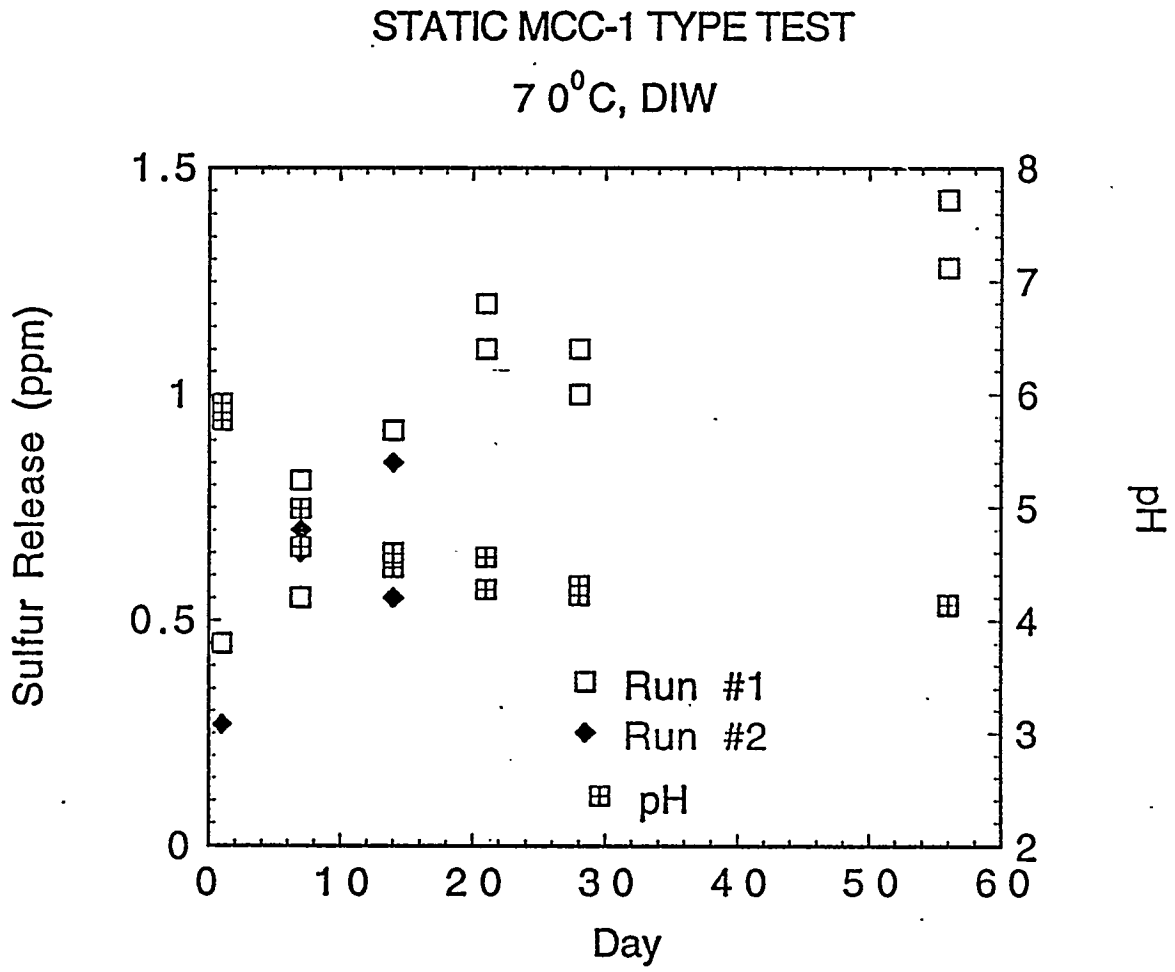

Figure 4.6. SPC Static Tests at 70°C in Deionized Water
Run #1 and Run #2 are different ICP analyses on the same sample.

The ICP results of the 70°C, 0.0107m LiOH buffer solution are shown in Table 4.10 and Figure 4.7. As expected, when the 70°C results were compared with the 90°C results for the 0.0107m LiOH buffer, lower total sulfur contents were found in the 70°C tests (for a given time period). As the buffering capacity of the LiOH buffer was exceeded, the pH of the solution began to decrease (dropping from an initial pH of 11.65 to about 7 after 56 days). There was an increased weight loss through the 28-day tests, which was consistent with the higher sulfur contents (compared to the DIW results at 70°C). If compared to the 90°C LiOH buffer results, the weight loss was significantly lower for the 70°C tests.

All ICP values reported are using the base/acid pretreatment technique. The two base/acid values in Table 4.9 and Figure 4.6 are values from different "ICP analyses" of the sample which had been archived. The TBD tests are still in progress. The comparison of corrosion rates between tests in DIW and in 0.0107m LiOH at 70°C is shown in Figure 4.8 and the difference was between 100 to 300 times from day one to day 56. This difference was much larger than the difference caused by temperature changes between tests at 70° and 90°C. The difference in sulfur release between 70° and 90°C was from 7 to 1.3 times for tests in 0.0107m LiOH, and from 4 to 10 times for tests in deionized water from day one to day 56. The sulfur release difference caused by temperature for tests in 0.0107m LiOH decreased with time while for the tests in DIW the difference increased with time.

Table 4.10. Results of the SPC Static Test at 70°C and 0.0107m LiOH

Sample	S (ppm) base/acid	pH (out)	% Weight Change
SPC-70-101-1	32 (32.7)	11.52	0.0017
SPC-70-101-2	26 (26.9)	11.53	0.0015
SPC-70-107-1	180 (190)	11.15	0.0083
SPC-70-107-2	160 (160)	11.25	0.0075
SPC-70-1014-1	260 (270)	10.28	0.0111
SPC-70-1014-2	260 (265)	10.38	0.0111
SPC-70-1021-1	290 (291)	9.23	0.0117
SPC-70-1021-2	290 (299)	8.98	0.0121
SPC-70-1028-1	310 (314)	8.25	0.0122
SPC-70-1028-2	300 (301)	7.97	0.0125
SPC-70-1056-1	340	6.86	-0.0138
SPC-70-1056-2	350	7.72	-0.0138
SPC-70-10TBD-1	In Progress	-	-
SPC-70-10TBD-2	In Progress	-	-

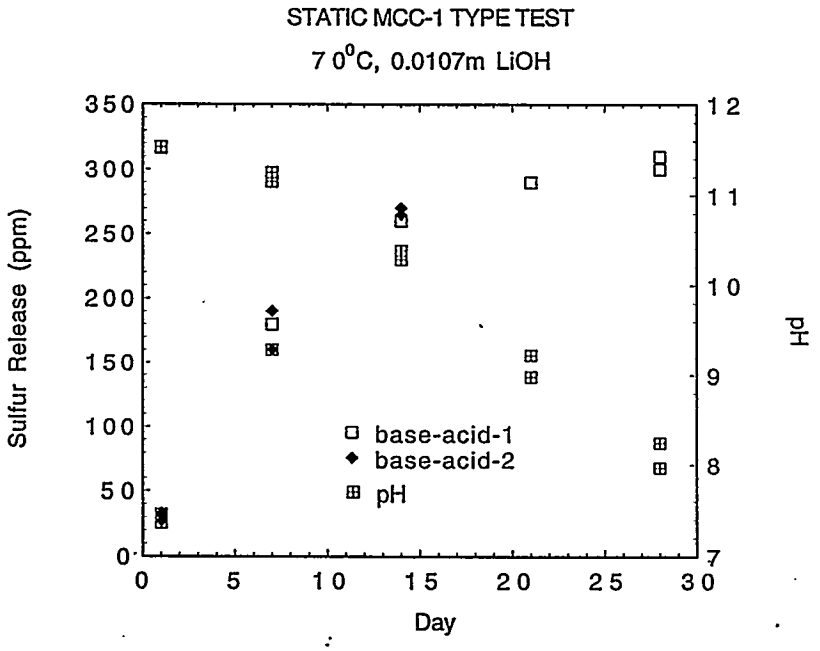

Figure 4.7. SPC Static Tests at 70°C and 0.0107m LiOH Buffer Solution. Run 1 and Run 2 are two different ICP analyses.

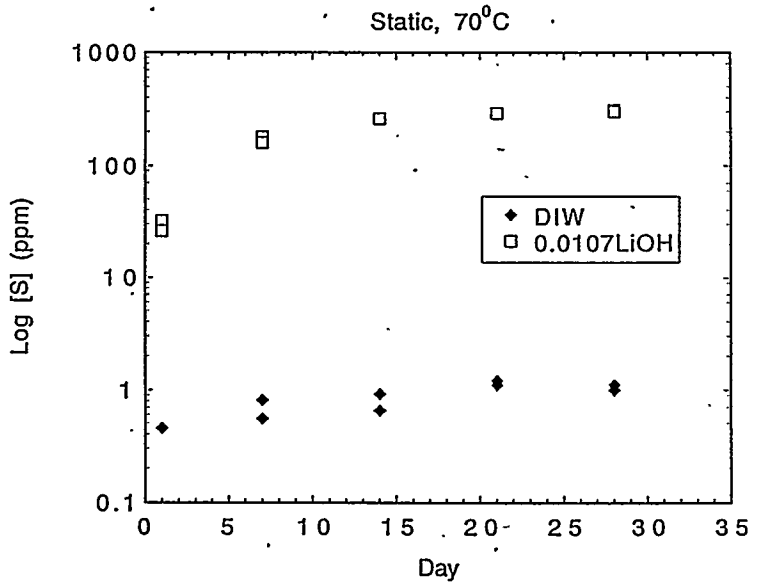

Figure 4.8. SPC Static Tests at 70°C in 0.0107m LiOH Buffer Solution and in Deionized Water.

As the temperature was reduced further, the expected decrease in sulfur release into solution was observed. The total sulfur contents in solution were well below the results for both 90°C and 70°C, as expected (Table 4.11). This was indicative of the temperature dependence on the reaction rate for the SPC monoliths. There was very little weight change through 56 days at 40°C, again consistent with the extremely low total sulfur values observed in DIW. As for the pH, the trend of decreasing pH values as a function of time remained; however, because of the lower temperature, the production of sulfur-related acids (reaction rates) appeared to be much slower. The pH of the system had yet to reach the equilibrium value of 3.5 after 56 days, even with no buffering capacity to exceed (i.e., DIW).

Table 4.11. Results of the SPC Static Test at 40°C and Deionized Water

Sample	S (ppm) base/acid	pH (out)	% Weight Change
SPC-40-D1-1	0.15 (0.23)	5.69	0.0001
SPC-40-D1-2	0.14 (0.17)	5.76	0.0005
SPC-40-D7-1	-	5.11	0.0002
SPC-40-D7-2	0.27 (0.32)	5.08	0.0003
SPC-40-D14-1	0.47 (0.32)	5.01	0.0001
SPC-40-D14-2	- (0.32)	4.67	0.0003
SPC-40-D21-1	0.44 (0.37)	4.60	0.0003
SPC-40-D21-2	0.32 (0.26)	4.77	-0.0001
SPC-40-D28-1	0.52 (0.39)	4.96	-0.0001
SPC-40-D28-2	0.44 (0.38)	5.50	0.0001
SPC-40-D56-1	0.72 (0.82)	4.44	0.000
SPC-40-D56-2	0.56 (0.53)	4.34	0.0003
SPC-40-DTBD-1	In Progress	-	-
SPC-40-DTBD-2	In Progress	-	-

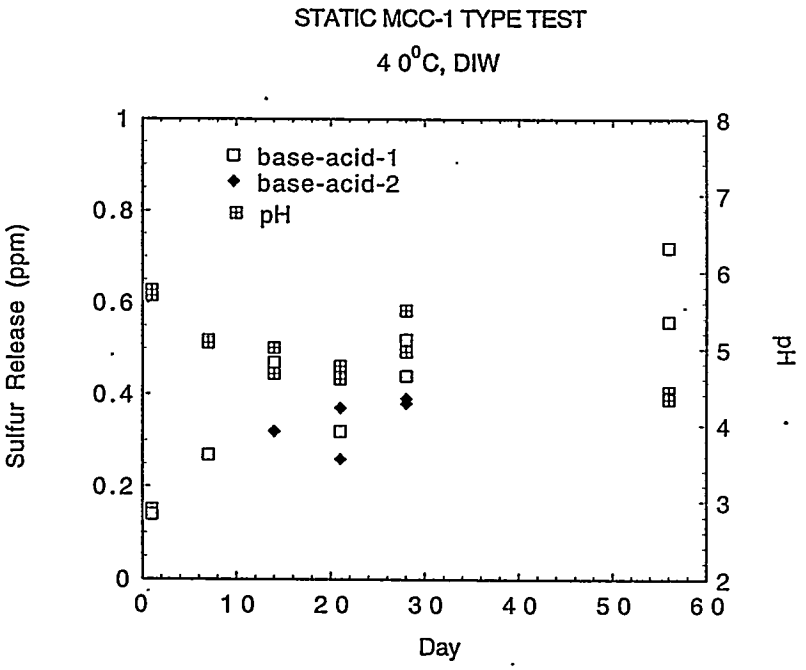

Figure 4.9. SPC Static Tests at 40°C and Deionized Water. Run 1 and Run 2 are two different ICP analyses.

Table 4.12. Results of the SPC Static Test at 40°C and 0.0107m LiOH

Sample	S (ppm) base/acid	pH (out)	% Weight Change
SPC-40-101-1	0.91 (0.76)	11.67	0.0003
SPC-40-101-2	0.92 (0.79)	11.68	0.0004
SPC-40-107-1	3.6 (3.6)	11.58	0.0002
SPC-40-107-2	3.6 (3.5)	11.56	0.0002
SPC-40-1014-1	7.3 (7.0)	11.56	0.0007
SPC-40-1014-2	8.1 (7.6)	11.56	0.0002
SPC-40-1021-1	11.5 (11.6)	11.62	0.0002
SPC-40-1021-2	11.2 (11.1)	11.63	0.0003
SPC-40-1028-1	15.6 (15.1)	11.57	0.0030
SPC-40-1028-2	14.9 (14.6)	11.57	-0.0001
SPC-40-1056-1	32.8	11.50	-0.0030
SPC-40-1056-2	33.1	11.52	-0.0024
SPC-40-10TBD-1	In Progress	-	-
SPC-40-10TBD-2	In Progress	-	-

The SPC corrosion rate and weight loss in 0.0107m LiOH at 40°C are shown in Table 4.12; the sulfur release data are also plotted in Figure 4.9. The sulfur concentration in the leachate increased linearly with time, but the released acids could not overcome the buffer capacity so that the leachate pH was essentially constant. The weight loss was also insignificant. The difference between the corrosion rate in 0.0107m LiOH and DIW was at a factor of 6 at the 1-day test and gradually increased to a factor of 55 at 56 days (Tables 4.11, 4.12 and Figure 4.10); 0.0107m LiOH was more corrosive over time, in comparison with DIW. The corrosion rate in 0.0107m LiOH decreased by about 40 times at the 1-day test and by 10 times at 56 days, when the test temperature decreased from 70° to 40°C. The temperature effects decreased with time. The corrosion rate difference in DIW was maintained at about 2 times throughout 1 to 56 days; i.e., the temperature effects did not change with time.

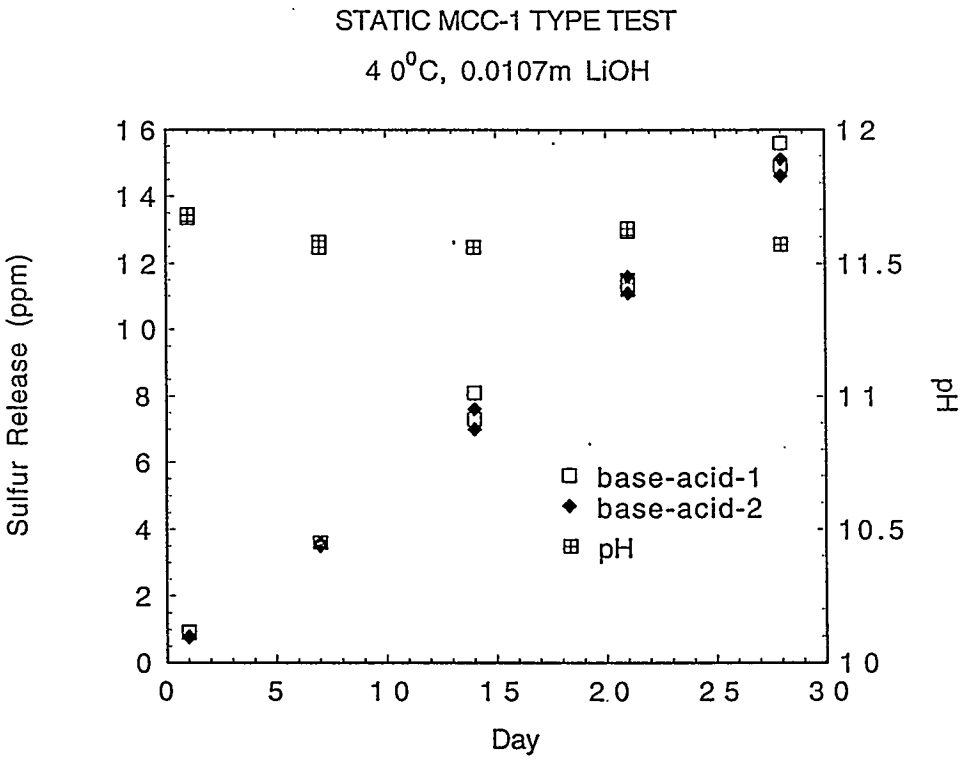

Figure 4.10. SPC Static Tests at 40°C and in 0.0107m LiOH Buffer Solution. Run 1 and Run 2 are two different ICP analyses.

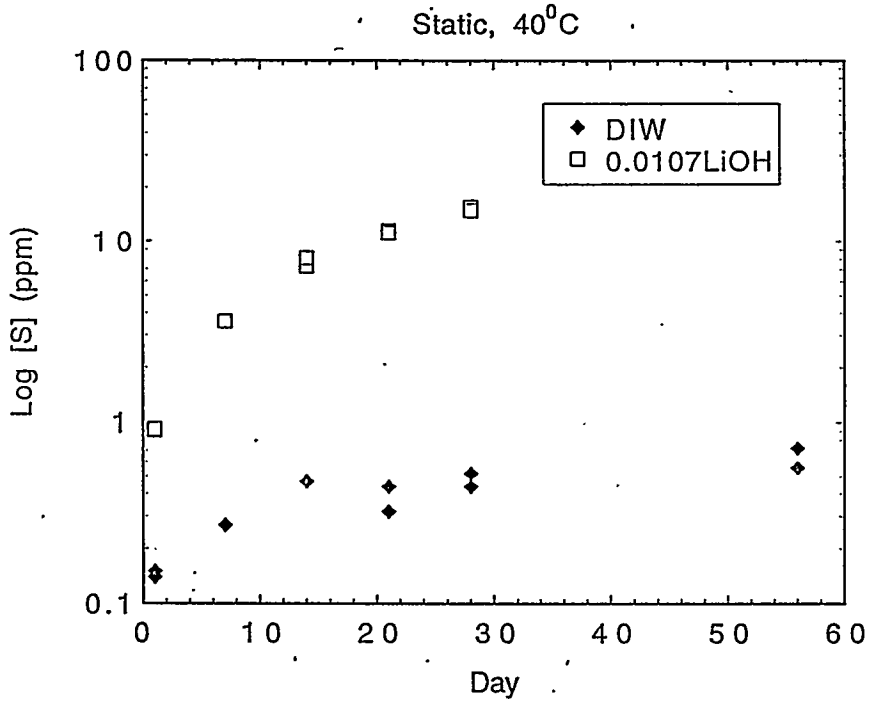

Figure 4.11. SPC Static 40°C Tests: 0.0107m LiOH versus the Deionized Water Buffer Solutions

Sulfur polymer cement was also leached at room temperature in both DIW and in 0.0107m LiOH buffer solution. The results for the tests in DIW are shown in Table 4.13 and Figure 4.15. The pH behavior appeared to have increased initially from about pH 5.6 at the 1-day test to about 6.5 in 14-day tests; then the pH backed down to the initial pH of about 5.6. The measurements had large variations, probably due to the low ionic strength of the solution, and because the leachate could be considered essentially at a constant pH..

These pH results were consistent with sulfur release results; i.e., the sulfur concentration was constant throughout the 1 to 56 days and showed no weight change during the tests, as shown in Table 4.13. This means SPC is very stable and insoluble in DIW at room temperature. The longer-term test is still in progress, and may provide valuable information to verify this observation.

The results for the test in LiOH buffers are shown in Table 4.14 and Figure 4.12. The sulfur concentration showed a linear increase with time throughout the 56-day test, while the solution pH was buffered at the same pH. The total weight loss during the test was insignificant. Figure 4.13 shows the relative dissolution behavior of SPC in 0.0107m LiOH and in DIW at room temperature. The difference between the corrosion rate in 0.0107m LiOH and DIW was at a factor of 2 at the 1-day test and gradually increased to a factor of 23 at 56 days (Tables 4.13, 4.14, and Figure 4.13); i.e., the longer the duration, the more corrosive 0.0107m LiOH was in comparison with DIW. The corrosion rate in 0.0107m LiOH decreased by about 2 times at the 1-day test to about 6 times at 56 days, when test temperature decreased from 40° to 20°C. The temperature effects were constant from 7 to 56 days. The corrosion rate difference between 40° and 20°C tests in DIW was insignificant during the early test periods and gradually increased to a factor of two at 56 days; i.e., the temperature effects were very small and increased slowly with time.

Table 4.13. Results of the SPC Static Test at 20°C and Deionized Water

Sample	S (ppm) base/acid	pH (out)	% Weight Change
SPC-20-D1-1	0.12	5.63	0.0008
SPC-20-D1-2	0.27	5.60	0.0001
SPC-20-D7-1	0.24	5.51	0.0006
SPC-20-D7-2	0.27	5.43	0.0002
SPC-20-D14-1	0.30	6.71	0.0006
SPC-20-D14-2	0.37	6.31	0.0006
SPC-20-D21-1	-	5.35	0.0003
SPC-20-D21-2	0.23	5.44	0.0003
SPC-20-D28-1	0.21	6.87	-0.0001
SPC-20-D28-2	0.25	5.55	0.00
SPC-20-D56-1	0.25	5.86	0.0004
SPC-20-D56-2	0.25	5.37	0.00
SPC-20-DTBD-1	In Progress	-	-
SPC-20-DTBD-2	In Progress	-	-

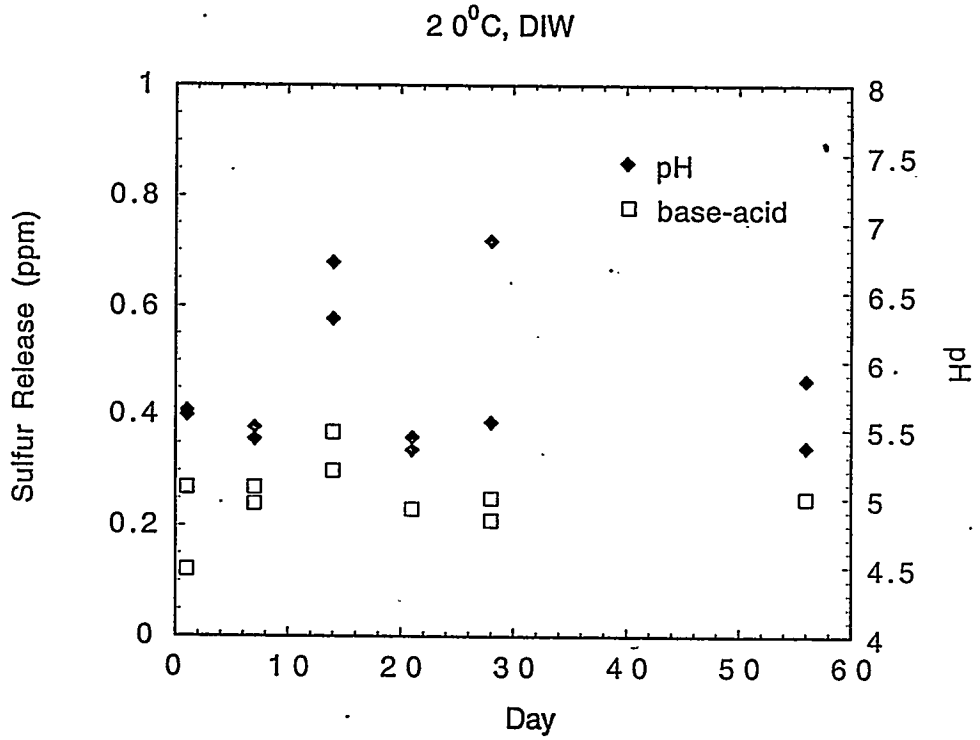

Figure 4.12. SPC Static Tests at 20°C in Deionized Water

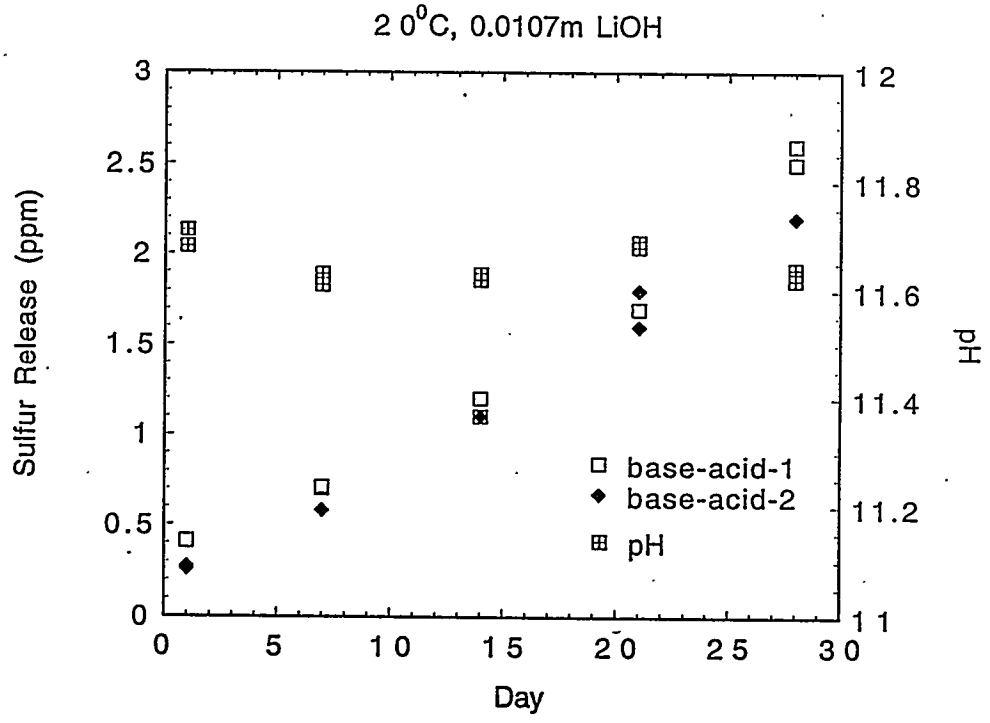

Figure 4.13. SPC Static Tests at 20°C in 0.0107m LiOH Buffer Solution. Run 1 and Run 2 are two different ICP burns.

Table 4.14. Results of the SPC Static Test at 20°C and 0.0107m LiOH

Sample	S (ppm) base/acid	pH (out)	% Weight Change
SPC-20-101-1	0.41 (0.27)	11.71	0.0003
SPC-20-101-2	- (0.26)	11.68	0.0004
SPC-20-107-1	0.70 (0.58)	11.63	0.0002
SPC-20-107-2	0.71 (0.58)	11.61	0.0004
SPC-20-1014-1	1.1 (1.1)	11.63	-0.0001
SPC-20-1014-2	1.2 (1.1)	11.62	-0.0009
SPC-20-1021-1	1.7 (1.8)	11.69	-0.0009
SPC-20-1021-2	1.7 (1.6)	11.68	-0.0003
SPC-20-1028-1	2.6 (2.2)	11.64	0.0030
SPC-20-1028-2	2.5 (2.2)	11.62	-0.0001
SPC-20-1056-1	5.8	11.57	-0.0012
SPC-20-1056-2	5.9	11.57	-0.0014
SPC-20-10TBD-1	In Progress	-	-
SPC-20-10TBD-2	In Progress	-	-

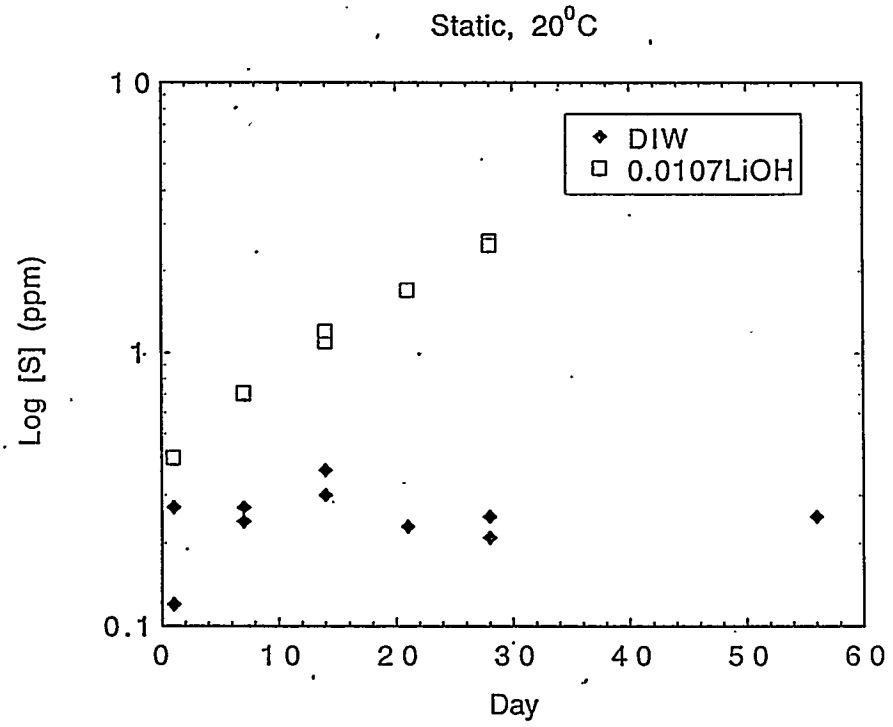

Figure 4.14. SPC Static 20°C Tests: 0.0107m LiOH versus the Deionized Water Buffer Solutions

4.2.3 Single-Pass Flow-Through Results

The single-pass flow-through tests were still in progress at the time of report preparation. Because the tests were terminated before completion, forward rates were unable to be calculated. **Preliminary data only are presented here.**

Table 4.15 shows the test conditions for the single-pass flow-through (SPFT) test performed on SPC at 90°C and pH 12. The sulfur concentration sampled at each of the 10-day tests showed decreasing concentration, which could indicate possible solution saturation or a solute effect on the SPC. This data may not useful in calculating the forward-reaction rate of SPC with water.

Table 4.16 shows the results for SPFT tests performed on SPC at 90°C and pH 10. The sulfur concentration is essentially constant over the 10-day test duration, which may generate a useful value of SPC forward-reaction rate at this test condition. This reaction rate is approximately 10-15 times lower than that at pH 12.

Table 4.17 shows the SPFT test results on SPC at 40°C in pH 12 buffer solutions. The sulfur release is an almost constant, possibly steady-state dissolution, under these test conditions. The reaction rate was approximately 100 times lower than the tests done at 90°C and pH 12. More data and analysis will be reported as the work progresses.

Table 4.15. Single-Pass Flow-Through Tests at 90°C and pH 12

Test Conditions:

Tests in duplicate
Test temperature: 90°C
0.0107m LiOH buffer solution
pH = 11.94 at RT (measured)
pH = 12.14 at 25°C (calculated)
pH = 10.56 at 90°C (calculated)
Flow rate: approximately 100 ml/day
Sample: monolithic
Status: 10-day test—terminated
Sample identification: SPC-X (FT-1)
Specific Surface Area: 401.13 mm^2
Mass: 0.9550 grams

Sample	Day	Sulfur (ppm)	pH (out)	Flow Rate (ml/day)
SPC-1 (FT-1)	1	405	11.21	101.26
SPC-2 (FT-1)	2	435	11.33	100.87
SPC-3 (FT-1)	3	340	11.59	99.99
SPC-4 (FT-1)	4	344	11.55	99.73
SPC-5 (FT-1)	5	288	11.68	100.94
SPC-6 (FT-1)	6	264	11.42	103.07
SPC-7 (FT-1)	7	277	11.42	99.81
SPC-10 (FT-1)	10	259	11.37	99.14

Table 4.16. Single-Pass Flow-Through Tests at 90°C and pH 9

Test Conditions:

Flow-through test temperature: 90°C
0.005m H_3BO_3 + 0.002m LiOH buffer solution
pH = 8.97 at RT (measured)
Flow rate: approximately 100 ml/day
Sample: monolithic
Status: 10-day test—terminated 6/18/95
Sample identification: SPC-FT-90-9-X
Specific Surface Area: 398.52 mm^2
Mass: 0.9544 grams

Analysis: Base/Acid—Samples treated with NH_3 and H_2O_2, then acidified to 2% HNO_3.

Sample	Day	Sulfur (ppm)	pH (out)	Flow Rate (ml/day)
SPC-FT-90-9-1	1	26.3	8.70	97.77
SPC-FT-90-9-2	2	46.3	8.60	96.35
SPC-FT-90-9-3	3	42.2	8.64	99.89
SPC-FT-90-9-4	4	38.3	8.68	99.28
SPC-FT-90-9-5	5	34.5	8.74	101.25
SPC-FT-90-9-6	6	32.3	8.73	100.88
SPC-FT-90-9-7	7	29.5	8.77	99.43
SPC-FT-90-9-8	8	25.6	8.54	101.28
SPC-FT-90-9-9	9	24.8	8.69	98.93
SPC-FT-90-9-10	10	24.1	8.74	101.68

Table 4.17. Single-Pass Flow-Through Tests at 40°C and pH 12

Test temperature: 40°C
0.0107m LiOH buffer solution
pH = 11.94 at RT (measured)
Flow rate: approximately 30 ml/day
Sample: monolithic
Specific Surface Area: 398.66 mm^2
Mass: 0.9504 grams

Sample	Day	Sulfur (ppm)	pH (out)	Flow Rate (ml/day)
Baseline	Pre-Test	(0.04)	11.92	
SPC-FT-40-1	1	3.27	11.89	30.92
SPC-FT-40-2	2	4.52	11.93	31.02
SPC-FT-40-3	3	5.40	11.91	30.89
SPC-FT-40-4	4	5.64	11.94	31.24
SPC-FT-40-5	5	4.97	11.93	31.00
SPC-FT-40-6	6	-	11.94	33.16
SPC-FT-40-7	7	5.61	11.82	32.23
SPC-FT-40-8	8	4.84	11.88	32.15
SPC-FT-40-9	9	4.99	11.89	34.03
SPC-FT-40-10	10	4.72	11.88	32.12
SPC-FT-40-11	11	4.94	11.88	32.70
SPC-FT-40-12	12	5.04	11.89	32.16
SPC-FT-40-13	13	4.69	11.91	30.00
SPC-FT-40-14	14	4.64	11.92	27.76

4.3 Summary

Results from the static MCC-type tests indicated that the reaction rate was highly dependent on both temperature and initial aqueous conditions. Higher temperature tests (i.e., 90°C) indicated that the SPC did not perform well under the conditions evaluated thus far. This could have been a result of the test temperature approaching or exceeding the "transition" temperature of the polymer. At room temperature, SPC was very stable and insoluble in water throughout the test duration in this project, where no pH change and/or weight loss were observed.

Based on the static tests, solution pH has the greatest effect on SPC corrosion. The corrosion rate in 0.0107m LiOH was at a factor of 2 higher at the 1-day test and at a factor of 23 higher at 56 days than those of tests in DIW at room temperature tests. These differences in sulfur releases at other temperatures are as follows: at a factor of 6 at 1-day and to a factor of 55 at 56-day tests in 40°C; at a factor of 100 to 300 from 1-day to 56-day in 70°C tests; and at a factor of 100 for 1-, 7-, and 14-day-tests at 90°C. The difference between the reaction rate in DIW and in alkali water increases with time and increases with temperature.

Based on the static tests, temperature affects SPC corrosion rate, but the effect is less than that of solution pH as discussed above. The temperature effects were different in DIW and in alkaline solutions:

- When test temperature changed from 40° to 20°C: The corrosion rate in 0.0107m LiOH decreased from 40° to 20°C by about 2 times in the 1-day test to about 6 times in 7 days, and the temperature effects were constant from 7 to 56 days. The corrosion rate difference in DIW was insignificant during the early test periods and gradually increased to a factor of two at 56 days; i.e., the temperature effects were very small and slowly increased with time.

- When test temperature changed from 70° to 40°C: The corrosion rate in 0.0107m LiOH decreased by about 40 times at the 1-day test and by 10 times at 56 days. The temperature effects decreased with time. The corrosion rate difference in DIW was maintained at about 2 times throughout of 1 to 56 days; i.e., the temperature effects did not change with time.

- When test temperature changed from 90° to 70°C: The SPC corrosion rate differed by 7 to 1.3 times for tests in 0.0107m LiOH, and by 4 to 10 times for tests in DIW from day one to day 56. The temperature difference for tests in 0.0107m LiOH decreased with time while the difference increased with time for the tests in DIW.

Activation energy calculated from the static tests may be misleading; too many variables were not under control (pH, oxygen fugacity, etc). Activation energy will be calculated from future data analysis of the single-pass flow-through tests.

Sulfur acids released from SPC drove down the pH to an equilibrium value of approximately 3.5. The starting pH of 11.82 decreased to approximately 9.0 in just one day and reached a constant value of approximately 3.5 after only 28 days at 90°C. However, the static tests at lower temperature or in DIW approached this pH much slower and no pH change was observed for tests at room temperature.

Results of the static MCC-type tests at 90°C precluded initiating vapor phase hydration tests at higher temperatures. The SPC "transition" temperature data from thermal analysis and thermal expansion tests indicate that tests performed above 90°C, and particularly above 100°C, would be invalid.

Several preliminary single-pass flow-through tests were completed at 90°C and 40°C. However, insufficient data were obtained to draw definitive conclusions about forward rates.

5.0 Sulfur Polymer Cement Formulation and Properties

From the initial sulfur polymer cement (SPC) characterization of the two primary lots, it was apparent that the formation and retention of beta sulfur was not merely a function of the SPC formulation. The thermal history was also crucial to the final phases found in SPC samples. There was significant lot-to-lot phase variation. For these reasons, SPC characterization was focused on the important properties that ultimately influence the long-term durability, processibility, reproducibility of SPC itself, and SPC concretes or waste forms. Special attention was paid to a potential new SPC formulation that improves the SPC in terms of chemical stability, mechanical compatibility, and processing conditions that are unique to SPC waste-form packaging.

5.1 Controlled Crystallization and Phase Identification in Sulfur Polymer Cement

The amorphous content plus the alpha and beta crystalline phase contents in the SPC were affected by many factors, particularly by the supercooling nature of elemental sulfur when cooled from a liquid.

Controlled cooling rate experiments were devised to study the effect of cooling rate on phase formation. Cooling rates were set and controlled through programmable computer controls. The cooling rate was set such that a fixed degree of SPC supercooling was maintained (25°C/min), a rate that simulated SPC cooling in a production waste form of 2 m x 2 m x 8 m (0.05°C/min).

To increase sensitivity and to correlate better with production SPC packaging, a large sample size (over 10 g) was used in the crystallization kinetics study. A thin thermocouple wire was embedded in each glass test tube as shown in Figure 5.1. Sulfur polymer cement samples were premelted in the tube at 140°C before the thermocouple was placed in position. The test-tube assembly was then placed in a silicon oil bath (Fisher, Precision 183) at 140°C and equilibrated 10 minutes before initiating the cooling schedule.

The oil bath temperature was controlled with a programmable temperature controller (Love Control, Model 32121-592-5150). Cooling rates for the oil bath were typically controlled between 0.05° to 5°C/min. For faster cooling rates (5° to 25°C/min), the test tubes were air-cooled. The fastest quenching was achieved using double copper plates (estimated faster than 100°C/min). Experiments using copper plates were not temperature-controlled.

Polymer modification of the SPC was also identified as an important factor influencing crystallization kinetics. Powder X-ray diffraction (XRD) was performed on a Philips X-Ray Diffractometer using a Cu source at 40kV/45mA. Powder SPC samples of various thermal histories and formulation (lot variation) were analyzed. The scanning rate was 1.5° theta/min in the 2-theta range of 5° to 75°. Semi-quantitative phase analysis in a given SPC specimen was achieved using a single crystal (alpha sulfur) background correction. The amorphous content included supercooled amorphous sulfur and the polymer used as a modifier in SPC, mainly cyclopentadiene.

SPC Cooldown Test Setup

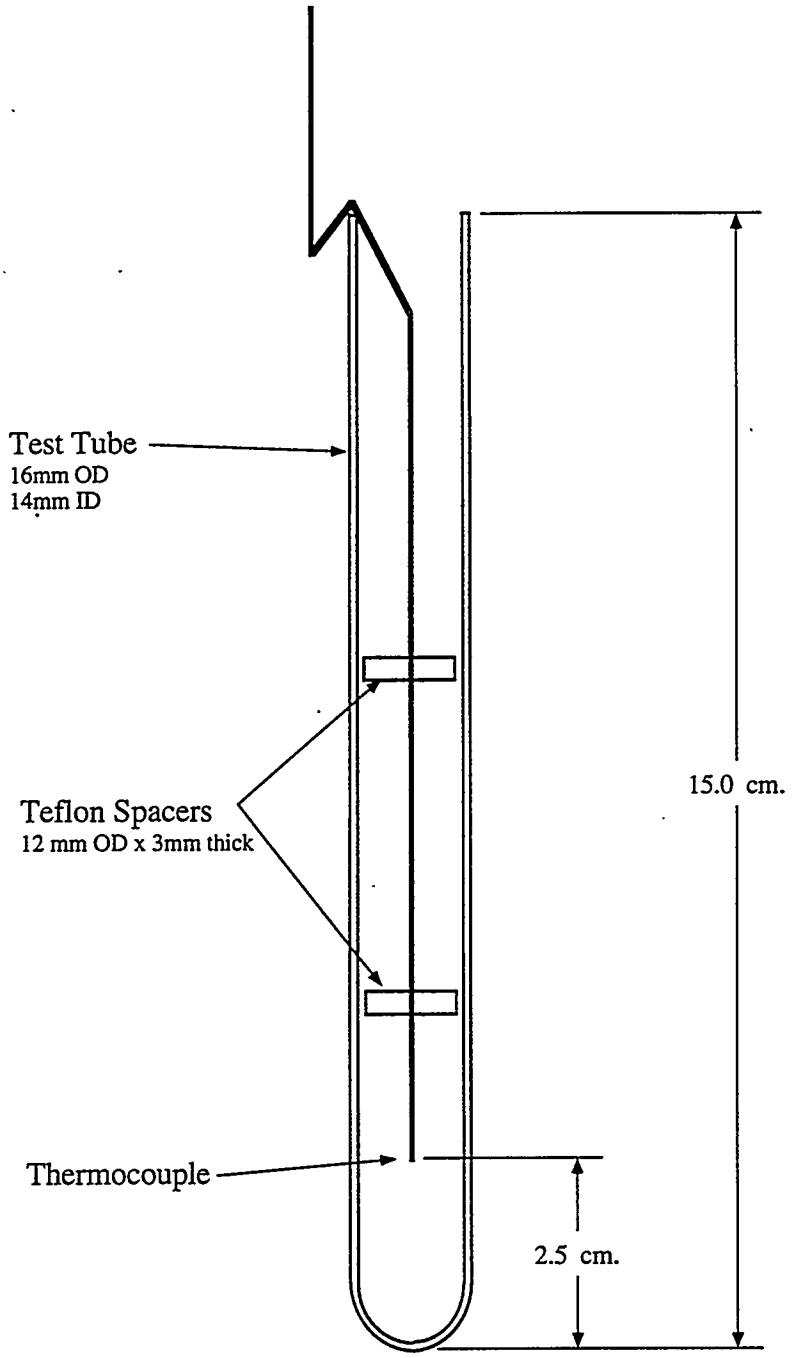

Figure 5.1. Typical Sample Holder and Temperature Sensor Configuration Used in Controlled Crystallization Studies. Test tubes are placed in a silicon oil bath which is programmed to cool at a given rate. A faster cooling rate is achieved by cooling test tubes in room air (5° to 25°C/min).

5.2 Polymers in Sulfur Polymer Cement and Their Reactions with Sulfur

Polymer modification of the SPC was also identified as an important factor influencing crystallization kinetics. The nature of the polymer and sulfur interaction was characterized by examining the energy spectrum of sulfur using X-ray photoelectron spectroscopy (XPS). The presence of the polymer species was identified with Fourier transform infrared (FTIR) spectroscopy and Raman spectroscopy. The reaction between sulfur and polymer was also studied using FTIR and Raman spectroscopy. A background XRD spectrum was used for semi-quantitative identification of polymers in SPC.

The suitability of SPC as a packaging or backfill material in terms of processibility was examined. Characterization specific to processibility included viscosity, the effect of curing (holding molten SPC at 130° to 140°C for various lengths of time). The temperature range where SPC had a lower viscosity without generating hydrogen sulfide was also determined and used as a reference for processing temperature.

5.3 Results and Discussion

5.3.1 Controlled Crystallization and Polymer Modification

Powder XRD is an effective and accurate method for identifying the various crystalline phases in SPC samples. An XRD pattern of sulfur in a single crystal alpha-phase is shown on the top of Figure 5.2; an XRD pattern of sulfur in a beta phase with some amorphous phase is shown at the bottom of Figure 5.2. The XRD patterns of alpha- and beta-sulfur crystals are extremely distinguishable, which makes XRD ideal for quantitative alpha- and beta-phase identification and measurement. By using a single-crystal alpha-sulfur spectrum as a reference for background subtraction, semi-quantitative measurement of the amorphous phases in SPC samples was also achieved. Table B.1 in Appendix B shows phase distributions for various SPC samples, covering a wide range of thermal histories. Alpha- and beta-phase distribution for the crystalline sulfur phases are represented in weight percent, while the amorphous phases are represented in volume percent of a sample.

The original invention by McBee, et al. (1982, 1983) was to stabilize (by way of polymer modification) the beta-to-alpha transformation so that the volume change associated is minimized. However, the formation and preservation of the beta phase is also dependent on the thermal history of the sample, in addition to the polymer stabilization.

Figure 5.3 shows the effect of cooling rate on the formation of the beta-sulfur phase. Cooling rate control from the SPC molten stage to solidification had a profound effect on the final phases present in SPC. The normal equilibrium crystallization path from a higher temperature is from melt to the beta phase, then to the alpha phase. Slower cooling rates (< 1.5°C/min) resulted in nearly all alpha phase at room temperature. Faster cooling rates increased the beta-to-alpha ratio; however, the amorphous content also increased due to the supercooling nature of sulfur.

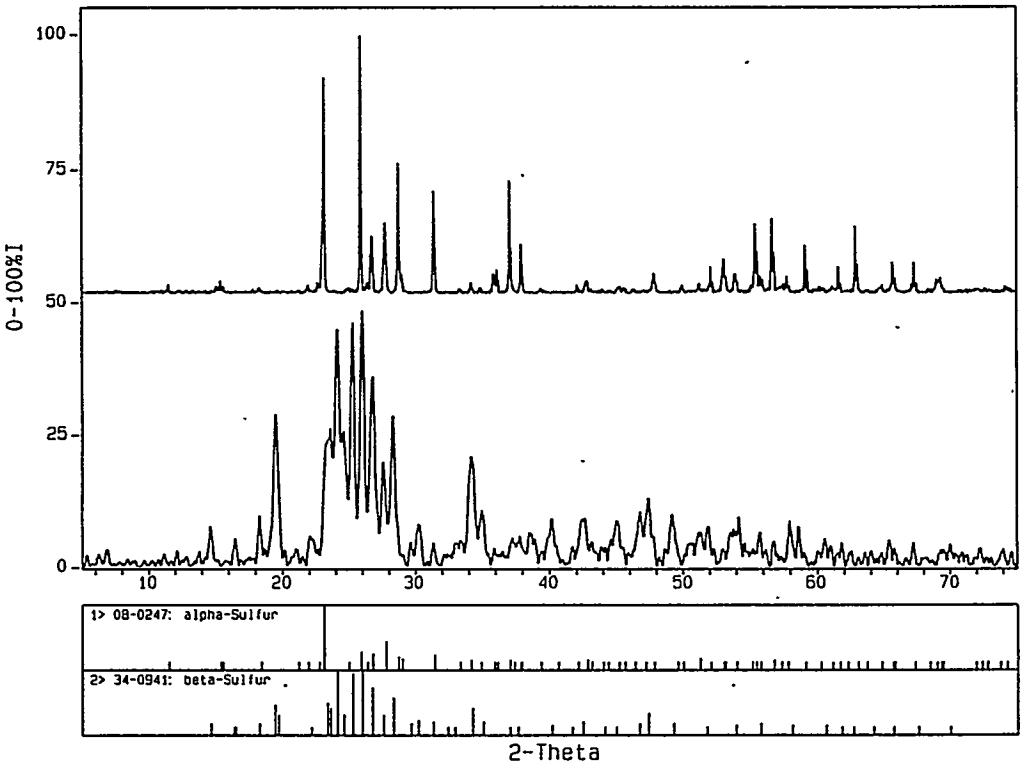

Figure 5.2. The XRD Patterns of Alpha and Beta Crystals are Extremely Distinguishable. XRD is ideal to identify between alpha and beta forms of sulfur. An accurate quantitative alpha and beta ratio can be readily established. Top is XRD of alpha single crystal; bottom is XRD of beta with some amorphous phases.

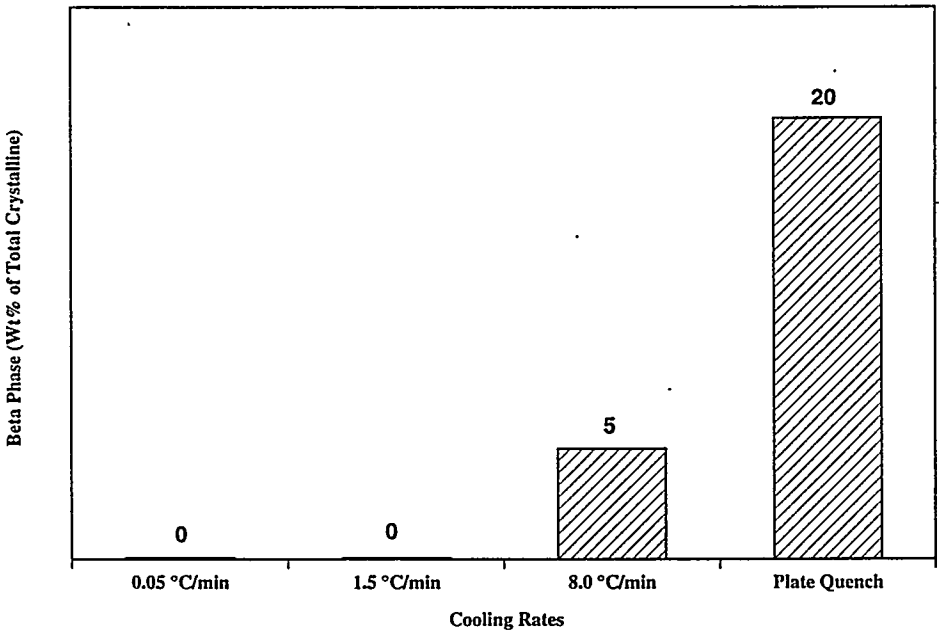

Figure 5.3. Beta Formation as a Function of Cooling Rates for SPC Lot PNNL 030695

The effect of polymer modification was also obvious. For pure elemental sulfur, no beta phase was detected using the cooling rates that ranged from 25°C/min to 0.05°C/min. It will be demonstrated later that when the polymers were fully reacted with sulfur in SPC, a cooling rate about 8°C/min stabilized the beta-sulfur phase so that no alpha phase was present at room temperature.

The effect of cooling rate and polymer modification on the peak crystallization temperature was also significant. For a cooling rate close to 25°C/min, pure sulfur showed a peak crystallization temperature at about 102°C, while polymer-modified sulfur (SPC lot 030695) showed a peak crystallization temperature of about 56°C, a 46°C difference. The difference was even greater when the same polymer-modified sulfur was cooled at 1.5°C/min (peak crystallization temperature about 112°C [see Figure 5.4]). Since chemical stability of different sulfur phases may differ significantly, knowing the degree of polymer modification and controlling the cooling rates accordingly may result in optimized long-term stability through sulfur-phase formation and control.

Polymers and sulfur were mixed and pre-reacted during the manufacturing process. Although the product is certified for polymer content, the completion of the chemical reaction between polymer and sulfur was not certified. Curing (holding molten SPC at the 140°C melting temperature over time) completes the reaction between the sulfur and modifying polymer.

The viscosity of SPC increases as curing time increases, which will be discussed later. Cured SPC exhibits completely different crystalline morphology and microstructure compared to uncured or pure sulfur. Figure 5.5 shows the effect of curing on the peak crystallization temperature for SPC 030695 and the same lot after 12 days of curing (holding the temperature at 140°C for 12 days). When more polymer was reacted with sulfur, as in the cured sample, peak crystallization temperature was suppressed and more crystalline phase was preserved at the higher symmetry, i.e., beta sulfur.

Figure 5.6 depicts the combined effect of cooling rate and polymer modification on the final phase in SPC. It suggests that to preserve sulfur in the beta form, polymer modification is necessary and the cooling rate has to be reasonably fast (8°C/min). For slower cooling rates (e.g., 0.05°C/min [shown in Figure 5.7]), there were two distinct temperature regions that showed crystallization, between 126° to 122°C, corresponding to the liquid/beta transformation, and between 108° to 104°C, corresponding to the beta/alpha transformation. The final crystalline form in all of the SPC sample was almost 100% alpha sulfur. This contrasted to the faster cooling rate curves (shown in Figure 5.5) where only one crystallization temperature region was detected and the final crystalline form was all beta sulfur (Figure 5.6), or a combination of alpha and beta sulfur.

Another important aspect of the polymer modification of sulfur is the control of crystalline morphology and microstructure. Without polymer modification, alpha-sulfur crystals show monoclinic morphology, like that in Figure 5.8. The crystal size was at least several millimeters. With polymer modification, the dominant microstructure was plate-like crystals of micron size (Figure 5.9). Such an interlocked, plate-like microstructure provides matrix mechanical integrity and also provides ways to relieve stress from a thermal expansion mismatch in SPC composite or concrete where LLW glass will be introduced.

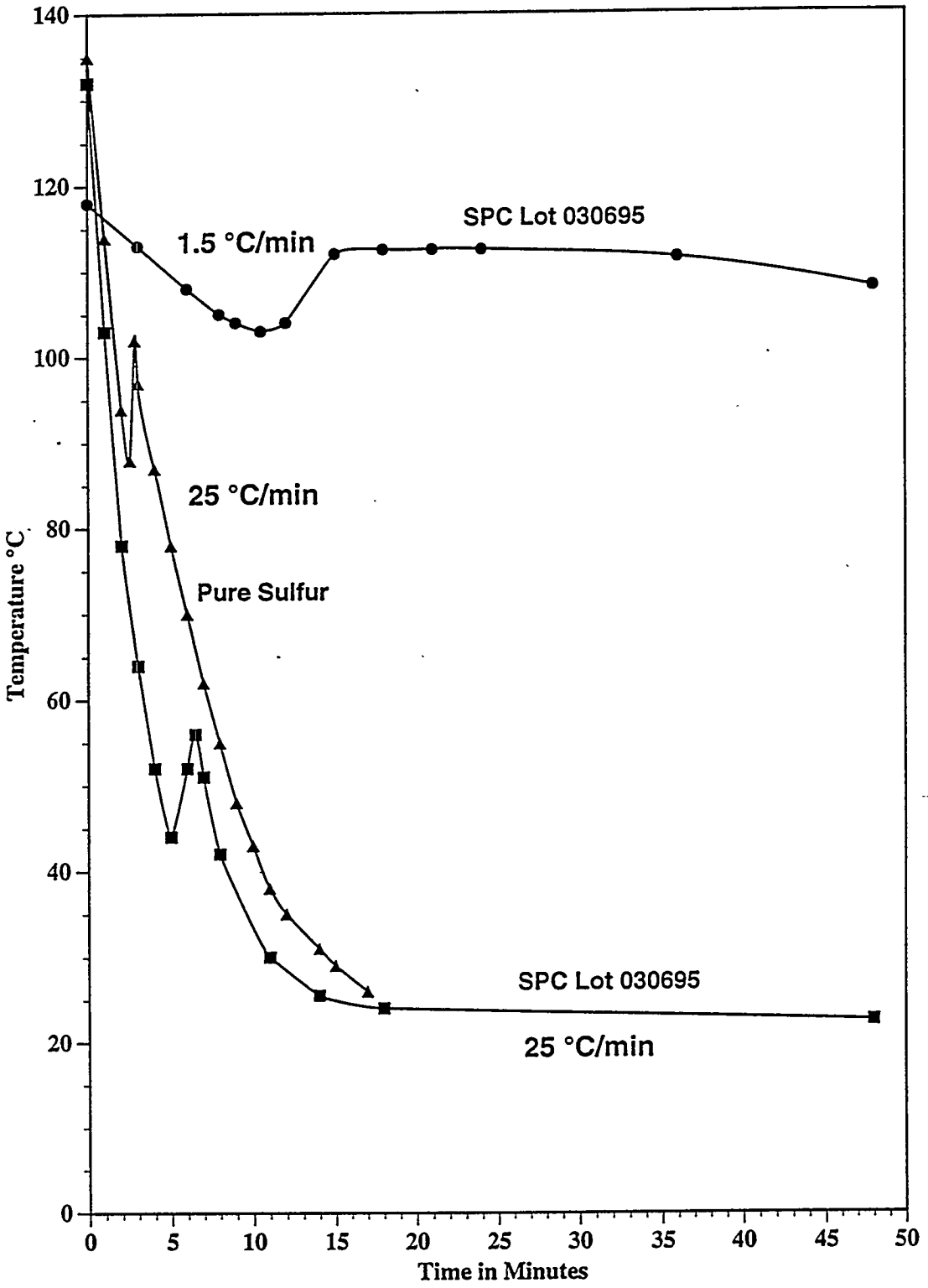

Figure 5.4. The Effect of Cooling Rate and Polymer Modification on the Peak Crystallization Temperature

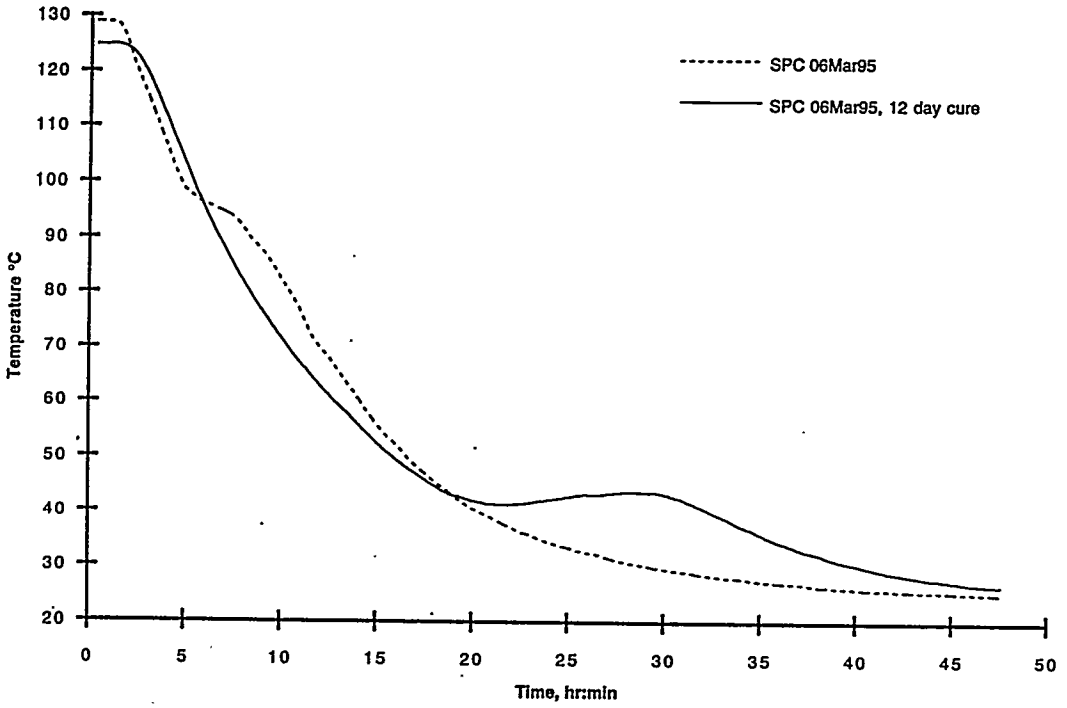

Figure 5.5. The Effect of Curing (Holding Melt Temperature for Several Days) on the Crystallization Behavior of SPC. The curing temperature was 140°.

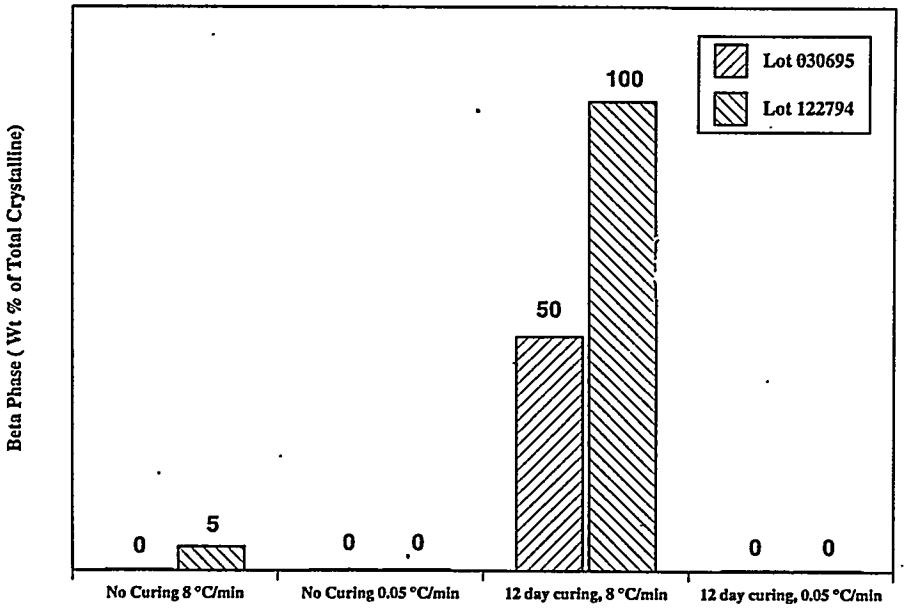

Figure 5.6. Beta Phase Formation as a Function of Cooling Rate and Polymer Modification. Beta phase is dominant when SPC is cured (140°C, 12 days) and is cooled at reasonably faster rate (8°C/min).

The role of polymer modification in SPC is not one of stabilizing the crystalline phases, as claimed by the inventors (McBee et al. 1982; 1983), but controlling of the microstructure. The interlocked plate-like, micron-sized microstructure helps to resist cracking and to tolerate any thermal expansion mismatch in SPC concrete. The microstructure shown in Figure 5.9 suggested that the polymer was likely present between plates and plate joints, much like the microstructure of a sea shell. The crystalline phase was always 100% alpha sulfur when the cooling rates were slower than 1.5°C/min, regardless of polymer modification and curing (Figures 5.3 and 5.6).

Canister center-line cooling rates for 2-, 1-, ½- and ¼-meter-diameter SPC concrete (50 vol% SPC, 50 vol% sand [sand represented waste glass]) were estimated to be slower than 0.008, 0.03, 0.12 and 0.5°C/min, respectively. Any sizable casting of SPC concrete will likely have a cooling rate sufficiently slow so that the final crystalline phase will be alpha sulfur. Therefore, the role of the polymer modifier in SPC cannot simply be to stabilize the beta crystalline phase, but to control the SPC microstructure as well to achieve mechanical integrity.

5.3.2 Thermal History and Sulfur Polymer Cement Formulation

It was suggested by the manufacturer that SPC lot 030695 contained more polymer; however, the polymer and sulfur reaction was more complete in SPC lot 122794. In addition, it was suggested by the inventor (McBee et al. 1982; 1983) that linear polymers are the end-product of the polymer and sulfur reaction (reactions 1 through 3 depicted below).

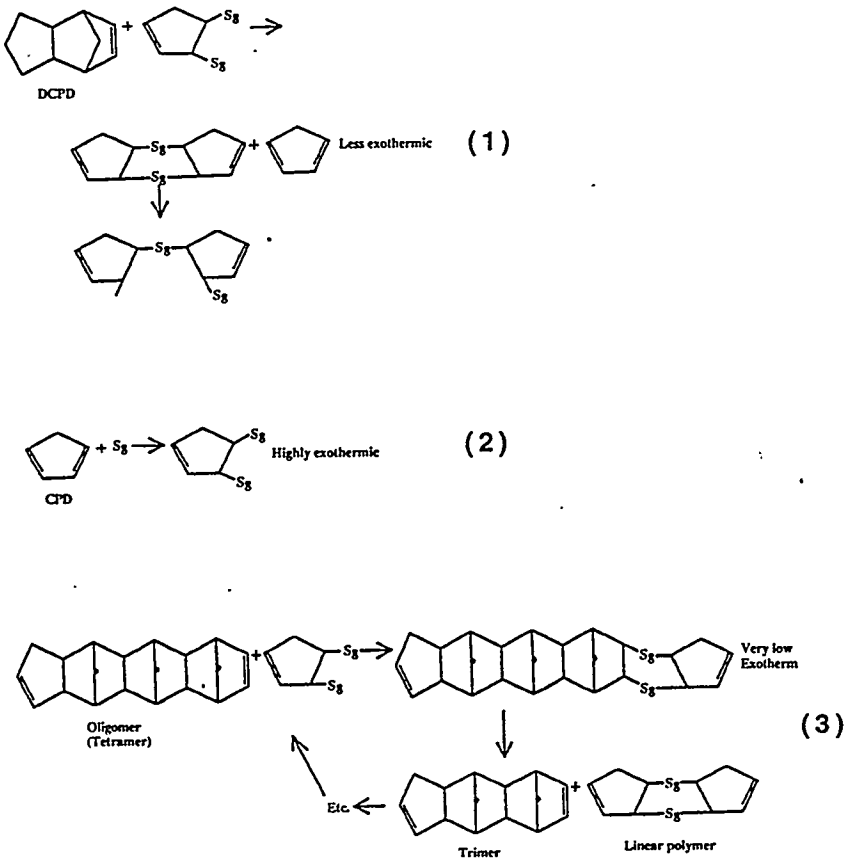

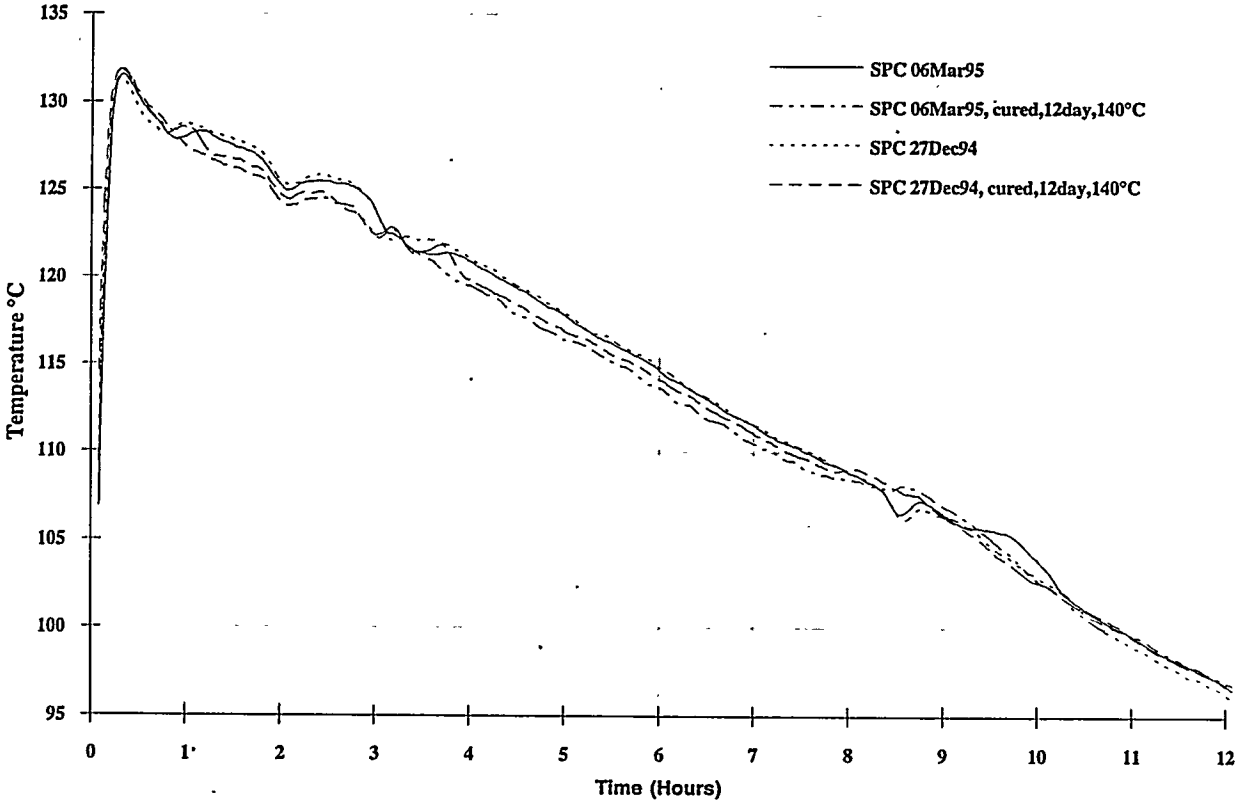

Figure 5.7. DTA Curves Showing Two Regions of Crystallization Associated with Liquid/Beta and Beta/Alpha Phase Transformation. When the cooling rate is slow, the polymer modification does not prevent beta/alpha transformation effectively.

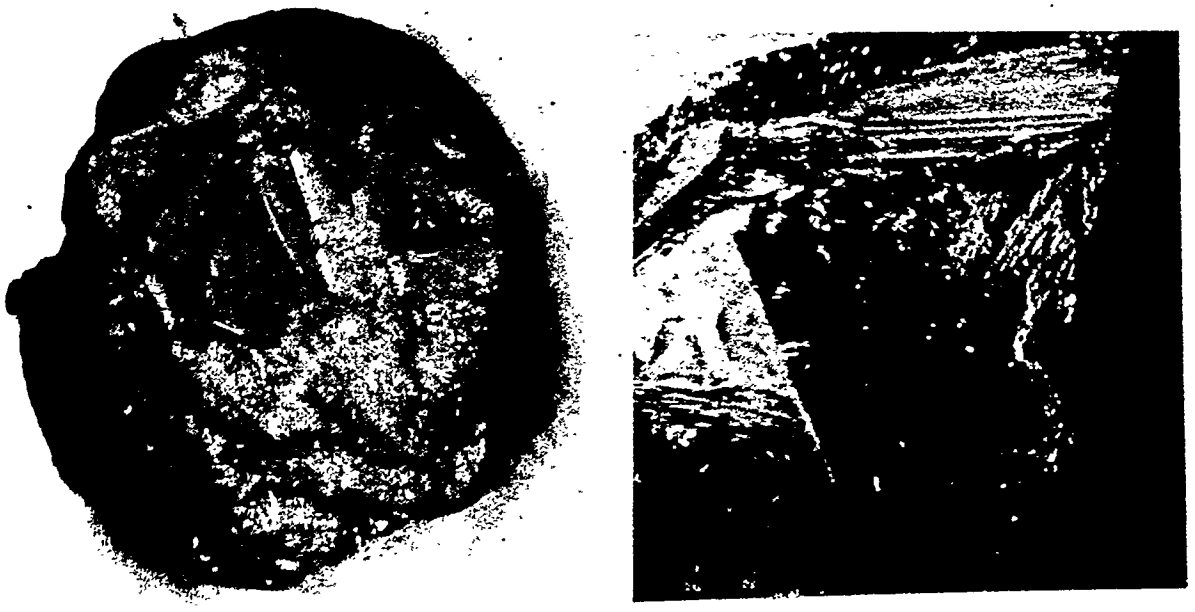

Figure 5.8. Typical Crystalline Morphology of Pure Elemental Sulfur Without Polymer Modification. Large monoclinic crystals are dominant.

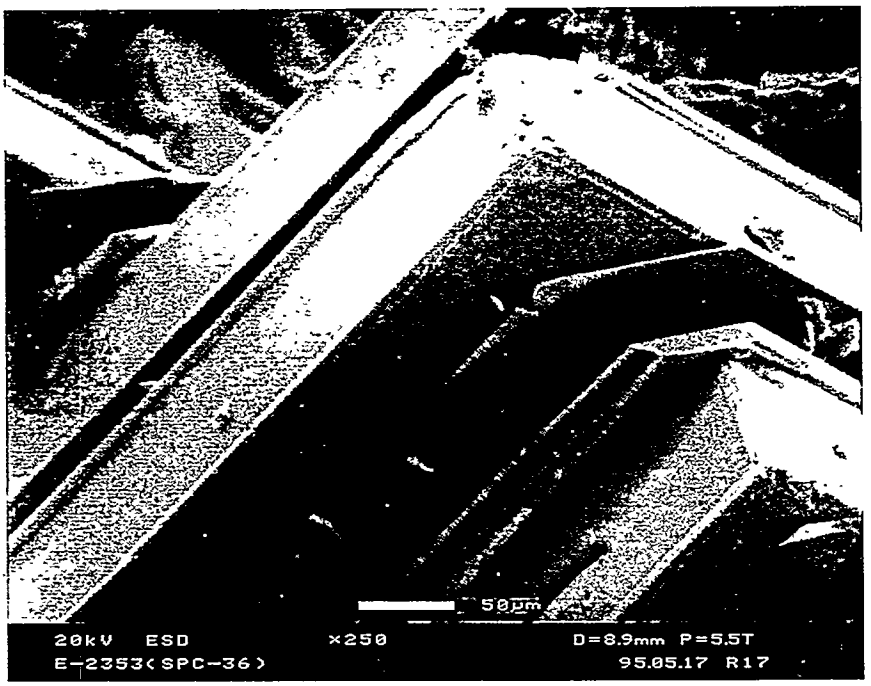

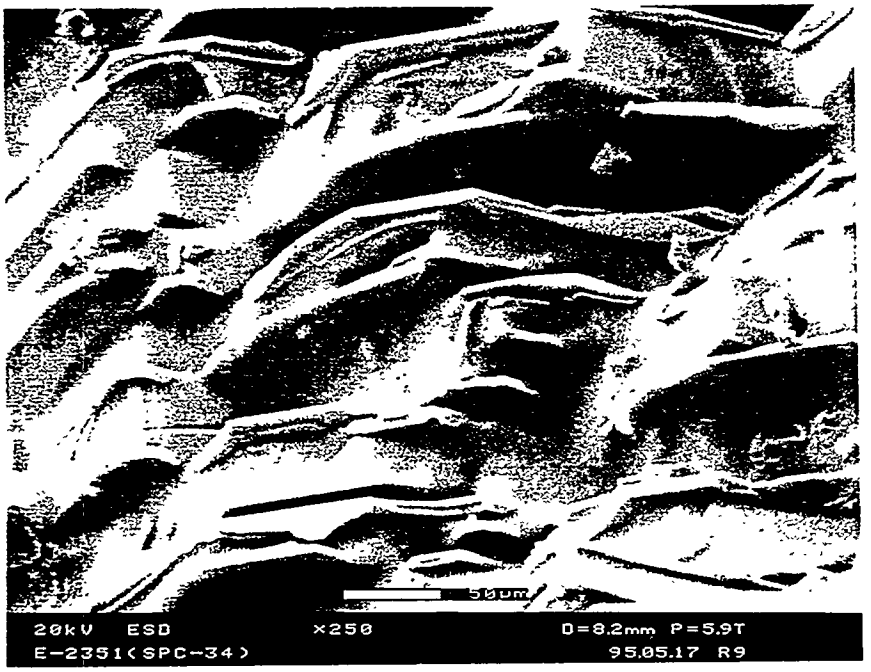

Figure 5.9. Typical Crystalline Morphology of Pure Elemental Sulfur With Polymer Modification. Interlocked plates are the dominant microstructure. SPC lot 122794 with 0.05°C/min cooling rate.

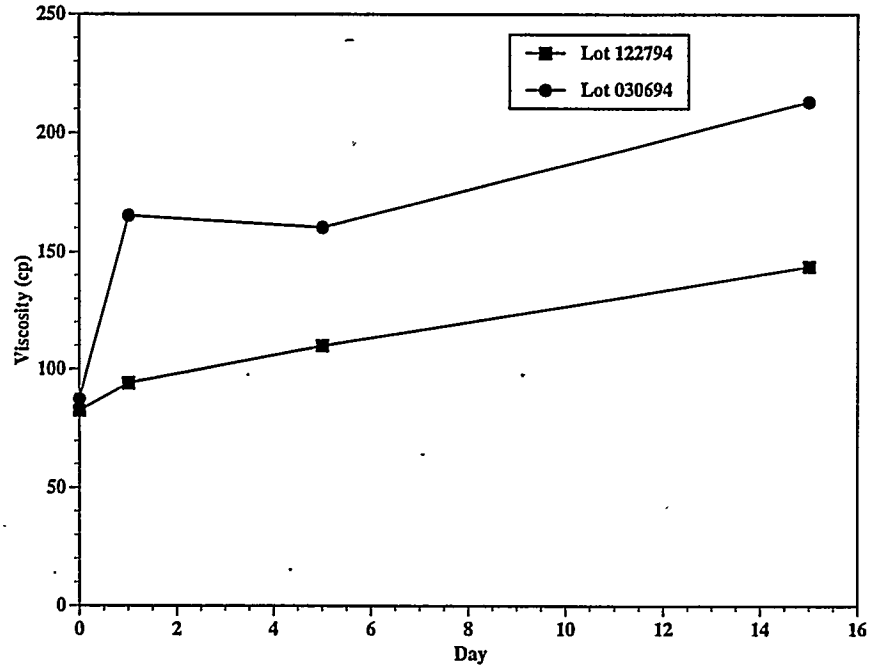

Figure 5.10. Viscosity of SPC (Lot 122794 and Lot 030695) as a Function of Curing Time at 135°C Curing Temperature (Curing is Holding the Melt at Temperature for Several Days)

The chemical analyses shown in Table 3.1 indicate that SPC lot 030695 does contain more polymer. However, the reaction between polymer and sulfur must be determined by other means. For example, the viscosity of SPC should increase as more polymer is reacted with the sulfur. Figure 5.10 plots viscosities of both SPC lot 030695 and lot 122794 as a function of curing time at 135°C. There was a significant increase in viscosity during the first 24 hours of curing for SPC lot 030695, indicating a significant amount of polymer and sulfur reacted. The higher viscosity of SPC lot 030695 also suggested it had a higher polymer content. The viscosities observed and their changes as a function of curing time correlated well with the manufacturer's estimates of polymer content and expected percent that would react.

The presence of unreacted polymer and the completion of the polymer-sulfur reaction through curing in SPC lot 030695 were also strongly supported by the FTIR measurement of the characteristic double bonds in the cyclopentadiene, which is the main modifying polymer constituent. The band at 3050/cm, shown in Figure 5.11, is consistent with C-H stretching. Since C-H is associated with C=C double bonds, the disappearance of C-H bonds suggested the consumption of C=C bonds, which generally leads to polymerization.

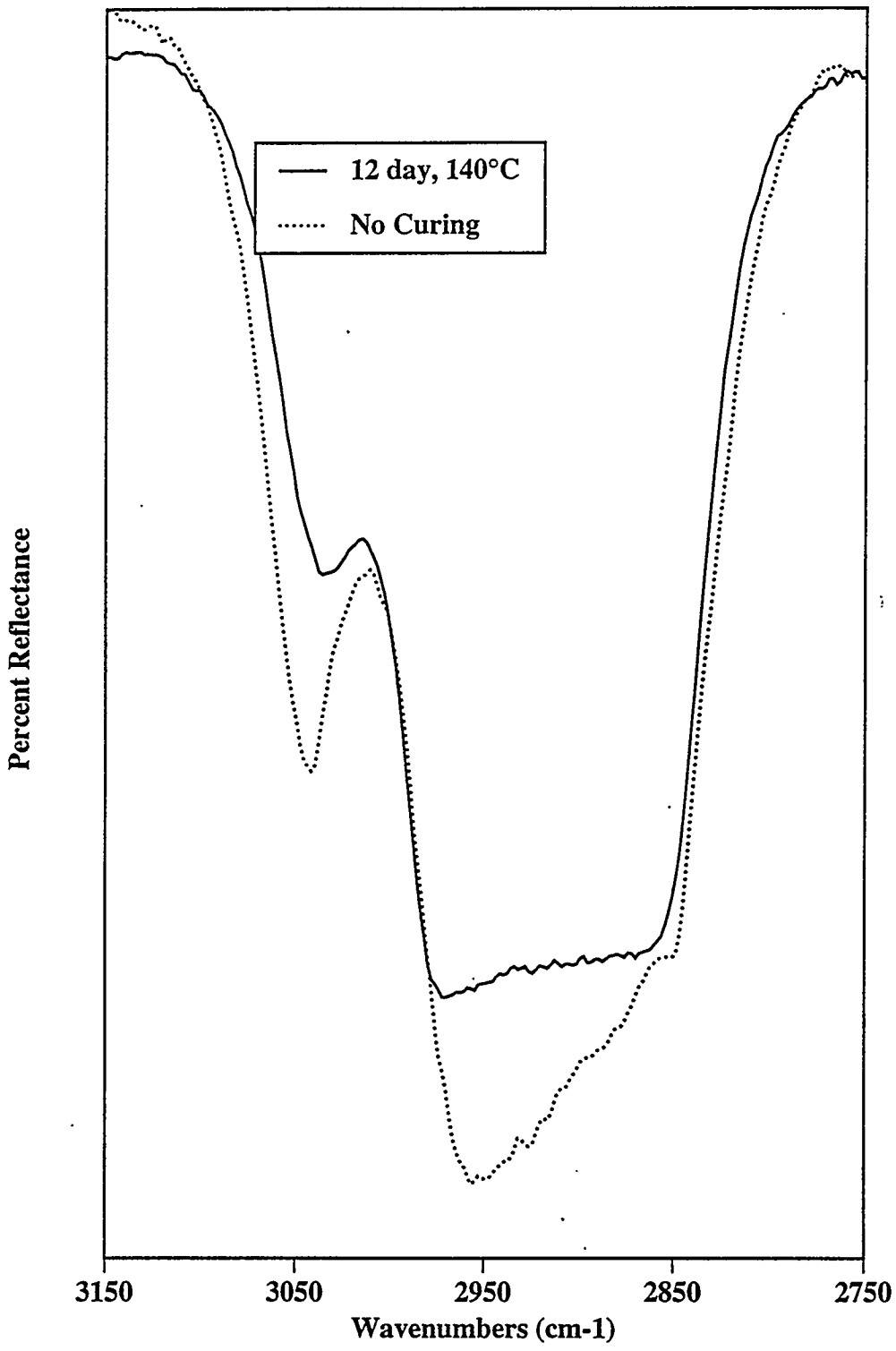

Figure 5.11. FTIR Spectrum Showing the Disappearance of Pentadyne Characteristic Double Bonds as the Polymer/Sulfur Reaction Completes

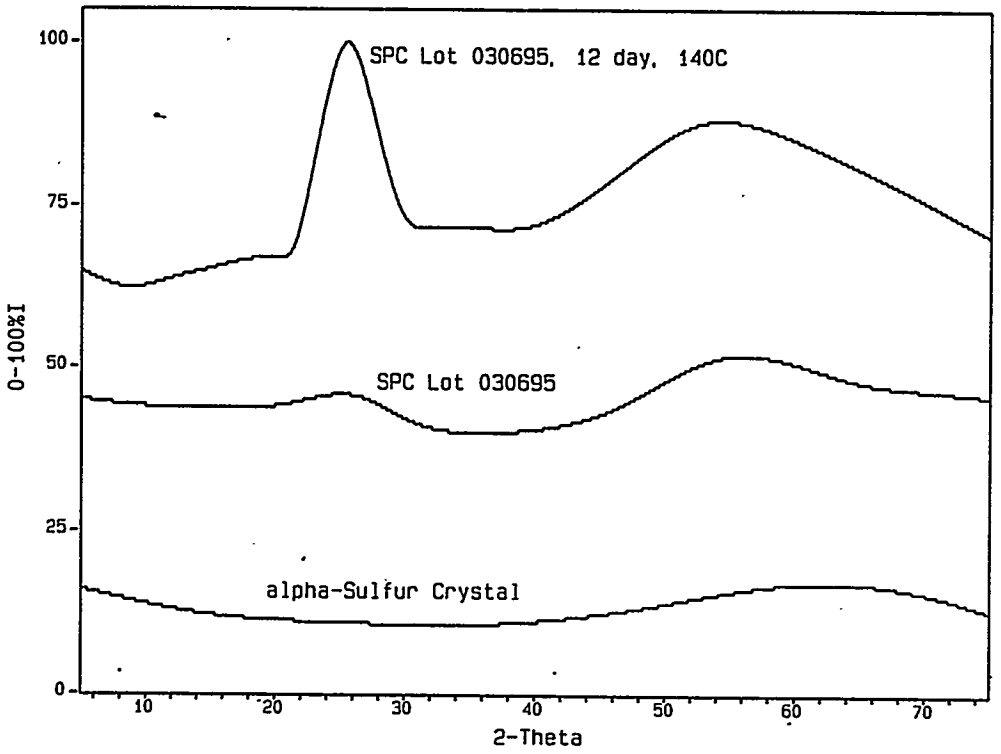

Figure 5.12. XRD Background Comparison of Single-Crystal Alpha Sulfur and Polymer-Modified Sulfur of Various Thermal Histories

This bond characterization is incomplete, since polymer-polymer reactions can cause the same change in the FTIR spectrum. Additional references such as dicyclopentadiene characterization are needed for conclusive results. However, with appropriate background subtraction, an XRD background spectrum can also identify the presence of polymer and its reaction. Figure 5.12 shows an extra background peak for SPC samples, compared to a single-crystal alpha sulfur that contained no polymer. This extra peak was likely associated with the presence of polymer.

The top XRD spectrum in Figure 5.12 corresponds to SPC lot 030695 after 12-day curing (holding the molten SPC at temperature at 140°C). The peak height increase and particularly the sharpening of the background peak for the polymer was consistent with reaction (3) in which oligomers, like tetramers, reduce the number of rings progressively as reaction (3) continued. This breakdown of oligomers (mixed species) unified the polymer species from oligomers to "monomers" (i.e., a single ring). Therefore, the sharpening of the polymer background spectrum was expected and can be an excellent indicator of the extent of the polymer-sulfur reaction. Further analysis concluded that XRD background peak sharpening corresponding to the polymer did not depend on the cooling rate or the final crystalline form of sulfur. The sharpening was solely a function of curing.

5.3.3 Sulfur Polymer Cement Processibility

Viscosity and volatility are important considerations for the large volume processing of SPC. Figure 5.13 plots the viscosities of pure sulfur and SPC as a function of temperature. Both SPC lot 030695 and lot 122794 were measured as-received without additional curing. Over the temperature range of 120° to 140°C, the viscosity did not change much; it stayed within 80 to 120 centipoise. Viscosities with this range are suitable for pouring, pumping, and draining.

Viscosities of pure sulfur were also measured. Early literature values for pure sulfur covered a greater temperature range and indicated a steep increase in viscosity starting at 158°C, which corresponds to the suggested sulfur polymerization (Tuller 1954).

Ideally, a high processing temperature should increase the fluidity of SPC and accelerate curing or the reaction between sulfur and polymer. The lower viscosity at the higher temperatures should also minimize the gas (air) voids in the SPC matrix and at the glass/SPC interface. Gas chromatography/mass analysis of SPC lot 030695 confirmed air entrapment in the SPC at lower temperatures.

Table 5.1 lists the dominant mass-to-charge ratio (M/Z) species for various compounds of interest to SPC. Referencing this table, Figure 5.14 becomes very informative. H_2O (M/Z=18), N_2 (M/Z=28), O_2 (M/Z=32) and CO_2 (M/Z=44) were all present in SPC lot 030695. Nearly all air and moisture entrapment was removed from this SPC under 584 mmHg vacuum (0.77 atmosphere) at 140°C (see Figure 5.14).

The additional detection of M/Z=32 was appreciable at temperatures above 150°C and was most dominant at 160°C. It is very likely the M/Z=32 corresponded to the formation of H_2S, which was reported by Darnell et al. (1992). M/Z=32 cannot be from O_2, due to retention time. The retention time for this species is 0.09 minute, while the retention time for O_2 is 0.33 minute. If there is an oxygen compound in the SPC, the reduction to release oxygen is not possible thermodynamically (Mattus et al. 1993; Tuller 1954). A temperature of 150°C sets the upper limit of SPC processing due to the release of H_2S. Not only is H_2S harmful, but according to Darnell et al. (1992), the formation of H_2S consumed the SPC polymer.

Table 5.1. Dominant M/Z for Important Gas Species Associated with SPC

Compound	M/Z 18	M/Z 28	M/Z 30	M/Z 32	M/Z 44
H_2O	x				
N_2		x			
O_2				x	
H_2S				x	
CO_2		x		x	x
NOx (?)			x		

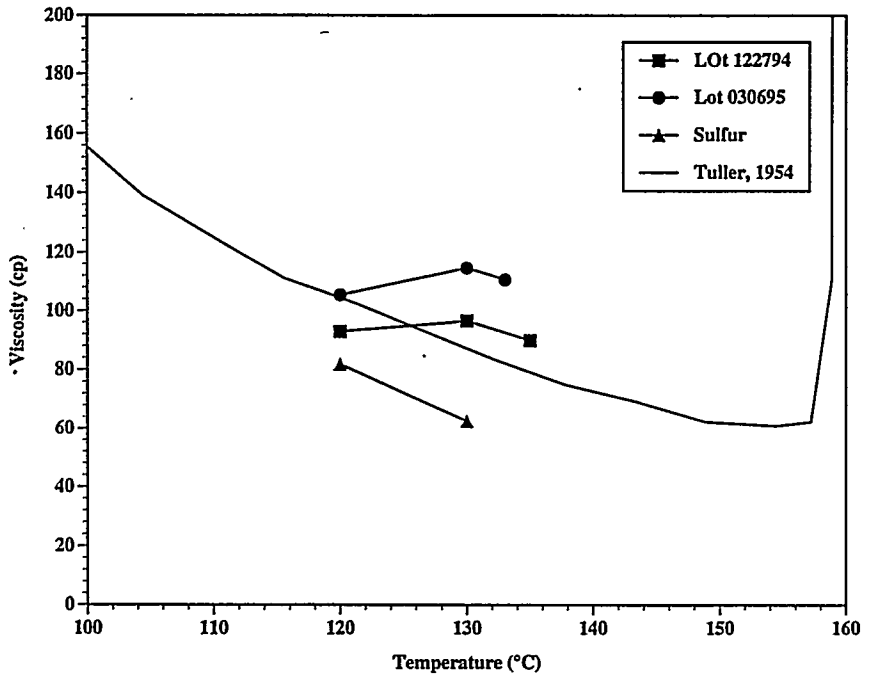

Figure 5.13. Viscosities of Pure Elemental Sulfur and SPC as a Function of Temperature. Literature values were also plotted for comparison.

5.4 Conclusions and Recommendations

The final phases in SPC depend not only on the polymer modification but also on the thermal history of the SPC. Polymer modification is necessary to retain the beta-crystalline sulfur at lower temperatures. When the cooling rates are slower than 1.5°C/min, the final crystalline phase is alpha sulfur regardless of the polymer modification.

The role of the polymer modification is not as important to stabilizing the beta sulfur form as it is in controlling the microstructure. Pure sulfur crystallizes and forms large alpha crystals (millimeters to centimeters). With the addition of polymer, the crystal growth is limited and controlled by the polymer in such a way that all crystals are plate-like of micron dimension.

A better understanding of SPC has been obtained in terms of its chemistry and thermal processing. New SPC formulations are possible. In particular, if control of the microstructure is most critical to achieve mechanical integrity of a sulfur cement, inorganic modifiers can be considered to impinge on the crystal growth. The same microstructure can be obtained without the use of organic species like polymer in SPC formulation.

Processing conditions have been defined in terms of temperature, processibility, reproducibility, and safety. Removal of entrapped air will reduce void volume. Curing at a higher temperature will complete the sulfur-polymer reaction.

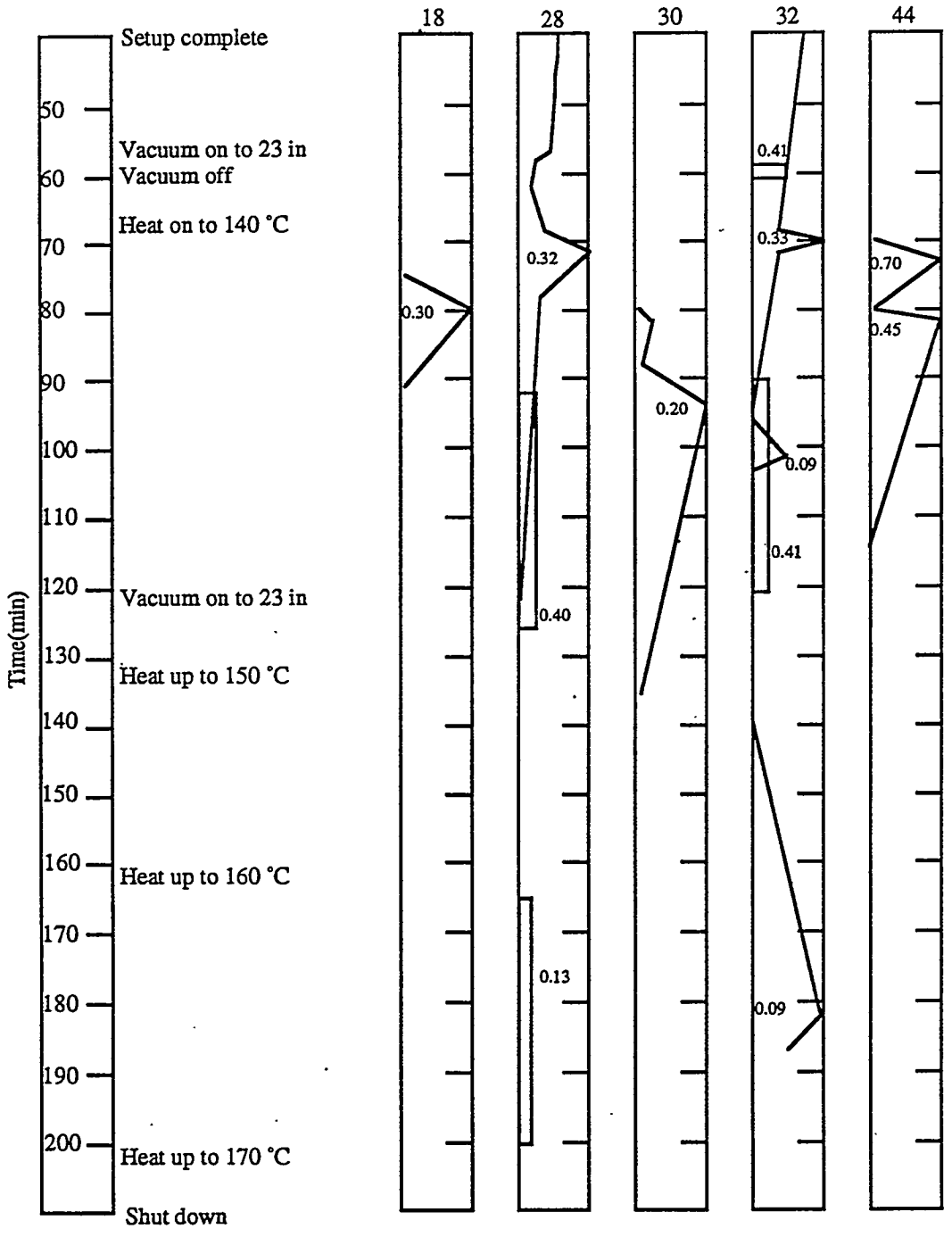

Figure 5.14. Detection of Gas Evolution from SPC as a Function of Temperature Under 0.77 Atmosphere Vacuum

6.0 Simulated Low-Level Waste Glass and Simulated Low-Level Waste Glass/Sulfur Polymer Cement Interface

The low-level waste (LLW) glass/sulfur polymer cement (SPC) interface characterization considered two crucial aspects, as follows:

- Determination of whether or not the glass-surface chemistry had been altered during the SPC melting and cooling processes, so that the glass dissolution mechanism might be altered. Since LLW glass dissolution has been characterized for performance assessment, predictions of long-term waste glass durability from models would be in error if the glass dissolution mechanism had changed after contact with the molten sulfur.

- Determination of whether or not the dissolution kinetics of a LLW glass change as a result of SPC encapsulation. The primary concern was the potential acid-base reaction between the sulfur in SPC and the LLW glass to accelerate glass corrosion. A worst case would be where cracking of SPC waste form happened at the LLW glass/SPC interface in the presence of water (i.e., groundwater), initiating an acid-base reaction. Simulation of this worst case would provide insight into the dissolution kinetics and the overall long-term stability of SPC LLW glass forms.

6.1 Glass/Sulfur Polymer Cement Interfacial Chemistry and Stability: Molten SPC

Simulated LLW glass/SPC interfacial chemistry and stability were examined for both the effect of molten SPC and/or water on the glass-surface chemistry, and the stability of SPC. Various simulated LLW glass-surface finishes (fractured, as-cast, polished, etc.) were exposed to molten SPC at 140°C for 12 days by suspending glass coupons into a molten SPC bath. To ensure good contact between molten SPC and glass, a vacuum was turned on periodically to remove any air bubbles at the interface. A freshly fractured glass surface of the same composition without exposure to molten SPC was used as a reference.

X-ray photoelectron spectroscopy (XPS) and secondary ion mass spectrometry (SIMS) depth profiles were obtained to determine the effect of molten SPC on glass-surface chemistry. Pseudo-line scanning analysis obtained by progressively moving an electron microprobe spot-scan was used to analyze the chemical composition across the glass/SPC interface. Overall interfacial chemistry and mechanical integrity were determined in this manner. This approach was also useful for detecting any sodium leached from the glass that may have diffused into the sulfur matrix.

6.2 Glass/Sulfur Polymer Cement Interfacial Chemistry and Stability: Aqueous Solution

Glass/SPC interfacial stability under aqueous conditions was also characterized. Polished LLW glass surfaces (6-μm diamond paste final polish) were used in all studies. Mineral oil was used for

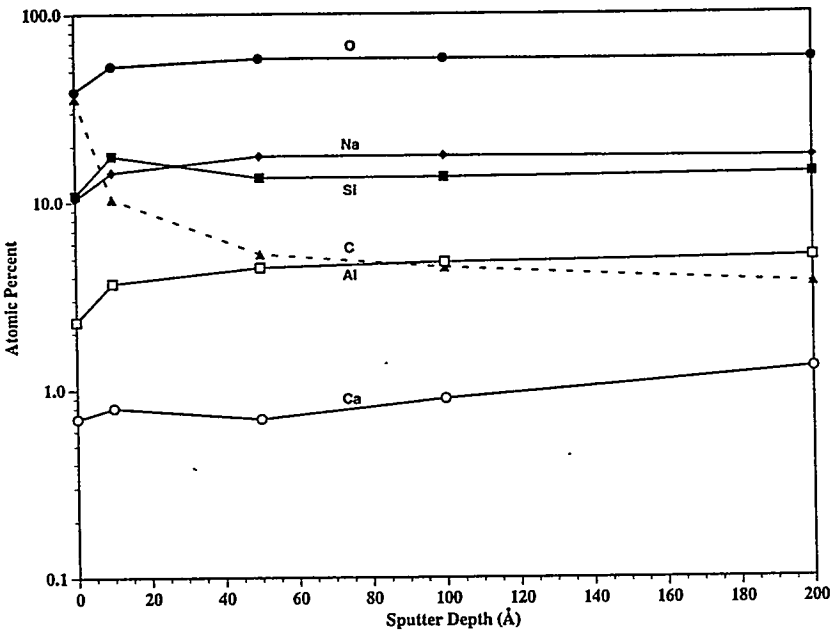

Figure 6.1. XPS Depth Profiles of As-Polished LD6-5412 Glass Surface. Glass surface was ground and polished with 6-μm diamond paste in mineral oil and cleaned with acetone.

grinding and polishing so that the polished surfaces were not exposed to water during sample preparation. The oil and residues on the glass surface were removed by acetone cleaning steps. Due to the mismatch in thermal expansion coefficients between LLW glass and SPC, large and crack-free interfaces were difficult to prepare.

Interfacial cracking and the effect of water at the glass/SPC interface were simulated by simply overlaying a polished LLW glass plate onto a smooth and flat piece of SPC lot 030695. The SPC plates were created by casting molten SPC onto flat Teflon sheets stretched over window-glass plates. This two-piece assembly was either immersed in deionized water at 50°C or in water vapor-saturated air at 50°C. Inert reference plates (quartz glass plates) were used in place of SPC plates (quartz is insoluble and contains no alkali). If there were continued acid-base reactions at the interface, then the surface-depth profiles for LLW glass in contact with SPC and in contact with quartz would have differed significantly.

Well bonded glass/SPC interfaces were created by embedding LLW glass fiber rods of 100μm to 2mm in diameter into molten SPC and then slowly cooled to solidify. Because of the smaller glass size and the compression of SPC onto glass when cooled from the melting temperature of SPC (140°C), the interfaces prepared were very tight mechanically. Polished cross-sections of such LLW glass fiber and SPC composites were exposed to deionized water at 50°C for up to 55 days.

A chemically inert filler (50 to 70 μm aluminum oxide powder) was mixed into the SPC to reduce its thermal expansion. Large LLW glass/SPC interfaces were prepared; typically, interfaces as large as 2 cm in diameter could be prepared without cracking.

6.3 Results and Discussion

6.3.1 Effect of Water on the Glass/SPC Interface

The experiments focused on two types of LLW glass/SPC interfaces, a tight or well-bonded interface and a loose or cracked interface. The loose or cracked interface represented the worst-case scenario in a disposal system where all the engineered barriers would have broken down, the SPC/LLW glass monolith would have many mechanical cracks at individual glass/SPC interfaces, and water would be present at the interfaces.

X-ray photoelectron spectroscopy depth profiling was a primary analysis tool used to reveal glass corrosion at the LLW glass/SPC interface. Figure 6.1 shows a reference depth profile for as-polished simulated LLW glass (LD6-5412). Na, O, C, Si, Al, and Ca profiles were collected and are shown. Sulfur was detected but was present much less than 1 atomic percent; it was not plotted in Figure 6.1. (Note: Table 3.21 indicates 0.21 wt% SO_3 in the nominal LD6-5412 simulated waste glass composition, which is equivalent to 0.05 atom% of sulfur. Data from XPS is generally reliable for .1 atom% or greater.) In this profile, the overall Na content is high and corresponds well with the 13.15 atom% shown in Table 3.21.

Also shown in Figure 6.1 is an artifact of grinding and polishing. Since the glass contained no carbon, the carbon line shown in Figure 6.1 is taken to be hydrocarbon contamination from either mineral oil and/or acetone cleaning. The carbon profile reaches a constant level at about 50 Å. Beyond 50 Å, all elements reach a constant concentration level. Elemental concentrations correspond well to expected values listed in Table 3.21.

Surface-depth profiles were obtained for the same polished surfaces after exposing them either to water or water vapor while in contact with SPC or inert quartz. Both water and water vapor exposure were done at 50°C for 312 hours. Depth profiles in Figure 6.2 were collected from a polished glass surface after water exposure, while depth profiles in Figure 6.3 were taken after water-vapor exposure. In both cases, the profiled surface was in constant contact with SPC plate (SPC lot 030695). Judging from the carbon profile, the grinding and polishing artifact was again present to about 50 Å, which was consistent with the control profile shown in Figure 6.1. The depth profiles for Si and Al were nearly comparable to the as-polished sample (compare Figures 6.2 and 3.35). There were, however, significant differences in the Na and Ca depth profiles.

In the case of water exposure, Na was depleted from the glass surface to about 25% of the expected level, even at a depth of 200Å (Figure 6.2). The Na depletion, on the other hand, was not detectable (Figure 6.3) from the surface exposed to saturated water vapor. Figure 6.4 compares the Na profiles. The Na control-depth profile from the as-polished sample is plotted for reference. The Na depth profile from the water-exposure-only sample (no SPC in contact) is also shown in Figure 6.4. Although one might expect a greater extent of depletion of Na on the surface in constant contact with SPC, due to the suggested acid/base reaction between sulfur and released Na, the water-exposure-only surface, Figure 6.4(d), indicated the greatest extent of Na depletion.

Table 6.1. Nominal LD6-5412 Glass Composition and Equivalents in Atomic Percent

Component	Nominal (wt%)	Element	Equivalent (atom%)
SiO_2	55.91	Si	18.95
Na_2O	20.00	Na	13.14
Al_2O_3	12.00	Al	4.79
B_2O_3	5.00	B	2.93
CaO	4.00	Ca	1.45
K_2O	1.46	K	0.63
Cl	0.35	Cl	0.20
F	0.29	F	0.31
SO_3	0.21	S	0.05
P_2O_5	0.19	P	0.05
Cs_2O	0.15	Cs	0.02
SrO	0.11	Sr	0.02
Cr_2O_3	0.04	Cr	0.01
Fe_2O_3	0.00	Fe	0.00
Others	0.29	O	57.83

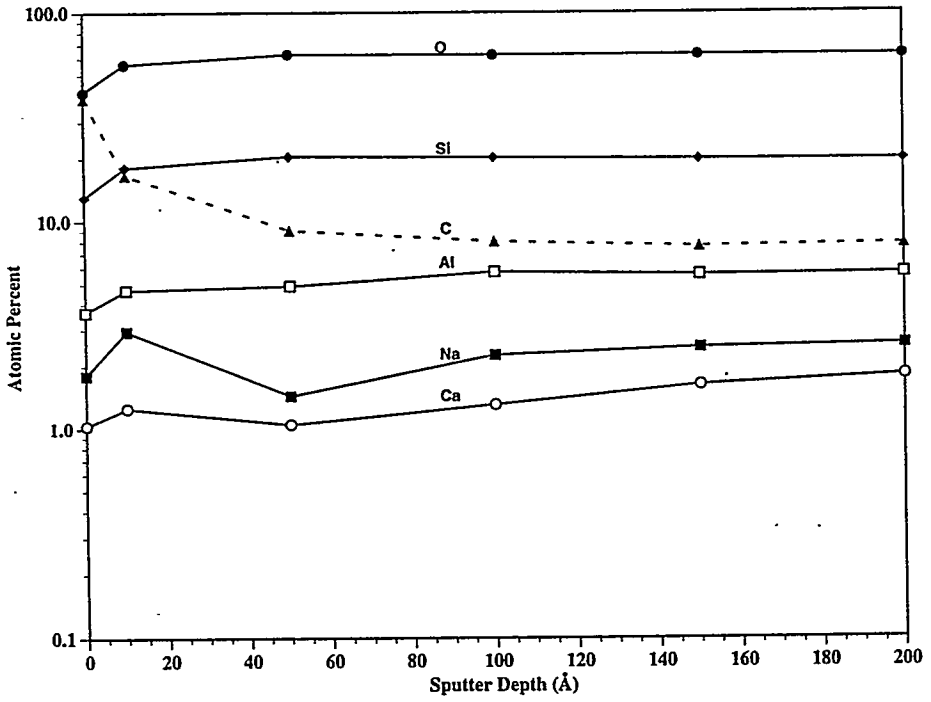

Figure 6.2. XPS Depth Profiles of Polished LD6-5412 Glass Surface After Exposing to Water at 50°C for 312 Hours. The sputtered surface was in contact with an SPC plate (lot 030695) while immersed in water.

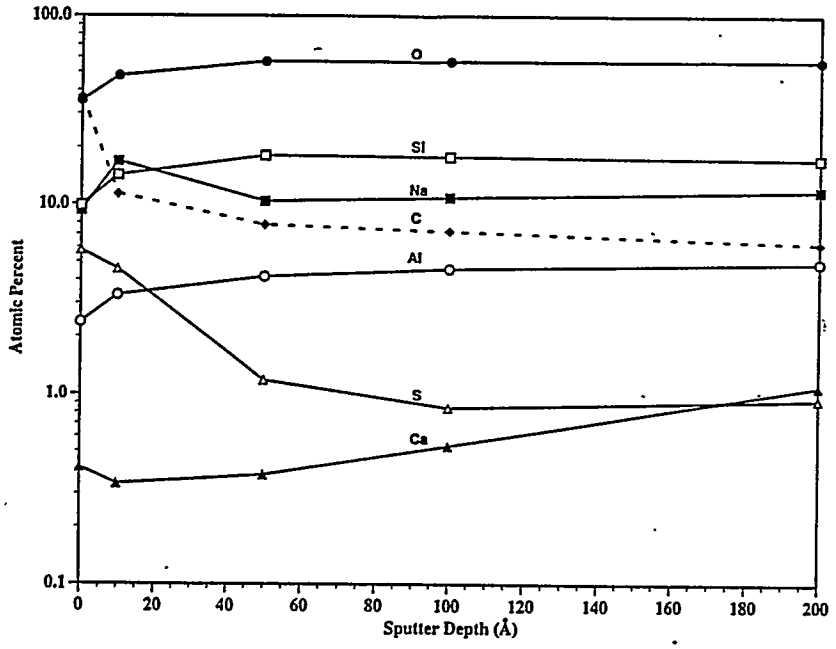

Figure 6.3. XPS Depth Profiles of Polished LD6-5412 Glass Surface After Exposing to Saturated Water Vapor at 50°C for 312 Hours. The sputtered surface was in contact with SPC (a plate of SPC lot 030695) during enclosure in water vapor.

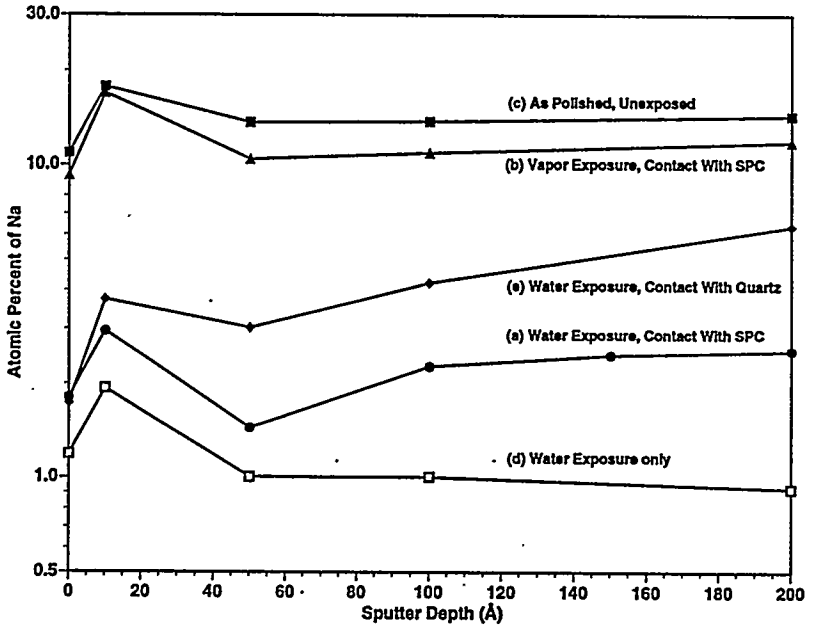

Figure 6.4. XPS Na Profiles: (a), (d) and (e) Water Exposure; (b) Vapor Exposure; (c) As-Polished Unexposed Surface. All exposures were at 50°C for 312 hours. The profiled surfaces were in constant contact with SPC plate (SPC lot 030695), except (d) where the profiled surface was exposed to water only, and (e) where the profiled surface was in contact with quartz.

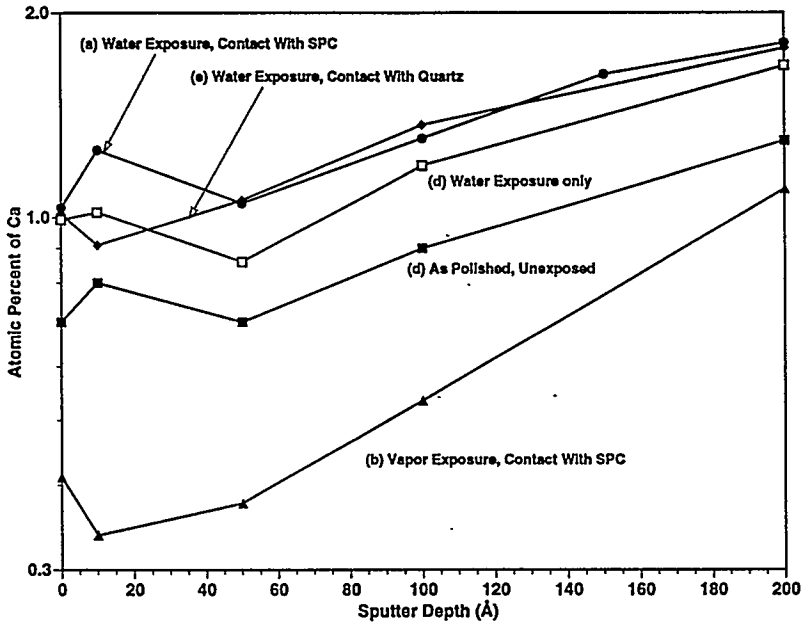

Figure 6.5. XPS Ca Profiles: (a), (d) and (e) Water Exposure; (b) Vapor Exposure; (c) As-Polished Unexposed Surface. All exposures were at 50°C for 312 hours. The profiled surfaces were in constant contact with SPC plate (SPC lot 030695), except (d) where the profiled surface was exposed to water only, and (e) where the profiled surface was in contact with quartz.

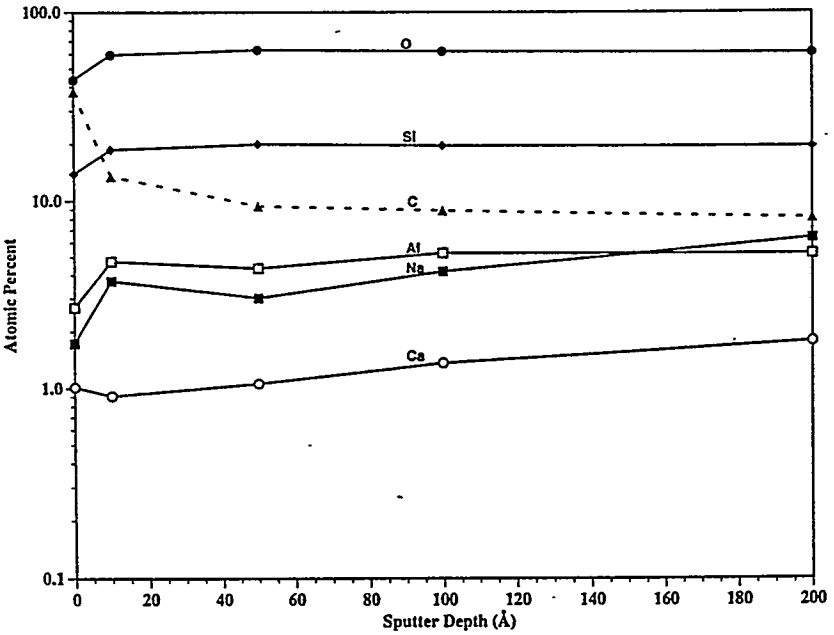

Figure 6.6. XPS Depth Profiles of Polished LD6-5412 Glass Surface After Exposing to Water at 50°C for 312 Hours. The sputtered surface was in constant contact with a quartz plate while immersed in water.

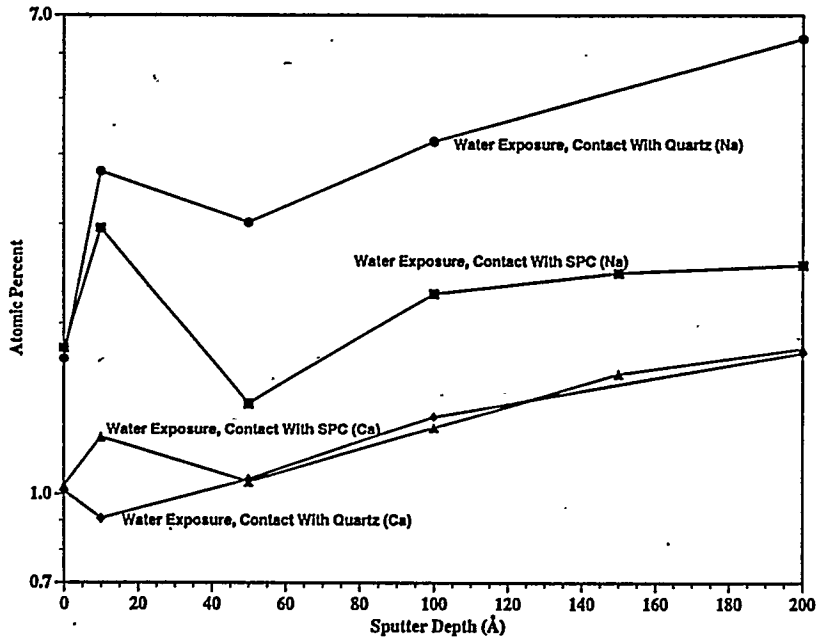

Figure 6.7. Effect of SPC at the Interface on LLW Glass Leaching Behavior. All profiled surfaces were exposed to water at 50°C for 312 hours. Quartz plates were used in place of SPC plates so that reference profiles could be obtained for comparison.

It is interesting to note that sulfur was detected (Figure 6.3) in significant amounts, even at the depth of 200Å in LLW glass-surface layer. The LLW glass surface was in contact with an SPC plate while exposed to 50°C water vapor. Also note that the depletion of Ca from the surface was much greater (Figure 6.3) compared to the case of water emersion (Figure 6.2).

Figure 6.5 compares the Ca depth profiles; the Ca control-depth profile was plotted for reference. The Ca depth profile for water exposure only (no SPC in contact) is also shown in Figure 6.5. Depletion of Ca in the case of water-vapor exposure seems to have been closely associated with the presence of sulfur. A similar trend in Ca depletion was detected from the glass surface in contact with molten SPC, which will be seen later. Further work is needed before an exact explanation can be given. The formation of calcium sulfate at the glass surface and the lowering of total free energy at the interface are likely causes of such a unique Ca and S interaction. To identify what effect SPC has on LLW glass corrosion behavior at the glass/SPC interface, parallel experiments identical to those discussed above were done using inert quartz plates instead of SPC plates. Figure 6.6 plots depth profiles for the polished LD6-5412 glass surface after water exposure at 50°C for 312 hours. The glass surface was in constant contact with a quartz plate (not an SPC plate).

Both Na and Ca profiles are compared in Figure 6.7. It seems that under the same water exposure conditions, sulfur at the glass surface promoted slight sodium leaching. Although more characterization is necessary before quantitative information can be obtained for comparing a SPC matrix with an inert matrix, it was clear that Na leaching could be reduced considerably in the presence of SPC when compared with no matrix (see Figure 6.4).

Well bonded simulated LLW glass/SPC interfaces were created with LD6-5412 fibers of various sizes by embedding the fibers in an SPC matrix. Cross-sections were cut and polished.

Figure 6.8 shows a typical cross-section of simulated LLW glass fibers in an SPC matrix. The interface was well bonded. These interfaces were very stable and showed no sign of opening or deterioration after 1330 hours (55 days) of water exposure at 50°C. The integrity of the interface was still obvious even under high magnification, as shown in Figure 6.9. If there were acid-base reactions between LLW glass and sulfur in SPC, and if such reactions were to continue, then one would see a deterioration of the glass/SPC interface. It was demonstrated in the present study that SPC corrosion was greatly accelerated in a basic medium like lithium buffer (pH = 10 or 12). See Section 4.0 on dissolution and corrosion of SPC.

It is also well known that sodium will leach out of glass and increase the solution pH. However, the rate of glass corrosion is such that the rate of Na leaching decreases as glass corrosion progresses. There may be an acid-base-type reaction at the very beginning of water exposure, but for these cases, it does not continue catastrophically.

As Figure 6.4 suggests, it is more advantageous to have SPC encapsulation than no encapsulation at all. Sodium leaching, for example, from the LLW glass surface was much greater when directly exposed to water. With a simple quartz or SPC plate covering the LLW glass surface, the sodium leaching was minimized significantly (see Figure 6.4).

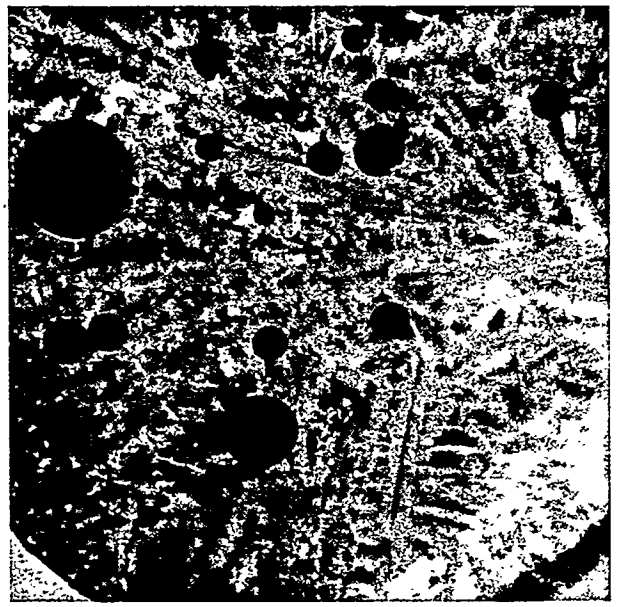

Figure 6.8. Typical Simulated LLW Glass/SPC Interface. Dark circular spots are cross-sections of LD6-5412 glass fibers.

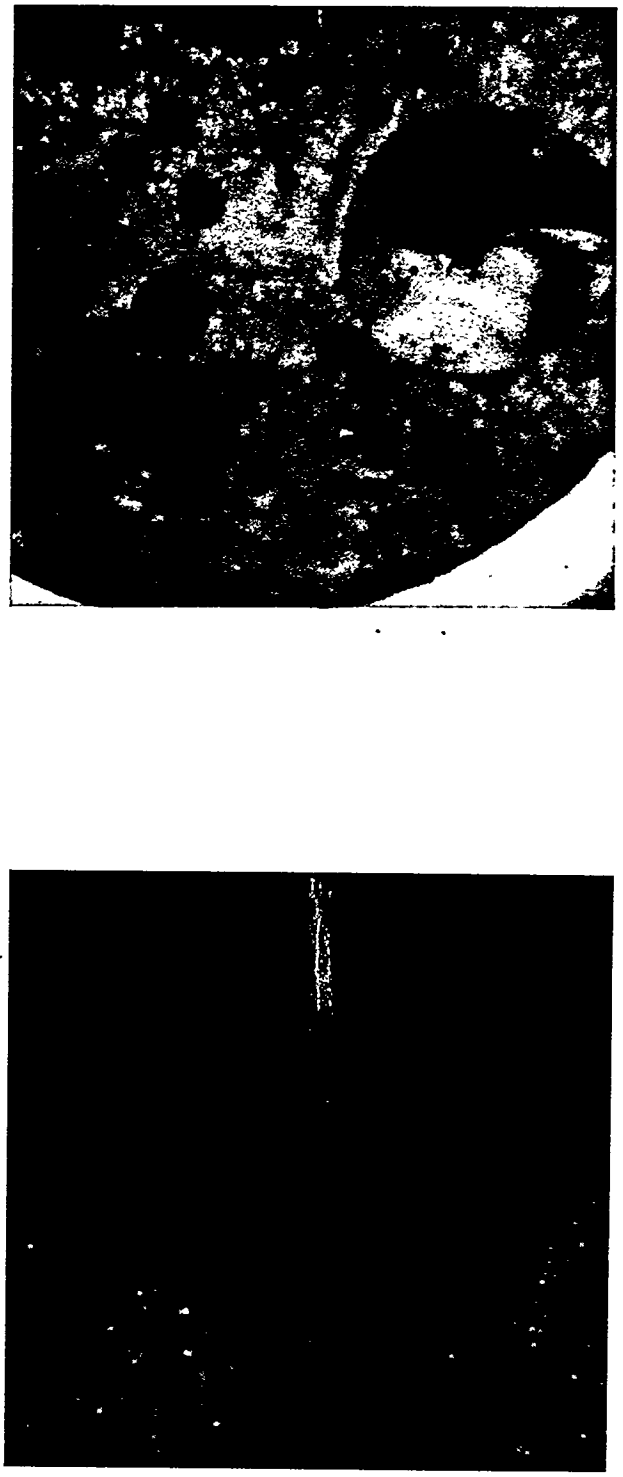

Figure 6.9. Typical Simulated LLW Glass/SPC Interface After Exposing to 50°C Deionized Water for 1330 Hours (55 Days). The LLW glass was prepared as fiber prior to embedding in SPC.

6.3.2 Effect of Molten SPC on Simulated LLW Glass Surface Chemistry

It takes at least 11 days for a 2m x 2m x 8m SPC waste form (50 vol% LLW glass) to cool from a molten state (140°C) to 80°C. A time period of 12 days was chosen to simulate the effect of molten SPC on glass surface chemistry.

Figure 6.10 shows a typical fractured, simulated LLW glass/SPC interface. This fracture was created from a prenotched glass rod. The glass surface was polished and exposed to molten sulfur for 12 days at 140°C. The fracture morphology suggests a reasonable interfacial bonding between glass and the SPC. It is fairly easy to obtain a flat fractured glass surface, especially when the glass is prenotched. However, if there was little or no interfacial bonding between the glass and SPC, the fracture surface would not resemble the fracture shown in Figure 6.10. Larger scale (submicron) simulated line scanning across the glass/SPC interface was performed by taking a series of spot scans using energy-dispersive X-ray (EDX). All spot-scan positions were numbered and are shown in Figure 6.10. The corresponding EDX spectra were plotted in Figure 6.11 for major elements of concern, Na, Si, S, Al, O.

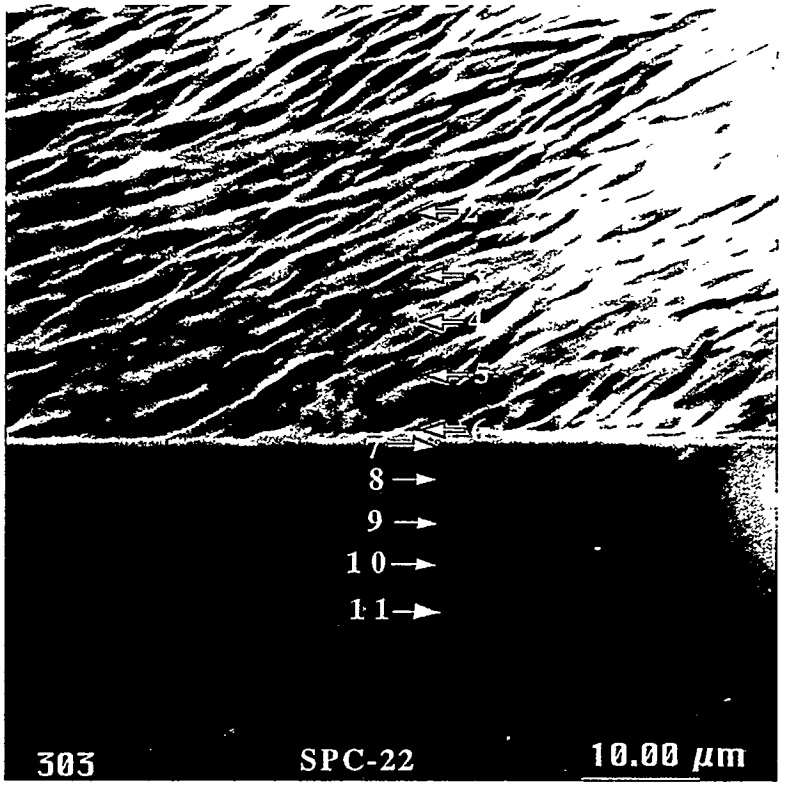

Figure 6.10. Typical Glass/SPC Interface Shows Reasonably Good Interfacial Bonding. This is LD6-5412 Simulated LLW Glass/SPC lot 030695 interface (fractured) after the glass had been in contact with molten SPC for 12 days at 140°C.

Due to the relatively large scanning area and spot positioning, spot scan 7 (shown in Figure 6.10) was at the glass/SPC interface (more on the glass side). For spectrum 7 (shown in Figure 6.11), a visible amount of sulfur was detected. About 8 microns away from the interface, the EDX scan (spectrum 8 in Figure 6.11) indicated no sulfur in the glass. This indicated that any sulfur penetration/diffusion into the glass was at a much shallower depth than 8 microns and the EDX scan would not have the resolution to reveal if the glass surface chemistry within the first micron layer had been altered by the molten sulfur.

Trace/small amounts of sodium were detected in spot scans 6, 5, and 4, as shown in Figure 6.11. No sodium was detected in spot scan 3, which was about 10 microns away from the interface. It is reasonable to assume that sodium was diffusing from the glass surface. Because SPC was in a molten state for 12 days, sodium could have migrated easily into the SPC, even to a depth of 10 microns as suggested by Figures 6.10 and 6.11.

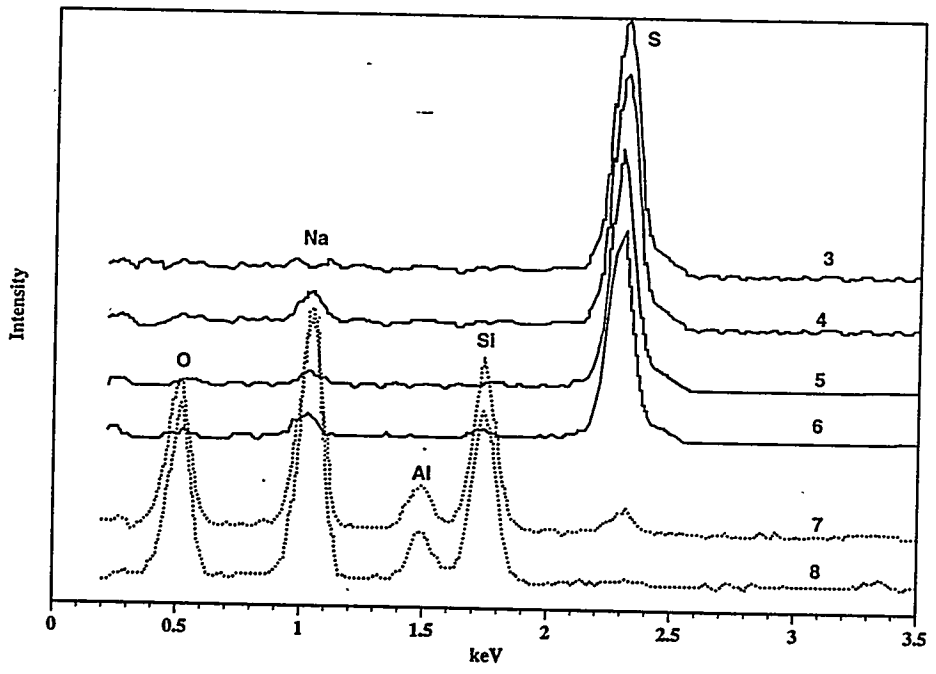

Figure 6.11. EDX Spot Scanning of Selected Chemical Compositions Across the Glass/SPC Interface. Spectrum numbers correspond to spots scanned. Refer to Figure 6.10 for spot positioning on the sample.

To reveal the effect of molten sulfur on the glass surface chemistry accurately, SIMS depth profiling was employed. A SIMS depth profile of a freshly fractured LD6-4512 glass was collected as reference and is shown in Figure 6.12. SIMS sputtering was a very effective technique; greater depths could be achieved in a shorter time, compared to other techniques like XPS sputtering. The SIMS sputtering technique is not suitable for shallow depth (<300Å) profiling. All elements reached an equilibrium or bulk concentration at a depth of about 500Å, for the reference surface profiling (Figure 6.10).

The SIMS depth profile for the identical fractured LD6-5412 surface after 12-day exposure to molten SPC (lot 030695) at 140°C is given in Figure 6.13. Both the sample and reference profiles corresponded closely beyond 500Å depth.

Depth profiles for Na, Ca and S showed a slightly different trend. A direct comparison of Na, Ca and S profiles is depicted in Figure 6.14. There was a moderate amount of sodium depletion at the surface layer. This is also suggested in Figures 6.8 and 6.9, where the trace/small amount of sodium was detected in the SPC adjacent to the LLW glass.

The Ca profile is most interesting. In relative percentages, more Ca (80%) was depleted at the surface than was Na (65%). More specifically, Ca is divalent and should have had orders of magnitude lower mobility when compared with Na. This surprising depletion of Ca may be explained by the chemical affinity between Ca and S and the stability of $CaSO_4$. Sulfur was detected at the surface at a much higher level than that in the bulk LD6-5412 glass (see Table 3.21). Similar, unexpected Ca depletion is also seen in Figures 6.3 and 6.5, as was discussed earlier.

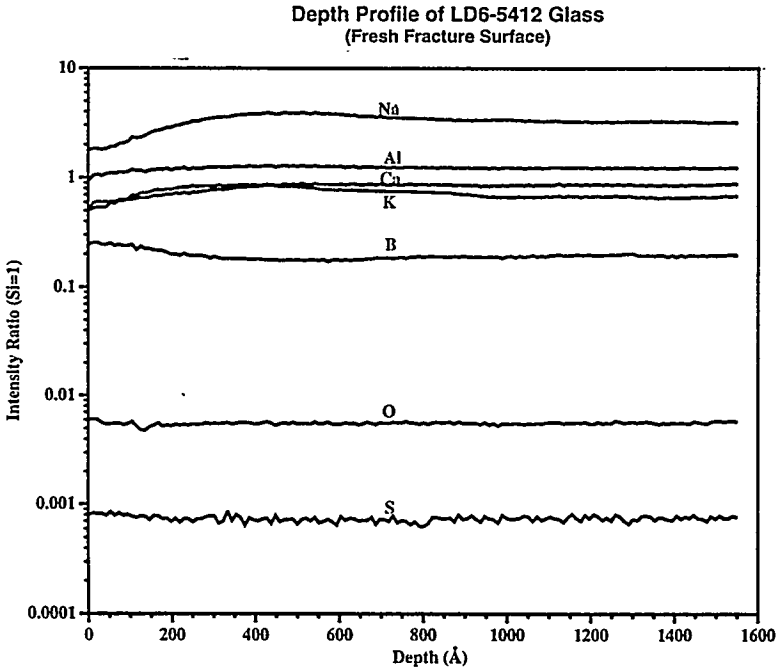

Figure 6.12. SIMS Depth Profile of a Freshly Fractured LD6-5412 Simulated Glass Surface

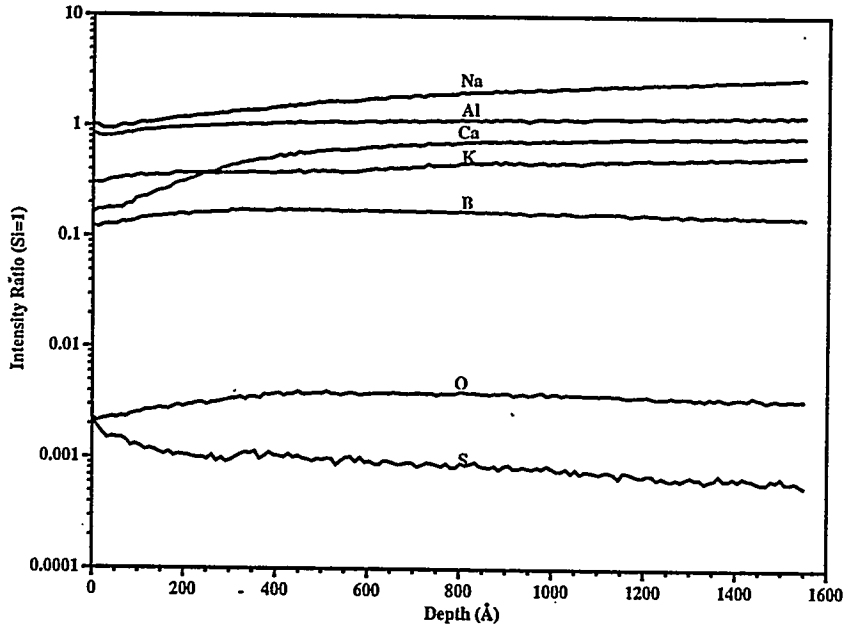

Figure 6.13. SIMS Depth Profile of a Fractured LD6-5412 Simulated LLW Glass Surface After Exposure to Molten SPC for 12 Days at 140°C

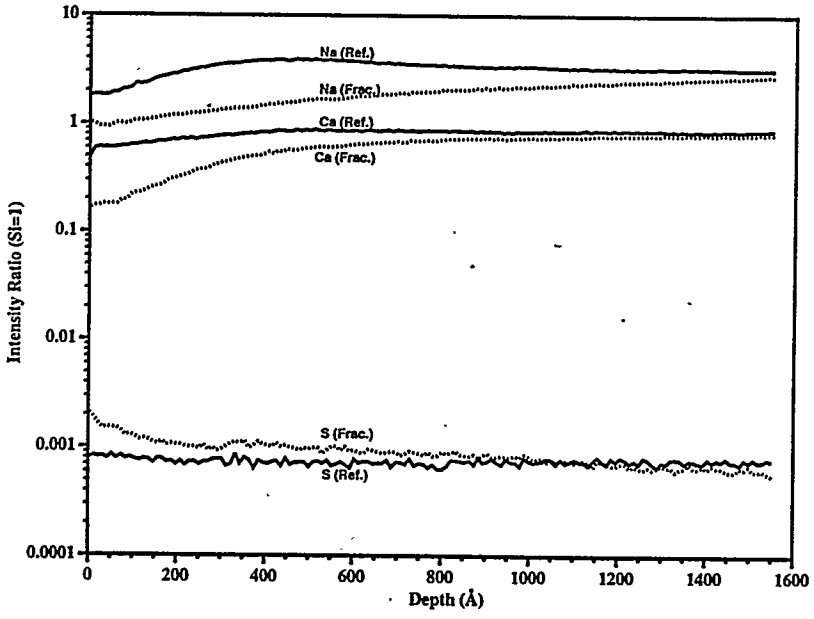

Figure 6.14. Comparison of Na, Ca, and S Depth Profiles of Fractured LD6-5412 Simulated LLW Glass Without Molten SPC Exposure (Designated Ref.) and With Molten SPC Exposure at 140°C for 12 Days (Designated Frac.)

These preliminary results showed that there was no major change in the glass surface chemistry that will in turn cause changes in the LLW glass dissolution mechanism. For example, sodium diffused from the LLW glass during a 12-day exposure to molten SPC at 140°C was not nearly as much as the leaching of glass after exposure to deionized water at 50°C for 312 hours (13 days). As Figure 6.4 indicates, nearly 90% of the sodium was leached from the glass surface for the entire sputtered 200Å depth. The actual depth could have been even greater. The same argument could be applied to Ca.

The glass surface chemistry change caused by extended exposure to molten sulfur (12 days at 140°C) was much less than the change caused by water exposure (50°C deionized water for 13 days). Therefore, it is not anticipated that the glass dissolution mechanism had been changed.

6.4 Conclusions and Recommendations

Simulated LLW glass surface chemistry changes very little after a 12-day exposure to molten SPC (during simulated processing of simulated LLW glass/SPC waste forms), as compared to changes caused by water exposure for a relatively short time at a lower temperature. There is no anticipated change in the glass corrosion mechanism.

The simulated LLW glass/SPC interface exhibited good wetting and bonding. The chemical affinity between calcium and sulfur that this investigation revealed should be explored further. A calcium sulfate thin layer could be created on the glass surface and may act as a barrier to preserve the interface.

The worst-case simulation indicated that SPC may accelerate the glass leaching at an early stage (within 13 days at 50°C) when compared with inert encapsulants like quartz. However, SPC encapsulation greatly minimized the glass leaching when compared with no encapsulation. This not only indicated the effectiveness of SPC encapsulation, but also indicated that the potential acid-base reaction between sulfur in SPC and glass may not be a concern from a kinetics point of view. Well bonded glass/SPC interfaces exposed to 50°C water for 1330 hours (55 days) had no detectable interfacial opening or deterioration.

7.0 Technetium Gettering Capability

7.1 Introduction

An important role of the sulfur polymer cement (SPC) or any matrix encapsulant, after the disposal system eventually breaks down from exposure to groundwater and/or moisture, is to serve as a getter for specific radionuclides. The capability of SPC to either adsorb or precipitate radionuclides that have been released from the waste glass is crucial to delaying and/or preventing the introduction of these radionuclides to the aquifer. Technetium-99 has been identified in performance assessment analyses as a mobile, significant contributor to dose in the exposure scenarios considered. Testing in fiscal year (FY) 1995 keyed on determining the capability of SPC to getter Tc, the mechanisms that cause the gettering, and the environmental conditions that control it.

Preliminary tests were performed in FY 1995 and are discussed below. These preliminary tests represent "scoping" tests; the data are reported strictly for reference and guidance for future studies. Care should be taken not to extend the conclusions beyond the reported data.

7.1.1 Experimental

All of the gettering tests used Tc(IV) as a pertechnetate (TcO_4^-) because it is expected to be the dominant species in solution in the Hanford Site vitrified low-level waste (LLW) glass disposal environment, and because it is readily soluble in water and exhibits very low adsorption tendencies. The SPC samples were in one of three forms: as-received granules (lot 030695); granules prepared by grinding a melted monolith (lot 030695); and monoliths melted from lot 122794.

Several experiments have been conducted to verify the pertechnetate-reducing efficacy of sulfur polymer cement. Thermodynamically, sulfur chemistry should dominate the system, reducing the pertechnetate species through sulfide-forming reactions, and removing the technetium from solution by adsorption on the SPC surface or by precipitation. It is believed that the progress of the reduction reaction is contingent upon the removal of dissolved oxygen from solution through the oxidation of elemental sulfur. As all of the dissolved oxygen is removed, reducing conditions are signaled by the production of hydrogen disulfide, at which time reduction of the pertechnetate also occurs.

The primary focus for these initial experiments was simply to demonstrate that technetium was removed from solution by the above-described mechanisms, so experiments were designed to achieve this result quickly. Because sulfur is insoluble in water, this set of conditions is only slowly achieved. For all of the tests described below, technetium activity was measured by mixing an aliquot of 0.45-μm-pore filtered solution with liquid scintillation cocktail and performing a count. The activity found in the samples was compared to an "activity blank" (spiked liquid with no SPC) that had been prepared identically to the samples contacting SPC.

An initial scoping experiment consisted of wetting 10 grams of crushed, granulated material (-20/+40 mesh) in 30 mL of deionized water in a 50-mL centrifuge tube. Technetium-99 (as pertechnetate) was spiked into each centrifuge tube at a concentration of 30 μCi/L (1.77×10^{-5} M). The tests were conducted at room temperature, in duplicate, and agitated end-over-end at 30 rpm.

Tubes were sacrificed at each sampling period. This experiment was conducted with crushed SPC in an as-received condition and also following remelting and cooling.

A second set of experiments was undertaken in response to obtaining inconclusive results (as will be discussed below) from the initial tests. The second set of experiments was conducted to eliminate the influx of atmospheric oxygen into the adsorption test container. The technique employed glass vials that were flame-sealed after they were filled with ground SPC and Tc-99-spiked DIW or Tc-99-spiked 0.01 M NaOH (DIW at pH 12 to approximate the alkaline environment of a leaching waste glass). These tests were also conducted with as-received SPC and remelted SPC. Each vial was filled with 0.2 grams of crushed SPC (-40/+70 mesh) and 2.0 mL of spiked solution, prepared as follows: A DIW solution was spiked to a Tc-99 concentration of 270 nCi/L (1.6×10^{-7} M) and the DIW-containing vials were filled. NaOH was added to the balance of this solution until a pH of 11.98 was reached. The pH 12 solution was then used to fill the appropriate vials at the same solid-to-liquid ratio mentioned above. Vials were quickly sealed using an oxygen/propane torch. An accurate weight was obtained for each vial before it was placed in an oven operating at 45°C. The weights were checked after several days to determine if the vials had been completely sealed.

A third set of experiments was conducted using rectangular-solid (monolith) samples cut from a sheet of remelted SPC. The SPC samples had a geometric surface area of 4.0 cm^2. These tests were conducted using 40 mL of Tc-99-spiked DIW in tightly sealed perfluroalkoxy (PFA) Teflon jars. The PFA jars were then placed inside polytetrafluoroethylene (PFTE) Teflon-lined, stainless-steel acid-digestion bombs and tightly sealed to preclude replenishment of dissolved oxygen. The test assembly was placed inside an oven operating at 70°C. These test containers were sampled at 7, 21, and 34 days and then resealed.

A fourth set of tests used the same sample type that was used in the third set as well as the same surface area-to-volume ratio, but the samples were heated to 70°C in a glass reflux-distillation apparatus so that the liquid was open to the atmosphere and evaporative loss was minimized. These tests were also sampled after 34 days (end of testing) of contact between the SPC coupon and the Tc-spiked DIW. Table 7.1 summarizes the experiments that have been conducted.

7.1.2 Results and Discussion

Samples of the liquids obtained from the first set of experiments were filtered through 0.45-μm-pore syringe filters following 4 and 7 days of contact with the granulated SPC. An aliquot of the filtrate was added to the liquid scintillation (LS) cocktail to determine the technetium activity. Activities in the filtrates were unchanged from initial activities, which indicated that no technetium had been removed from solution. The pH of liquids following contact with SPC ranged from 4.8 to 5.5 (pH of a DIW blank measured 5.5). Results at the subsequent sampling periods (31 and 62 days) also showed no loss of Tc from solution. However, because each of the centrifuge tubes was individually spiked, there were slight variations in activities between the activity blanks and the SPC-contacted solutions. These variations may have masked reductions in Tc activities because the spike concentrations were fairly high, necessitating use of small aliquots for LS counting. The confounding effects of initial-spike variability may have been especially significant because of the possibility that adsorption kinetics at room temperature are slow. Technetium reduction may also have been slowed by two other factors, oxygen replenishment through the centrifuge tubes and lack of particle wetting.

Table 7.1. Summary of Experimental Test Conditions for Pertechnetate Reduction using Sulfur Polymer Cement

	Matrix 1	Matrix 2
Specimen Morphology	-20/+40 mesh	-40/+70 mesh
Specimen Treatment	As-Received, Remelted	As-Received, Remelted
Temperature, °C	Room Temperature	45°
Solution(s)	DIW	DIW, 0.01 M NaOH
Technetium Conc., Ci/L	3.0×10^{-5}	2.7×10^{-7}
Approx SA/V, cm^{-1}	10 g SPC/30 mL	0.2 g SPC/2 mL
Agitation	End-Over-End @ 30 rpm	None
Container Type	Poly. Centrifuge Tube	Flame-Sealed Vial
Sampling Periods, days	4, 7, 35, 62	20, 40, 54, 67
Results	Inconclusive	Tc Reduced $\leq$ 25% @ 20 d and 67 d (most reduced 50%)

	Matrix 3	Matrix 4
Specimen Morphology	Monolith	Monolith
Specimen Treatment	Remelted	Remelted
Temperature, °C	70°	70°
Solution(s)	DIW	DIW
Technetium Conc., Ci/L	2.0×10^{-7}	2.0×10^{-7}
SA/V, cm^{-1}	0.1	0.1
Agitation	None	None
Container Type	PFA (Teflon) in Pressure Vessel	Reflux (No Seal)
Sampling Periods, days.	7, 21, 34	27
Results	No Reduction	No Reduction

Granules of SPC were observed floating on the surface of the water, even though the specific gravity of the material is roughly twice that of water (2.07 g/cm^3). In addition, the bulk density of the particles appeared reduced (to the naked eye) either by electrostatic repulsion and/or by entrapping small bubbles of air.

There has been speculation that the hydrophobic behavior demonstrated by some of these particles could be attributed to the grinding technique. The particles were ground using a hand-powered, rotating-disc mill. The steel discs have an adjustable spacing for producing different particle sizes. The grinding discs also have milled grooves to feed the material efficiently. Over the course of grinding some SPC was "smeared" into the grooves and built up, so it was assumed that the material not only fractured but also abraded and friction-heat-fused, producing melt-polished surfaces.

It is believed that these particles may have been difficult to wet because of the presence of such polished surfaces. Furthermore, there is a possibility that a net electrostatic charge built up on the particles during grinding which may have resulted in the particles repelling one another and altering the physical behavior of the particles. These observations are presented here as experimental artifacts that may have effects that would not be observed in their intended repository role.

The second set of experiments was conducted to eliminate the influx of atmospheric oxygen into the adsorption test container and gave positive results for pertechnetate reduction. Following exposure periods of 20, 40, 54, and 69 days, selected vials were opened and the contents were filtered through a 0.22-μm-pore filter. One mL of this filtrate was added to 15 mL of scintillation cocktail to determine Tc-99 activity, and the balance was used to determine pH. For the first sampling, at 20 days, technetium activities in tests conducted with DIW were reduced to approximately 83% of the original activities, while technetium activities in tests conducted at pH 12 were reduced to approximately 75%. No significant difference was observed between SPC in its as-received and remelted conditions. It was concluded that remelting most likely has no impact on the capability of SPC to reduce pertechnetate (see Figure 7.1). The pH of DIW solutions dropped from approximately 6.6 to 3.4 following exposure to SPC for 20 days, while the pH of the 0.01 M NaOH solutions dropped from 12.0 to approximately 7.2 over the same period.

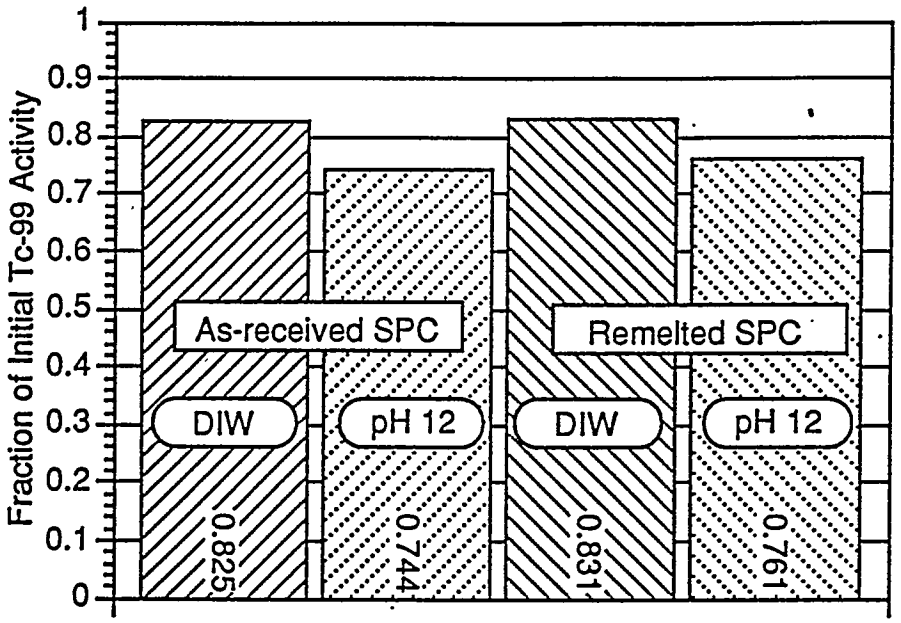

Figure 7.1. Fraction of Initial Activity of Tc-99 After 20 Days Exposure to Either As-Received or Remelted SPC Granules in DIW or pH 12 Solution. Flame-sealed vials were used to eliminate oxygen (270 Nci/L Tc-99).

Five additional "pH-12 adjusted" samples were analyzed following 40, 54, and 69 days of exposure. Results from these samples are included in Table 7.2. No decreasing trend of technetium activity is apparent in the data. It is not clear, at this point, whether these results indicate the development of a reaction-site saturated system that is incapable of producing any further pertechnetate reduction, or whether a minute diffusion of oxygen is occurring and an equilibrium has been produced, or, simply, whether the reduction reaction(s) are proceeding at a slow pace.

A third set of experiments, initiated to eliminate uncertainties concerning particle wetting, used rectangular specimens of SPC with geometric surface areas of 4.0 cm^2 (monoliths). The SPC samples were placed in tightly sealed PFA Teflon containers to prevent oxygen replenishment, but were opened for sampling at 7, 21, and 34 days and then resealed. The tightly sealed containers were placed in an oven operating at 70°C. These tests generated no liquid samples which showed any reduction of technetium activity, and therefore no pertechnetate reduction.

The fourth set of experiments using a reflux-distillation apparatus (open to the atmosphere) also showed no pertechnetate reduction following 34 days of exposure of Tc-spiked DIW to SPC monolith coupons.

It was anticipated that achieving positive results from tests employing SPC monoliths would be slow, given the reduced surface area available for reduction reactions to occur. The lack of positive

Table 7.2. Technetium-99 Solution Activities Found Following Exposure to Sulfur Polymer Cement Granules

Elapsed Exposure Time, days (SPC granules in Tc-spiked DIW, pH 12)	Fraction of Initial Tc-99 Activity
20	0.74, 0.76
40	0.78
54	0.51, 0.65
69	0.75, 0.74

results for these tests is consistent with the results obtained from tests using granulated SPC. Specifically, even though an enormous excess of sulfur was nominally available, pertechnetate reduction was slow and reactions only removed, at most, fifty percent of pertechnetate from solution (one flame-sealed vial test). When extrapolating these results to tests employing reduced reactive surface area, it is easily understood why positive results are yet to be achieved with monolith samples. Given the available data, these monolith test results cannot be used to establish the sensitivity of the reaction system to oxygen, nor to generally indicate whether surface wetting might play a significant role in the physics of the reaction.

7.2 Summary

Sulfur polymer cement was used in a variety of tests to assess its ability to serve as a reductant for pertechnetate ion. Although verification of this reducing ability was demonstrated, that positive result was not quickly produced. Pertechnetate reduction was assumed to have occurred if the amount of Tc-99 found in solution by liquid scintillation counting, following contact with SPC, was less than its initial concentration. The reduced technetium species was assumed to be adsorbed on the surface of the SPC, to precipitate from solution, or to be filtered from solution using a 0.45-μm-pore filter. Initial experiments using granulated SPC failed to produce positive results because, conducted at approximately 25°C, reaction kinetics were too slow to observe reaction progress, and/or the test containers (centrifuge tubes) were too permeable to atmospheric oxygen and prevented reducing conditions from developing.

A subsequent experiment used granulated SPC contained in flame-sealed glass vials used pertechnetate-spiked (pH 12) DIW that was 100x less concentrated than Tc concentrations used in the first test, and was conducted at 45°C. This setup eliminated the influx of oxygen, changed the Tc concentration to a level facilitating detection of small reaction progress, and increased the speed of thermal kinetics. This test produced approximately 25% pertechnetate reduction at seven days contact (75% still in solution). Although the lowest values for pertechnetate solution concentration were found at 54 days (approximately 50% and 65%) other concentrations found in samples taken at 40 and 69 days did not differ significantly from the initial 75% value.

The results of the scoping tests identified a few of the important test parameters and represent a starting point for a more comprehensive test matrix. Conclusions or generalizations about the Tc gettering capability of SPC should not be extended out of context of the reported data.

Experiments with SPC monolith samples, conducted concurrently with the flame-sealed vial experiments, produced no positive results within the available 34-day test period. This negative result is believed to be primarily attributable to the reduced amount of surface area available for reaction, but the reactions may also have been slowed by oxygen influx when sampling the containers at 7 and 21 days.

Clearly, although SPC has a demonstrated capability to remove pertechnetate from solution by reduction reaction, if SPC is to be used in a repository to prevent the escape of pertechnetate, then a more thorough understanding of the reaction kinetics and necessary reaction conditions is needed. Of primary importance is the answer to whether or not the conditions necessary for the reduction reaction can develop under the anticipated repository environment. Furthermore; it is suggested that the technetium species produced by the reduction reaction be carefully studied for redox stability. These experiments have not addressed the long-term stability of the reduction reaction products. Given the slow and incomplete progress of the pertechnetate/SPC reduction reaction, reaction reversibility and equilibrium needs to be carefully considered.

8.0 Compressive Strength

As part of the evaluation of sulfur polymer cement (SPC) as a matrix material for low-level waste (LLW) glass, the mechanical strength of the material was measured. This section discusses the preparation of test specimens and contains the test results for both pure SPC and composites of simulated LLW glass and SPC, in both the as-prepared state and after gamma irradiation, to the lifetime dose calculated to result from residual (mainly Sr and Cs) radionuclides dissolved in the LLW glass.

8.1 Experimental Considerations

8.1.1 Specimen Preparation

Compression testing was chosen to evaluate these materials because of the simplicity in specimen fabrication plus the general applicability of the results to analysis of the suitability of the material for permanent disposal. Consideration of the size scale of the LLW glass as cullet indicated that a specimen diameter of 2.5 cm and a length of 5 cm would be an adequate size for sampling purposes. This length-to-diameter ratio is also proper according to the specification used to guide the work (ASTM 1988).

Specimens were molded in Teflon because of its nonreactive nature. The Teflon was in the form of tubes with an inside diameter of 2.5 cm, approximately 15 cm long, closed on the lower end by a suitable steel pipe cap and with a Teflon gasket to provide a nonreactive bottom surface. The containers were immersed in a silicone oil bath at 140°C; SPC was melted in them. All mechanical testing used SPC lot 122794. The best technique for obtaining a nearly bubble-free outer surface was to immerse the containers in room-temperature water, so that the SPC at the Teflon-SPC interface froze first to form the outer surface. The Teflon mold had a slight (0.25°) taper in its inside surface to aid in ejecting the SPC specimens. The specimens were easily ejected by use of a small hand press.

Production of LLW glass/SPC composites was somewhat more involved. The rather low (approx 20 cp, similar to water) viscosity of molten SPC and the higher density of glass than SPC indicated that the LLW glass would sink quickly in the SPC and would pack on the bottom of the mold at the packing density for the size distribution of the glass, approximately 60 vol%. No attempt was made to produce specimens at a lower volume percent glass loading than the natural packing density, since this packing density would invariably occur in practice. First, a volume of SPC sufficient to fill interstices between glass, plus an allowance for a shrinkage void, was melted in the 140°C oil bath. Then 60 g of simulated LLW glass, sufficient to fill the mold to a height of 4.5 cm, was added to the container. The glass initially cooled the top SPC below its melting point and stayed at the SPC surface. As heat was transferred to the glass and the top SPC melted, the glass particles fell through the molten SPC to the bottom of the container. After the first specimens showed spherical air bubbles at the outer surfaces, several remedial measures were considered to eliminate these voids. Although vacuum evacuation was effective in eliminating the bubbles, it was found that thorough stirring of the settled glass would accomplish the same result, and would assist the glass to pack at its maximum density. After stirring, the mold was quenched into water as for the pure SPC. Forty specimens of pure SPC and SPC-glass

composites were prepared, to provide at least seven specimens in both the as-prepared and gamma-irradiated conditions, plus specimens for later testing after exposure to leaching environments.

8.1.2 Irradiation of Test Specimens

In addition to testing as-prepared materials, it was desirable to determine whether gamma irradiation would produce changes in SPC binder material mechanical properties. Previous calculations[a] indicated that the lifetime dose to a matrix material surrounding a large bed of composite material would be no more than 1E8 rads.

The gamma facility (3720 Building) was used to provide such a dose to the test material. This facility includes several tubes for irradiation, calibrated for dose rates from about 150 to 1,500,000 rads/h. Tube 1, with a current dose rate of 1.46E6 rads/h, was available and capable of providing the target dose in 68.5 hours.

Specimens were packaged in a container of high-density polyethylene and inserted to the peak dose rate position on 4-14-95 and were retrieved 68.5 h later on 4-17-95. During the irradiation it was assumed that gamma heating of materials such as glass and sulfur would be low, so it was probable that specimens were at the facility water temperature, 17°C. Visual observations of all specimens indicated no obvious changes due to the irradiation. Density measurements by Archimedes' Method indicated that as-prepared SPC had a density of 1.927 g/cc and the irradiated material was 1.9315 g/cc, a difference of only 0.2%.

8.1.3 Specimen Preparation for Mechanical Testing

To meet the requirements of ASTM C773-88, test specimens must be parallel to the testing forces, and the specimen ends must be closely parallel, within 10 microns. The combination of soft, brittle SPC with hard and brittle glass is very difficult to shape to such high tolerances, so a slightly different method was used to produce test specimens that would meet the requirements. First, as-molded specimens had tapered outer surfaces from the mold, and also showed a visible curvature, making them difficult to grip for normal machining operations. Ends were made parallel and perpendicular through use of a custom, machinist-built collet; the ends were trimmed using a combination of steel tooling for the SPC and diamond tooling for the composite specimens. Using this technique, all specimens were supplied with ends perpendicular and parallel within 50 microns.

To produce specimens with ends parallel within 10 microns, the test cylinders were attached to Plexiglas™ plates (using a thickened epoxy [J B Weld, Sulphur Springs, TX]) with mechanical properties similar to the specimens themselves. To keep the Plexiglas plates parallel during gluing, the specimens were placed in jigs which provided positive alignment of the end plates. Figure 8.1 shows the loading plates and gluing jigs in use.

The alignment of the loading machine faces, which pressed against the specimen end plates, was checked and found to be accurate within 3 microns. This was done by using a material made to check

(a) Higley, B. A. 1995. Personal communication.

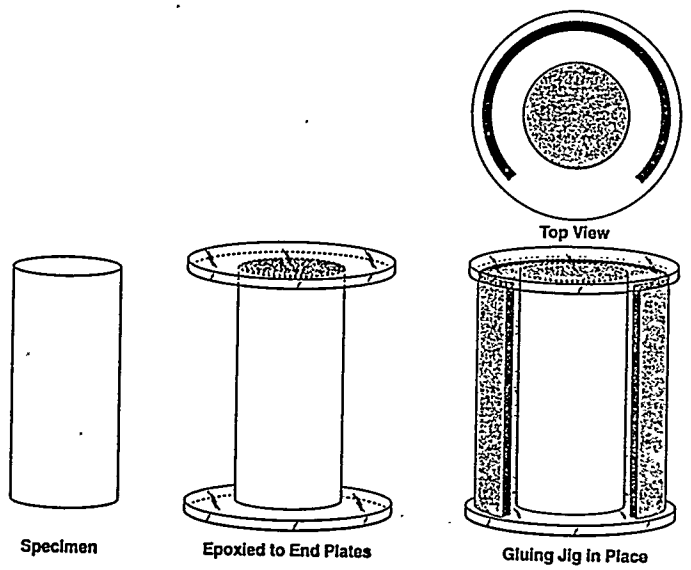

Figure 8.1. Schematic Drawing of Method for Gluing Compression Test Specimens of Either Simulated LLW Glass/SPC Composites or Neat SPC to Parallel End Plates

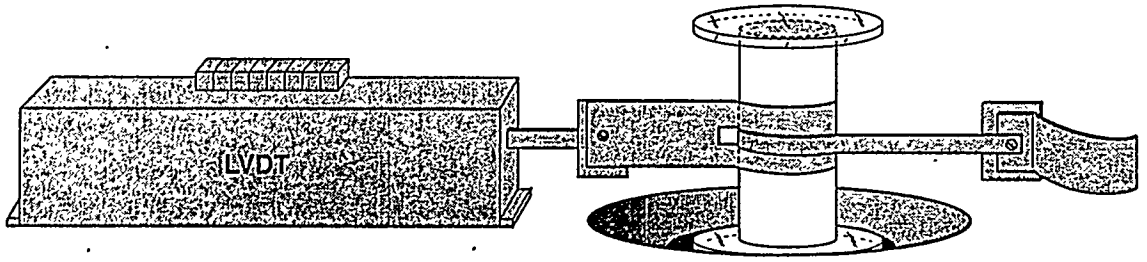

Figure 8.2. Instrument Used to Measure Circumferential Strain of Compressed Simulated LLW Glass/SPC Composites or Neat SPC Specimens

bearing clearances in automobile engines.[a] This material indicates clearance in assembled bearings by the width to which it spreads when clamping force is applied. The material was applied betweentwo of the end plates, then placed in the test machine and pressed in the load frame until it flattened to approximately 3 mm. Spreading of the gauge material was extremely uniform; there was no evidence that the test machine loading faces had measurable nonparallelism.

During the mechanical testing, it was planned that the force applied to the specimen would be measured as a function of the movement of the testing machine crosshead. To provide additional information on the mechanical response of test specimens, the strain of selected specimens was also measured in the hoop (circumferential) dimension by using a device constructed at PNNL from available parts. Figure 8.2 is a drawing of the device, which consisted of a stainless-steel band 100-microns thick which encircled the specimen, fixed at one end and attached to a linear variable differential transformer (LVDT) on the other. As the specimen was compressed, its hoop dimension increased, and the device measured the increase.

Other pre-test preparations included checking to be certain that all calibrations were up-to-date and attaching a computer to the output of measuring instruments for data analysis.

8.2 Results and Discussion

All testing was conducted in a mechanical testing laboratory, at a room temperature of 70°F, controlled within ±3°F. All loading was done at a cross-head speed of 0.025 cm/min, which corresponded to an approximate compressive strain rate of 0.5%/min. To guard against flying fragments of test material, a band of stretchy adhesive tape[b] was applied to each specimen before testing.

The main observation made during testing was that the SPC and SPC/glass composites were comparatively tough materials in the as-prepared condition. Failure in all cases was by longitudinal splitting at the outer surface of the test specimens, caused by the high hoop strain there. Even after failure, and at an approximate axial strain of 6%, the pure SPC specimens supported a stress of 35 MPa, as shown in Figure 8.3. The composites were generally weaker and more brittle, but supported a stress of about 18 MPa after being strained 1.5%; see Figure 8.4.

Typical SPC and composite specimens after testing are shown in Figures 8.5 and 3.53, respectively. Note the multitude of axial cracks. These cracks formed at the outer surface of the specimen, propagating inward as the strain limits of the material were sequentially exceeded.

The main effect of the glass in the composite material is to stiffen the SPC, as would be expected from its higher elastic modulus, and to decrease the strain at maximum stress. The composite specimens were more brittle than the all-SPC specimens, and were slightly weaker. The slight weakness was probably caused by comparatively weak bonding at the glass-SPC interfaces. Close

---

(a) Plastigage Clearance Indicator, Perfect Circle, Toledo, Ohio

(b) Polyken Tape, Polyken Technologies, Westwood, Massachusetts.

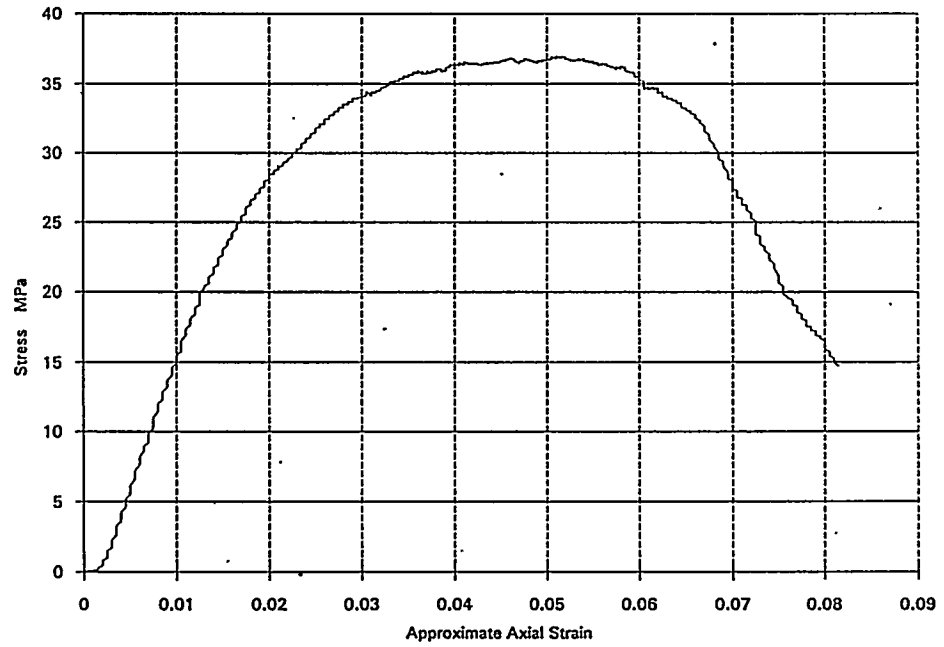

Figure 8.3. Typical Stress-Strain Curve for Neat Sulfur Polymer Cement

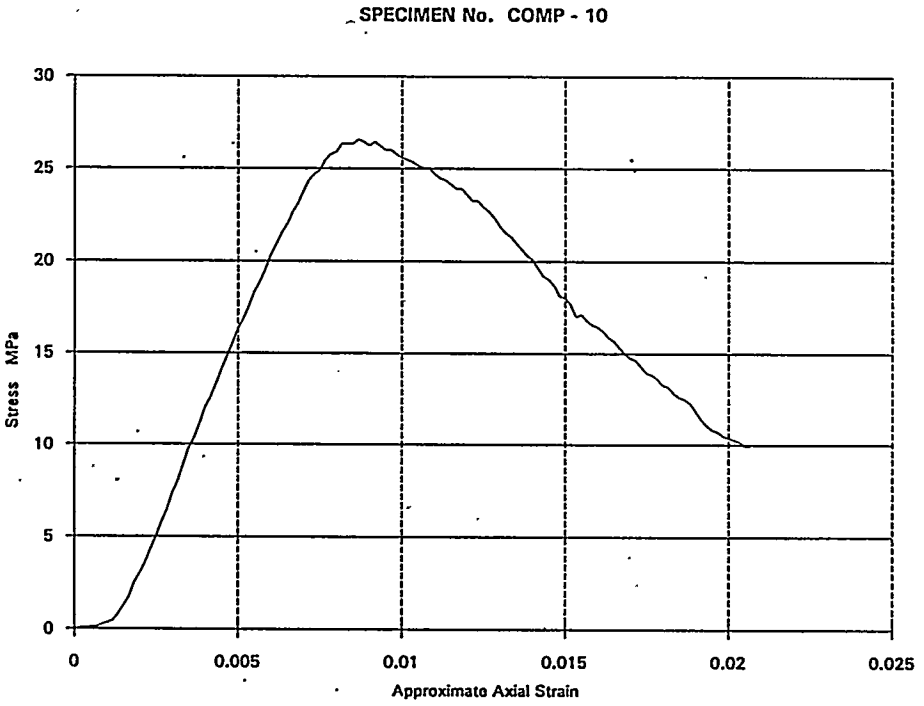

Figure 8.4. Typical Stress-Strain Curve for Sulfur Polymer Cement-Simulated LLW Glass Composite

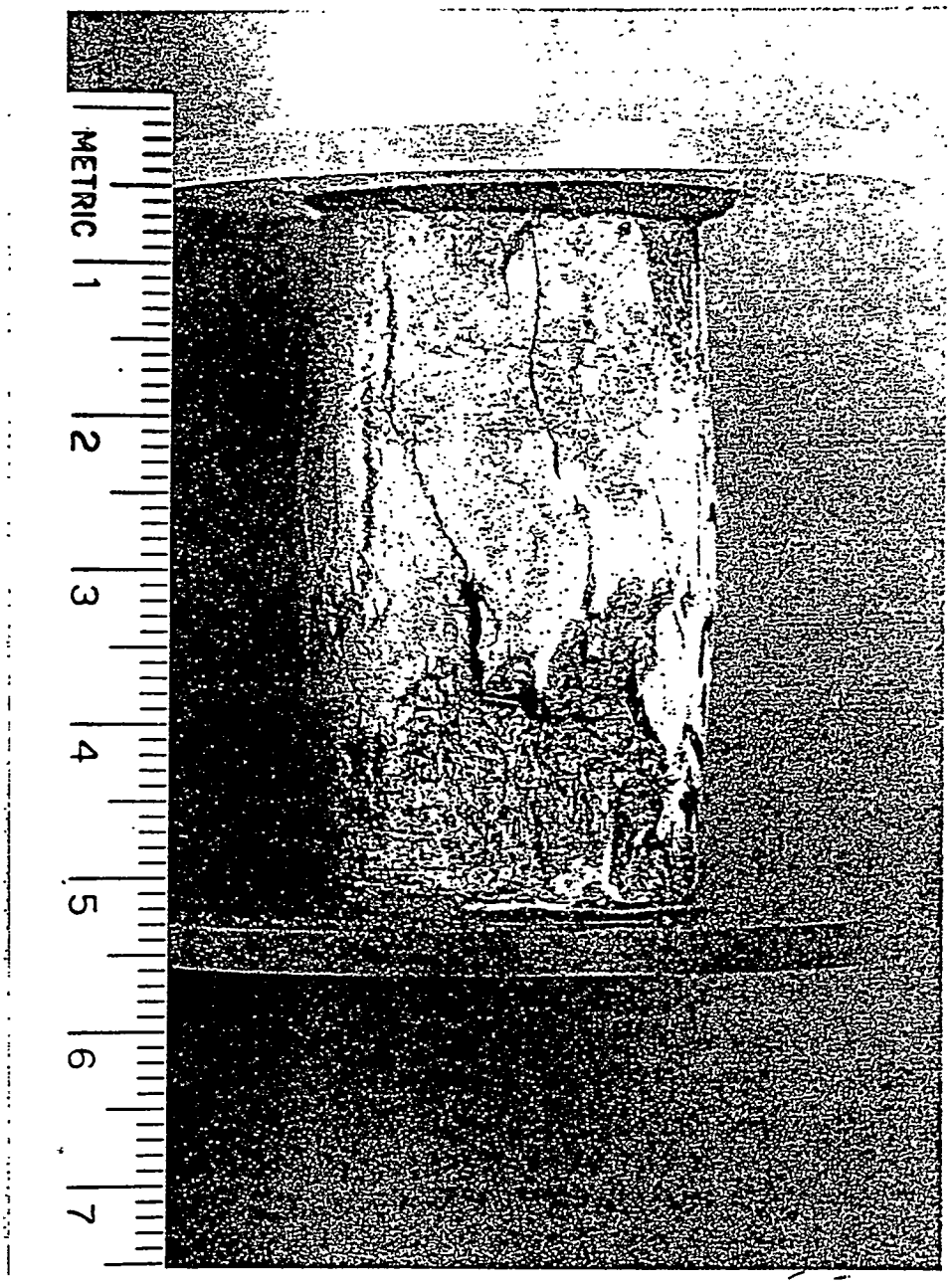

Figure 8.5. Photograph of Failed Neat Sulfur Polymer Cement Specimen

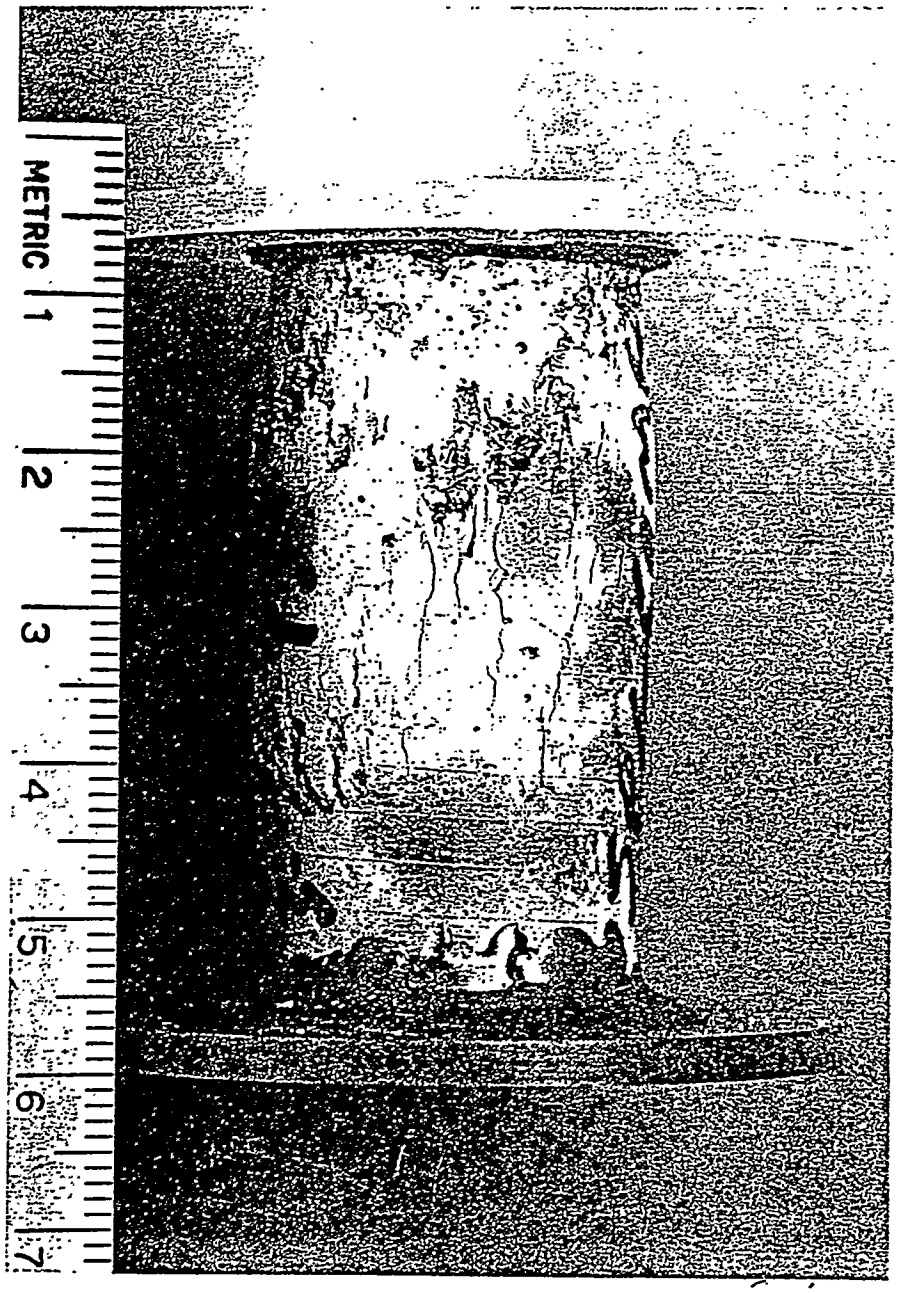

Figure 8.6. Photograph of Failed Sulfur Polymer Cement-Simulated LLW Glass Composite Specimen

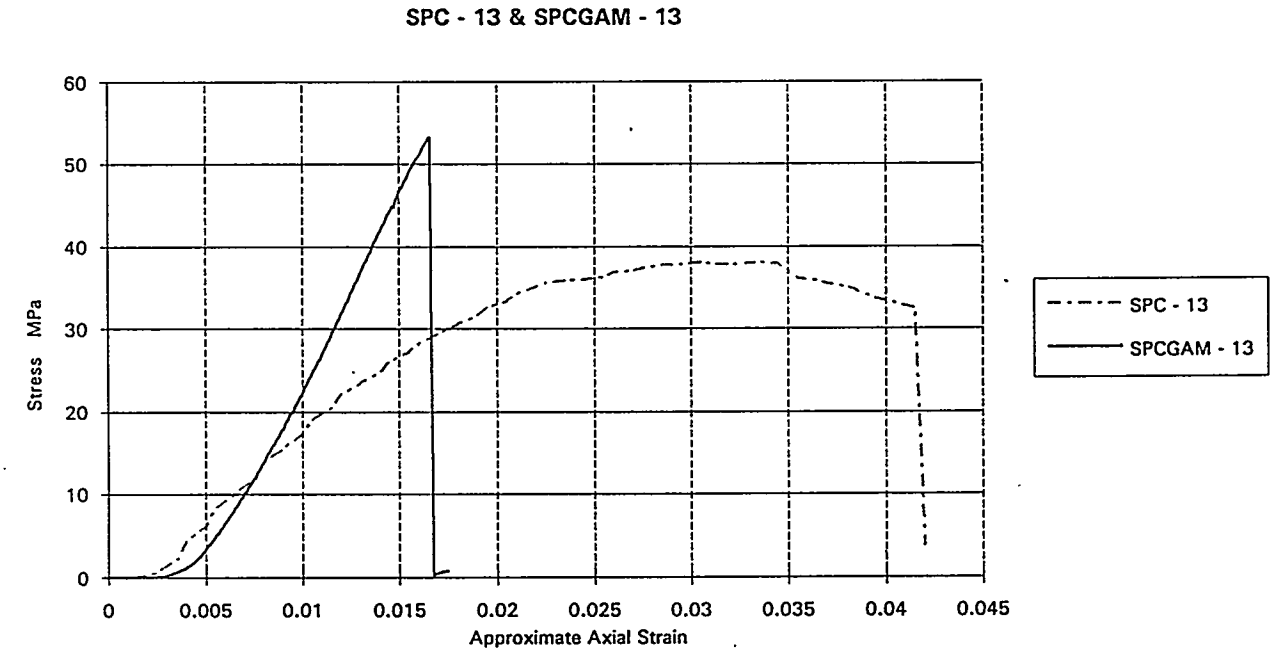

Figure 8.7. Comparison of Typical Stress-Strain Curves for As-Prepared and Gamma-Irradiated Neat Sulfur Polymer Cement

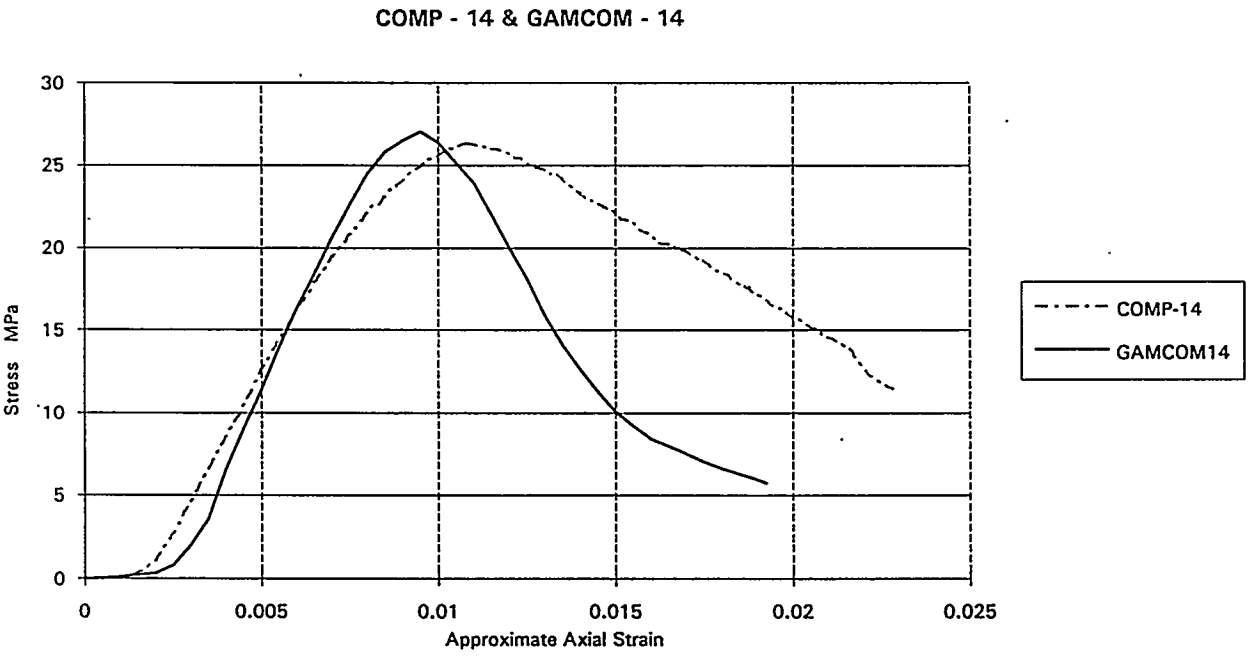

Figure 8.8. Comparison of Typical Stress-Strain Curves for As-Prepared and Gamma-Irradiated Sulfur Polymer Cement-Simulated LLW Glass Composites

examination of tested composite specimens revealed that the fracture path was predominantly at the glass-SPC interfaces.

Gamma-irradiated SPC was much stiffer than non-irradiated material, and failed in a more brittle fashion at a higher stress. Figure 8.7 compares typical irradiated and non-irradiated SPC specimens. Although the irradiated SPC was almost 50% stronger than the non-irradiated material, it failed completely at about one-third the strain at which the nonirradiated SPC retained most of its peak compressive strength. The effect of gamma radiation on composite specimens was similar but not as profound (see Figure 8.8); the gamma-irradiated material was stiffer but showed a similar compressive strength to its nonirradiated counterpart.

Table 8.1 contains values for peak stresses and strains for all specimens tested, as well as average values for peak stresses observed in the four specimen types. Table 8.1 also contains approximate values for the stiffness computed from the slope of the stress-strain curves at small values of strain, in the portion of the curve that was approximately linear.

Figure 8.9 shows the method used to calculate this stiffness. The area chosen for analysis was determined by visual inspection of the stress-strain curves, and the slope was determined by the least-squares method on the corresponding data. In cases where the load curve was irregular in appearance, the slope was not determined. At least three slopes were determined for each type of specimen tested.

Figure 8.10 is a plot of circumferential strains as a function of applied stress for all four specimen types. The same trends of relative ductility in SPC versus composites and in the effects of gamma irradiation were also seen in these measurements.

The reason for the increase in the stiffness and strength of SPC as a result of gamma irradiation is not known. A literature search revealed no relevant information on the effects of gamma radiation on sulfur. To at least provide some evidence for judging speculations, specimens of SPC, both as-prepared and after gamma irradiation to 1E8 rads, were examined by differential scanning calorimetry (DSC) and X-ray diffraction (XRD). Results were inconclusive; DSC showed almost identical endothermic peaks for the alpha-beta transition and melting for both as-fabricated and gamma-irradiated SPC. X-ray diffraction indicated that alpha sulfur was the major phase in both as-prepared and irradiated SPC, and a barely measurable difference in the amount of beta sulfur present (about 3 wt% nonirradiated, 5 wt% irradiated). It was possible that the gamma irradiation produced some crosslinking between the eight-member rings in the sulfur structure, in the same way crosslinking occurs in common polymers. Alternately, the organic additive cyclopentadiene may have been crosslinked by the radiation. Polymers such as polyethylene are substantially stiffened and strengthened by such crosslinking. However, there was no conclusive evidence that crosslinking occurred in the SPC.

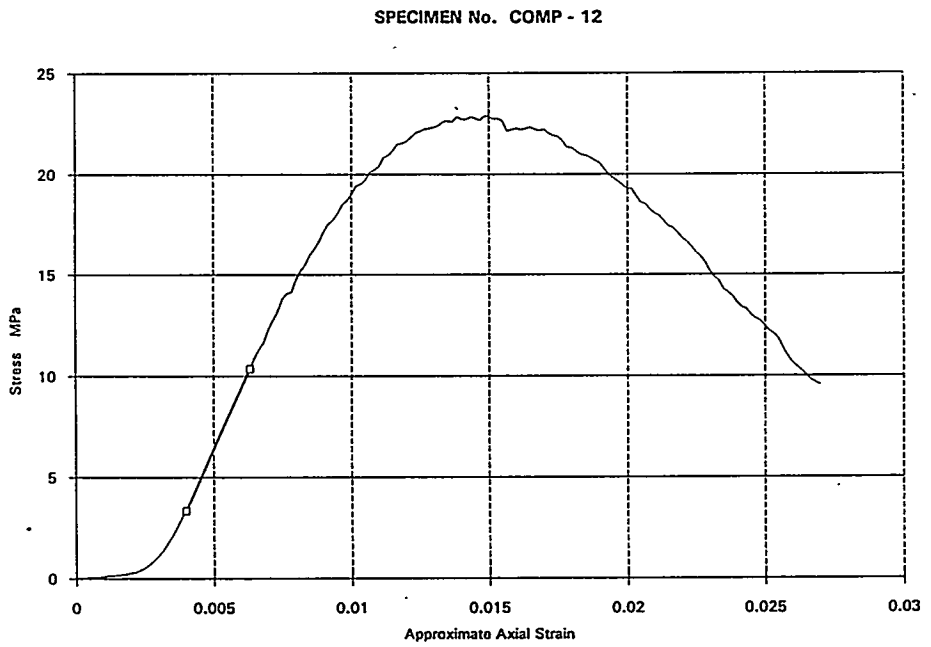

Figure 8.9. Stress-Strain Curve for Sulfur Polymer Cement-Simulated Glass Composite, Showing Region in Which Slope was Determined

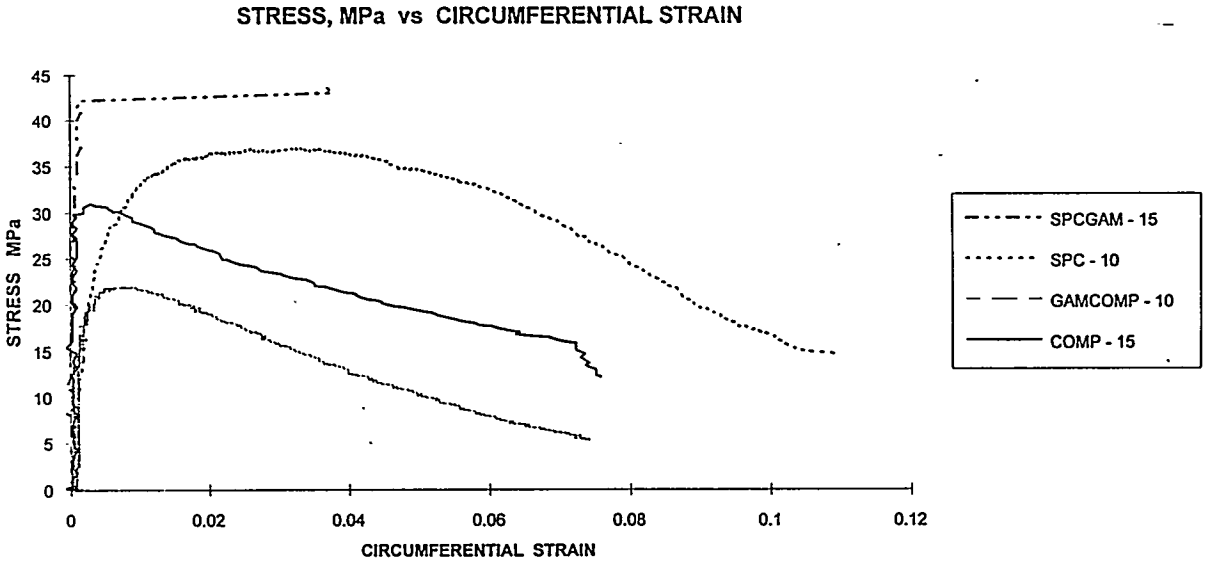

Figure 8.10. Circumferential Strain as a Function of Applied Stress for Neat SPC (SPC-10), Gamma-Irradiated Neat SPC (SPCGAM-15), and Simulated LLW Glass/SPC Composite, Prior to (COMP-15) and After Gamma Irradiation (GAMCOMP-10)

8.3 Conclusions

Sulfur polymer cement, both neat and in composite form with simulated LLW glass, is a fairly strong material capable of mechanical damage without catastrophic failure.

Gamma irradiation to projected lifetime dose stiffens and strengthens the SPC by an unknown mechanism.

Table 8.1. Summary of Mechanical Test Data for Four Specimen Types

Specimen Type and Serial #	Maximum Stress, MPa	Strain @ Max. Stress, %	Stiffness, MPa
SPC[(a)]-10	36.97	5.1	1864
SPC-11	42.07	3.8	
SPC-12	34.23	4.7	1855
SPC-13	38.10	3.1	
SPC-14	38.14	4.0	2180
SPC-15	33.61	4.1	1843
SPC-16	37.63	5.3	
Averages	37.25	4.3	1860
Std. Dev.	2.81	0.8	185
SPCGLAS[(b)]-10	26.60	0.9	
SPCGLAS-11	24.52	1.2	3232
SPCGLAS-12	22.88	1.4	
SPCGLAS-13	24.60	1.1	3379
SPCGLAS-14	26.34	1.1	
SPCGLAS-15	30.98	1.1	4564
SPCGLAS-16	29.06	1.1	
SPCGLAS-17	23.58	1.2	3683
Averages	26.07	1.1	3531
Std. Dev.	2.79	0.1	870
SPCGAM[(c)]-10	57.79	1.6	4788
SPCGAM-11	43.61	1.4	
SPCGAM-12	63.92	1.7	4952
SPCGAM-13	53.20	1.7	4154
SPCGAM-14	51.76	1.6	4605

(a) Pure SPC, no glass.
(b) SPC/simulated LLW glass composites.
(c) Gamma-irradiated pure SPC.

Table 8.1. Summary of Mechanical Test Data for Four Specimen Types (Continued)

Specimen Type and Serial #	Maximum Stress, MPa	Strain @ Max. Stress, %	Stiffness, MPa
SPCGAM-15	43.53	1.5	4114
SPCGAM-16	39.68	1.8	3490
Averages	50.50	1.6	4415
Std. Dev.	8.71	0.7	544
SPCGLASGAM[(a)]-10	21.93	1.0	4062
SPCGLASGAM-11	29.47	0.6	6335
SPCGLASGAM-12	17.10	0.6	4515
SPCGLASGAM-13	37.16	0.7	6064
SPCGLASGAM-14	27.05	1.0	4896
SPCGLASGAM-15	18.42	0.8	3513
SPCGLASGAM-16	21.71	0.9	3458
SPCGLASGAM-17	35.34	0.9	6109
Averages	26.02	0.8	4860
Std. Dev.	7.53	0.1	1179

(d) SPC/simulated LLW glass composites, gamma irradiated.

9.0 References

American Society for Testing and Materials. 1988. *Standard Test Method for Compressive (Crushing) Strength of Fired Whiteware Materials*. C773-88, Philadelphia, Pennsylvania.

Boomer, K. D. 1990. "Functional Requirements Baseline for the Closure of Single-Shell Tanks." WHC-EP-0338, Westinghouse Hanford Company, Richland, Washington.

Darnell, G. R., W. C. Aldrich and J. A. Logan. 1992. "Full-Scale Tests of Sulfur Polymer Cement and Non-Radioactive Waste in Heated and Unheated Prototypical Containers." EGG-WM-10109, Idaho National Engineering Laboratory, Idaho Falls, Idaho.

Feng, X. 1995. "Evaluation of Phase II Glass Formulations for Vitrification of Hanford Site Low-Level Waste." PVTD-T3B-95-206. Pacific Northwest Laboratory, Richland, Washington.

Kalb, P. D., J. H. Heiser, III, and P. Colombo. 1991. "Polyethylene Encapsulation of Nitrate Salt Wastes in Waste Form Stability, Process Scale-Up, and Economics." BNL-52293, Brookhaven National Laboratory, Upton, New York.

Kim, D. 1994. "Vitrification Technology Development Project Evaluation and Recommendation of Candidate Glass Systems for LLW Vitrification, Glass Formulation Technical Status Report." Pacific Northwest Laboratory, Richland, Washington.

Los Alamos Technical Associates. 1994. "Low-Level Tank Waste Disposal Study, WHC-SD-W378-ES-001, Rev. 0." WHC-SD-W378-ES-001, Rev. 0. Richland, Washington.

McBee, W. C., and T. A. Sullivan. 1982. *Modified Sulfur Cement*. U.S. Patent 4,311,826.

McBee, W. C., and T. A. Sullivan. 1983. *Modified Sulfur Cement*. U.S. Patent 4,391,969.

Ringwood, A. E. 1980. "Safe Disposal of High-Level Nuclear Waste: A New Strategy." *Fortschrieschrittene Minerals* **58**:149.

Wiemers, K. D., J. E. Mendel, A. A. Kruger, L. R. Bunnell, and G. B. Mellinger. 1992. "Preliminary Assessment of Candidate Immobilization Technologies for Retrieved Single-Shell Tank Wastes." PNL-7918, Pacific Northwest Laboratory, Richland, Washington.

Appendix A

Appendix A

Product Packaging Issues

I) Glass/Matrix Properties

A - "Representativeness" of testing (composite material testing protocols)

B - Physical

1) mechanical properties
2) glass geometry effects/packing
3) radiation effects on matrix physical properties
4) thermal expansion mismatches - cracking

C - Chemical

1) biodegradation under Hanford-relevant conditions
2) toxicity
3) thermodynamic stability ($S \rightarrow SO_4$)
4) matrix chemisorption/gettering capabilities
5) short-term aqueous durability - PCT, MCC-1, TCLP
6) long-term aqueous durability - flow-through, vapor phase, long-term static (PCT) test
7) glass-matrix material interface chemistry
8) radiation effects on matrix chemical properties
9) compatibility with sediments and pore solutions from near-field geology
10) compatibility with other barrier materials

D - Other Properties

1) flammability/combustibility
2) thermal diffusivity
3) permeability
4) gaseous emissions
5) unsaturated moisture content

II) Processing

A - Retrievability

B - Processability

C - Matrix processing effects on glass properties

D - Operations/risk of using matrix material

E - Glass geometry and size (large monoliths, marbles, cullet, etc)

F - Glass loading/fraction filled

G - In-plant pumpability (not for waste glass transport)

H - Post-treatment after forming glass/matrix monolith

III) Project Interfaces

A - Glass Formulation - formulation changes, component limits

B - Melter Technology (processing) - glass shape, geometry

C - Performance Assessment - modelling information

Appendix B

Appendix B

Table B.1. Crystalline and Amorphous Phases in Various Forms of SPC as a Function of SPC Formulation and Thermal History *

	Crystal (wt %)		Amorphous		
ID	Alpha	Beta	vol %	Color	Sample Description
SPC-07	~100	~0	25	yellow	Powder of SPC mostly from surface rubbing during, for example, shipping and handling. Collected from as-received SPC lot 122794.
SPC-08	~100	~0	20	yellow	SPC (lot 122794) grain with fractured interior showing yellow color. Compare with SPC-07.
SPC-09	~30	~70	55	dark gray	SPC (lot 122794) grain with fractured interior showing dark gray color. Compare with SPC-08.
SPC-10	~95	~5	35	yellowish gray	Found in as-received SPC (lot 122794). Nearly crumbling. Compare with SPC-07.
SPC-11	~100	~0	20	yellow	As-received SPC (lot 030695) chips. Compare with SPC-09.
SPC-12	>95	<5	35	dark gray	SPC cylinder for mechanical testing. Prepared by casting molten SPC (lot 122794) into Teflon tubes.
SPC-13S	~100	~0	?		Surface scanning. MCC-1 tested (pH 7, 28 days). ID=SPC-73-1.
SPC-13P	~100	~0	35		Powder scanning. MCC-1 tested (pH 7, 28 days). ID=SPC-73-1.
SPC-14S	~0	~0	100		Surface scanning. MCC-1 tested (pH 12, 7 days). ID=SPC-127-2.
SPC-14P	~100	~0	25		Powder scanning. MCC-1 tested (pH 12, 7 days). ID=SPC-127-2.
SPC-15	~80	~20	60		Expected to be amorphous. SPC (lot 030695), melted at 140°C, quenched between copper plates.

	Crystal (wt %)		Amorphous		
ID	**Alpha**	**Beta**	**vol %**	**Color**	**Sample Description**
SPC-35XXX	100	0	0		Single crystal sulfur. Sulfur was extracted from SPC (lot 030695) using CS2. Alpha crystals were obtained by slowly evaporating CS2.
SPC-30	100	0			SPC (lot 030695) cooled from 140°C at 1.55°C/min.
SPC-32	100	0			Pure sulfur cooled from 140°C at 25°C/min. ID: VWR Sulfur (sublimed).
SPC-33	100	0			SPC (lot 030695) cooled from 140°C at 0.2°C/min.
SPC-34	100	0			SPC (lot 122794) cooled from 140°C at 0.2°C/min.
SPC-35	100	0			Pure sulfur cooled from 140°C at 0.2°C/min. ID: VWR Sulfur (sublimed).
SPC-36	100	0			SPC (lot 030695) cooled from 140°C at 0.05°C/min.
SPC-37	100	0			SPC (lot 122794) cooled from 140°C at 0.05°C/min.
SPC-38	100	0			SPC (lot 030695) cooled from 140°C at 0.35°C/min. SPC was held at 140°C for 12 days before cooling.
SPC-100	100	0	30		SPC (lot 030695) remain after CS2 extraction.
SPC-101	0	0	100		SPC (lot 122794) remain after CS2 extraction.
SPC-102	100	0	20		SPC (lot 030695) air cooled from 140°C.
SPC-103	95	5	35		SPC (lot 122794) air cooled from 140°C.
SPC-104	50	50	75		SPC (lot 030695) air cooled from 140°C. SPC was held at 140°C for 12 days before cooling.
SPC-105	0	100	30		SPC (lot 122794) air cooled from 140°C. SPC was held at 140°C for 12 days before cooling.
SPC-106	100	0	20		SPC (lot 122794) cooled from 140°C at 0.05°C/min.
SPC-107	100	0	25		SPC (lot 030695) cooled from 140°C at 0.05°C/min.
SPC-108	100	0	30		SPC (lot 030695) cooled from 140°C at 0.05°C/min.. SPC was held at 140°C for 12 days before cooling.
SPC-109	100	0	30		SPC (lot 122794) cooled from 140°C at 0.05°C/min. SPC was held at 140°C for 12 days before cooling.
SPC-I	95	5	30		SPC (lot 122794) MCC-1 coupon.
SPC-II	95	5	35		SPC (lot 122794) MCC-1 coupon.

* Note: Alpha and beta forms are expressed in wt% of all crystalline phases only, while amorphousness is expressed in vol% of the entire SPC sample.

Comments: Spalling or crumbling was observed where solid amorphous phase was converted to alpha. See samples SPC-01, SPC-10.

Appendix C

Evaluation of Alternate Matrix Materials

Appendix C

Evaluation of Alternate Matrix Materials

The purpose of this work was to review possible alternatives to the sulfur polymer cement (SPC) being studied as a matrix material for packaging low-level waste (LLW) glass prepared from Hanford Site tank waste cleanup operations. The primary source reviewed was WHC-SD-W378-ES-001, Rev. 0, "Low-Level Tank Waste Disposal Study" (LATA 1994). This document is comprehensive, current, and contains an evaluation of most, if not all, reasonable matrix materials, including processing considerations. The majority of the literature reviewed contained methods of immobilizing waste by adding the waste directly into the material. There was very little literature on a dual-package waste-form system such as that being proposed for Hanford Site LLW.

One of the options being evaluated for LLW immobilization is the dissolution of these wastes (composed mainly of sodium nitrate) as oxides in a suitably designed glass. Previous testing (Kim 1994) has indicated that a glass could be designed to contain more than 20% sodium oxide while still meeting durability requirements. Such LLW glass could be cast into monoliths from the melter, and its radiation hazard would be low enough to permit handling as a granular bulk material until final disposal. The sheer volume of the waste glass also favors bulk handling; present plans call for a glass production rate of up to 200 MT/day.

While production of the glass in a granular form is simple, requiring only a water quench from the melter, disposal of such a material will require a matrix substance to bind the granules together into a coherent solid. Several matrix materials were evaluated; the leading candidate from that study was sulfur polymer cement (SPC), a material developed for the construction industry in which commercial-grade sulfur is mixed with organic additives such as cyclopentadiene to retard the solid-state phase transformation which would otherwise occur at 95.3°C (LATA 1994).

According to the patents on SPC (McBee 1982; 1983), the additive acts to retain the SPC in its high-temperature beta phase. The beta-alpha phase transformation is accompanied by a volume change which, unless suppressed, could reduce or destroy the mechanical integrity of the sulfur. Sulfur polymer cement was developed as an alternative to concrete made with standard Portland cement, to be used to construct floors or other structures which will be exposed to acid environments. Such environments quickly destroy Portland concrete, while SPC concrete is very durable under acidic conditions. SPC concrete is prepared differently than conventional concrete, in that the SPC is added to heated sand-and-gravel aggregate in a heated mixer, where it melts during mixing. The hot SPC concrete is placed and finished before it hardens by cooling below the melting point of the SPC. This is in marked contrast to Portland concrete, which hardens by a hydration reaction of the cement portion.

The flaws of various alternatives to SPC as a matrix material for vitrified Hanford LLW are presented below. A "short list" of candidate alternates is presented, together with an assessment of the importance of those flaws, plus the issues that must be addressed before these matrix materials can be judged to be sufficiently viable to justify further evaluations.

C.1 Bitumen

Possible Radiolytic Gas Build-Up and Swelling

This is probably a valid point at lifetime gamma doses around 10^8 rads and is a confounding factor in any accelerated radiation test with this material. Diffusion rates of various gases in bitumen are needed for modeling purposes.

High Creep Rate

For composites where there is glass-to-glass contact, the glass is the supporting member for the composite. There should be little if any creep.

Fire

Fire hazards during processing (equipment washdown, mixing operations) can be avoided by process and equipment design and fire protection. The possibility of fires over the long term is valid, and may represent an unacceptable flaw for this matrix. Oxygen exclusion, by such a simple technique as soil burial, may be the only guarantee against fire after disposal.

C.2 Polymer-Modified Cement

Possible Radiolytic Gas Build-Up

All polymers have this problem, but there are substantial differences in the magnitude of radiolytic gas build-up in different polymers. A literature search for appropriate cement-modifying polymers with good radiation resistance appears to be justified.

Alkaline Environment for Glass

This environment is possibly an unacceptable flaw for polymer-modified cement (or any hydraulic cement), but typical cement pH values should be used to make this judgement. Glasses also differ in their capability to resist caustic environments, and the durability of glass being considered could be tested in appropriate environments before rejecting this option.

Residual Permeability

The purpose of the polymer additive is to reduce the permeability of the concrete. A literature search should be conducted for permeability numbers, and these should be used in modeling to determine whether or not cement is sufficiently tight.

C.3 Glass Matrix

Fusion of the matrix with the LLW glass probably involves sufficiently high temperatures that interdiffusion of the two compositions is likely. This is an unacceptable flaw for glass, and it should not be considered further as a matrix.

C.4 Low-Melting Metals and Ceramics

Because of the high expense of low-melting metals and ceramics, this alternative is unacceptably flawed.

C.5 Polymers

Expense

Economic considerations will tend to force the use of polyethylene (recycled polyethylene is a possibility). This is an acceptable flaw; Brookhaven National Laboratory (BNL) work shows polyethylene to be a strong contender (Kalb et al. 1991).

Polyethylene Radiation Resistance

Polyethylene has very good radiation resistance, generates no gases, and crosslinks up to a gamma dose of about 10^8 rads. After this total dose, several percent shrinkage can occur. The effect of this shrinkage depends on the strain-to-failure of irradiated polyethylene.

C.6 Resin Sand

Resin sand is mentioned only briefly in the LATA report and is not defined. The term is taken to mean the sand used in foundry work that to which phenol formaldehyde resin has been added as a bonding agent that is polymerized by heat. Such a matrix material would be very inexpensive, but would be very porous and thus could not be seriously considered as a matrix likely to improve leach resistance.

C.7 Swelling Clays

Although not mentioned in the LATA report, swelling clays are included here for the sake of completeness. These clays would be inexpensive; processing would consist of mixing it with the glass, then pressing the mixture to some defined shape at pressures of several thousand pounds per square inch. If such a shape could be restrained against swelling when contacted by water, then exclusion of water could be essentially total. To provide this restraint, the containment would have to be extremely durable. Ramming the glass-clay mixture into a drilled shaft in solid rock would provide the necessary durable restraint, for instance. The expense involved in such a process makes it speculative at present, and it is not included in the "short list" below.

Of the six alternatives to SPC, bitumen, polymer-modified cement, and polyethylene appear to have acceptable or minor flaws. With bitumen the issue is long-term fire avoidance, and it may be possible to guarantee this by design of the disposal conditions. Polymer-modified cement has several processing advantages, and its acceptability probably depends upon its permeability to water, studies of which should be available in the relevant literature. Polyethylene appears to be viable, but more refined calculations of lifetime radiation dose, together with high-dose information recently available from BNL work, are required to assess its long-term performance further.

PNNL-10947
UC-721

DISTRIBUTION

No. of
Copies

OFFSITE

2 DOE Office of Scientific and Technical Information

ONSITE

1 DOE Richland Operations Office

NR Brown	K6-51

5 Westinghouse Hanford Company

CR Eiholzer	H0-36
JS Garfield	H5-49
BA Higley	H5-27
FA Mann	H0-36
GF Williamson	H5-03

36 Pacific Northwest National Laboratory

X Feng	P8-44
AM Fillion	P7-72
DL Gladwell	K9-80
BP McGrail	K2-44
PF Martin	P8-37
YB Peng	P8-44
P Sliva (22)	K6-48
PJ Turner	P7-33
JH Westsik, Jr.	K9-80
Publishing Coordination	K1-06
Technical Report Files (5)	